FLUORESCENCE STUDY OF NATURAL ANTHRAQUINONES AND CHEMICAL CONSTITUENTS OF *Boesenbergia stenophylla*

NABILA ELYANA BINTI ADNAN

FACULTY OF SCIENCE
UNIVERSITY OF MALAYA
KUALA LUMPUR

2018

FLUORESCENCE STUDY OF NATURAL ANTHRAQUINONES AND CHEMICAL CONSTITUENTS OF *Boesenbergia stenophylla*

NABILA ELYANA BINTI ADNAN

DISSERTATION SUBMITTED IN FULFILMENT OF THE REQUIREMENTS FOR THE DEGREE OF MASTER OF SCIENCE

DEPARTMENT OF CHEMISTRY
FACULTY OF SCIENCE
UNIVERSITY OF MALAYA
KUALA LUMPUR

2018

UNIVERSITY OF MALAYA

ORIGINAL LITERARY WORK DECLARATION

Name of Candidate: Nabila Elyana binti Adnan

Matric No: SGR140009

Name of Degree: Master of Science (Except Mathematics & Science Philosophy)

Title of Project Paper/Research Report/Dissertation/Thesis ("this Work"): Fluorescence Study of Natural Anthraquinones and Chemical Constituents of *Boesenbergia stenophylla*

Field of Study: Natural Product Chemistry

I do solemnly and sincerely declare that:

(1) I am the sole author/writer of this Work;
(2) This Work is original;
(3) Any use of any work in which copyright exists was done by way of fair dealing and for permitted purposes and any excerpt or extract from, or reference to or reproduction of any copyright work has been disclosed expressly and sufficiently and the title of the Work and its authorship have been acknowledged in this Work;
(4) I do not have any actual knowledge nor do I ought reasonably to know that the making of this work constitutes an infringement of any copyright work;
(5) I hereby assign all and every rights in the copyright to this Work to the University of Malaya ("UM"), who henceforth shall be owner of the copyright in this Work and that any reproduction or use in any form or by any means whatsoever is prohibited without the written consent of UM having been first had and obtained;
(6) I am fully aware that if in the course of making this Work I have infringed any copyright whether intentionally or otherwise, I may be subject to legal action or any other action as may be determined by UM.

Candidate's Signature Date:

Subscribed and solemnly declared before,

Witness's Signature Date:

Name: Dr. Choo Yeun Mun

Designation: Senior Lecturer

[FLUORESCENCE STUDY OF NATURAL ANTHRAQUINONES AND CHEMICAL CONSTITUENTS OF *BOESENBERGIA STENOPHYLLA*]

ABSTRACT

Anthraquinones have significant economic values as dyes and pigments and attracted many interests in advanced studies focusing on optical spectroscopy and photochemistry properties. However, these studies are based on unnatural anthraquinones obtained synthetically. The present dissertation work focused on the fluorescence study of natural anthraquinones isolated from *Morinda citrifolia*. Ten known anthraquinones obtained from the roots of *M. citrifolia* have been subjected to the fluorescence study. The effects of substituent groups and intramolecular hydrogen bonding on the fluorescence properties were investigated. The present dissertation work also focused on the phytochemical studies of *Boesenbergia stenophylla. B. stenophylla* from the family of Zingiberacea, is a perennial rhizomatous herb that can be found in the highland areas of Sarawak, Malaysia. In the present study, two new and two known compounds were isolated from *B. stenophylla.* All the compounds were isolated and characterized using extensive chromatographic and spectroscopic methods. Several of these compounds were selected for antioxidant assay for their ferric reducing antioxidant power (FRAP).

Keywords: Photophysical properties, anthraquinones, intramolecular hydrogen bonding, *Boesenbergia stenophylla,* essential oil.

[KAJIAN PENDAFLUOR PADA ANTRAKUINON SEMULAJADI DAN KANDUNGAN KIMIA DALAM *BOESENBERGIA STENOPHYLLA*]

ABSTRAK

Antrakuinon mempunyai nilai-nilai ekonomi yang signifikan sebagai pewarna dan pigmen dan menarik banyak minat dalam kajian lanjutan yang menumpukan pada sifat spektroskopi optik dan fitokimia. Walaubagaimanapun, kebanyakan kajian hanya berdasarkan kepada antrakuinon yang diperoleh secara sintetik. Disertasi ini memfokuskan kepada kajian pendaflour dari antrakuinon semulajadi yang diperoleh daripada *Morinda citrifolia.* Sepuluh sebatian yang telah dikenalpasti daripada akar *Morinda citrifolia* untuk keperluan pendafluor. Kesan pengganti dan ikatan intra-hidrogen molecular terhadap pendafluor dikaji. Disertasi ini juga fokus kepada kajian fitokimia tumbuhan *Boesenbergia stenophylla. B. stenophylla* adalah dari keluarga Zingiberacea, merupakan herba dari baka rhizomatous yang boleh dijumpai di kawasan tanah tinggi Sarawak, Malaysia. Dalam kajian ini, dua sebatian baru dan dua sebatian yang telah diketahui telah di asingkan dari ekstrak *B. stenophylla.* Kesemua sebatian ini telah diasingkan dan dicirikan menggunakan kaedah kromatografik dan spektroskopik. Beberapa sebatian yang telah diasingkan telah dipilih untuk kajian antioksidan sebagai kajian dalam kuasa antioksidan pengurangan ferric (FRAP).

Kata kunci: Sifat-sifat fotofizikal, antrakuinon, ikatan intra-hidrogen molekular, *Boesenbergia stenophylla,* minyak pati.

ACKNOWLEDGEMENTS

First and foremost, praise be to Allah the Almighty for providing me this opportunity and granting me the capability to proceed successfully. This thesis appears in its current form due to the assistance and guidance of several people. I would therefore like to offer my sincere thanks to all of them.

I take pride in expressing my utmost respect and sincere gratitude to my supervisor Dr. Choo Yeun Mun for her restless support and advice in guiding me throughout this research work. I would also like to thank Dr. Hairul Anuar Tajuddin for his encouragement and mentorship.

I would like to appreciate the help from the administrative division of the Chemistry department, and also to the staff of the NMR, MS, IR and UV team for their assistance and services.

I would also like to thank my lab members Ms. Yap Ann Chee, Mrs. Siti Rabeah Fadzil, and Mrs. Nur Atiqah binti Mohd Nasuha , for their care, assistance and friendship during the ups and downs in the lab. I am grateful to many friends for sharing their friendship, insights and experiences, especially Ms. Amy Nuzwir Wateh, Mrs. Fatirah Muhamad Sarih, Mrs. Phoebe Primus and Ms. Noridayu Omer.

And last but not least, I wish to thank my family for their invaluable support and constant encouragement throughout my study.

TABLE OF CONTENTS

LIST OF FIGURES

LIST OF TABLES

LIST OF SYMBOLS AND ABBREVIATIONS

ABTS	:	2,2-azinobis(3-ethyl-benzothiazoline-6-sulfonic acid)
CC	:	Column Chromatography
CD_3OD	:	Deuterated Methanol
$CDCl_3$	:	Deuterated Chloroform
$-CH_3$	:	Methyl
$CHCl_3$	:	Chloroform
CHO	:	Aldehyde
CNS	:	Central Nervous System
COSY	:	Correlation Spectroscopy
CTCL	:	Centrifugal Thin Layer Chromatography
DEPT	:	Distortionless Enhancement by Polarization Transfer
DiEt	:	Diethyl Ether
DMAAQ	:	Dimethylaminoanthraquinone
DPPH	:	2,2- diphenyl-1-picrylhydrazyl
ergs	:	Unit of energy
ESI	:	Electrospray Ionization
ET	:	Electron Transfer
Fe	:	Ferrous
$FeCl_3$	:	Ferrous Chloride
$FeSO_4$	:	Ferrous Sulphate
$FeSO_4.7H_2O$	:	Ferrous Sulphate Heptahydrate Solution
FRAP	:	Ferric Reducing Antioxidant Power
H	:	Hydrogen
HAT	:	Hydrogen Atom transfer

HCl	:	Hydrochloric Acid
Hex	:	Hexane
HMBC	:	Heteronuclear Multiple Bond Correlation
HPLC	:	High Performance Liquid Chromatography
HRESIMS	:	High Resolution Electrospray Ionization Mass Spectrometry
HSQC	:	Heteronuclear Single Quantum Coherence
IR	:	Infrared Spectroscopy
J	:	Coupling Constant
MAAQ	:	Methylaminoanthraquinone
MeOH	:	Methanol
MS	:	Mass Spectrometry
NaCl	:	Sodium chloride
NIR	:	Near-Infrared
NMR	:	Nuclear Magnetic Resonance
OEt	:	Ethoxy
OH	:	Hydroxyl
OMe	:	Methoxy
ORAC	:	Oxygen Radical Absorption Capacity
PTLC	:	Preparative Thin Layer Chromatography
Q-TOF	:	Quadrapole Time-of-Flight
SOD	:	Superoxide Dismutase
TEAC	:	Trolox Equivalent Antioxidant Capacity
TLC	:	Thin Layer Chromatography
TPTZ	:	2,4,6-Tris(2-pyridyl)-1,3,5-triazine
UV	:	Ultraviolet

LIST OF APPENDICES

CHAPTER 1: INTRODUCTION

1.1 Luminescence spectroscopy

Luminescence is the emission of light from a substance occurring from an electronically excited state. Luminescence is formally divided into two categories, fluorescence and phosphorescence; depending on the nature of the excited states. In the excited singlet states, electron in the excited orbital is paired (by opposite spin) to the second electron in the ground-state orbital. Subsequently, the excited electron returns to the ground state in its allowed spin rapidly and followed by emission of a photon. The emission rates of fluorescence are typically 10^8 s^{-1} with typical lifetime of approximate 10 ns (10 x 10^{-9} s). Luminescent compounds can be of very different kinds. For example, organic compounds are aromatic hydrocarbons (napthalene, anthracene, phenanthrene, pyrene, perylene), fluorescein, rhodamines, and coumarins (Figure 1.1) (Lakowicz, 2013). Examples for inorganic compounds are uranyl ion, lanthanide ions, doped glasses, and crystals (Lakowicz, 2013; Valeur & Berberan- Santos, 2012).

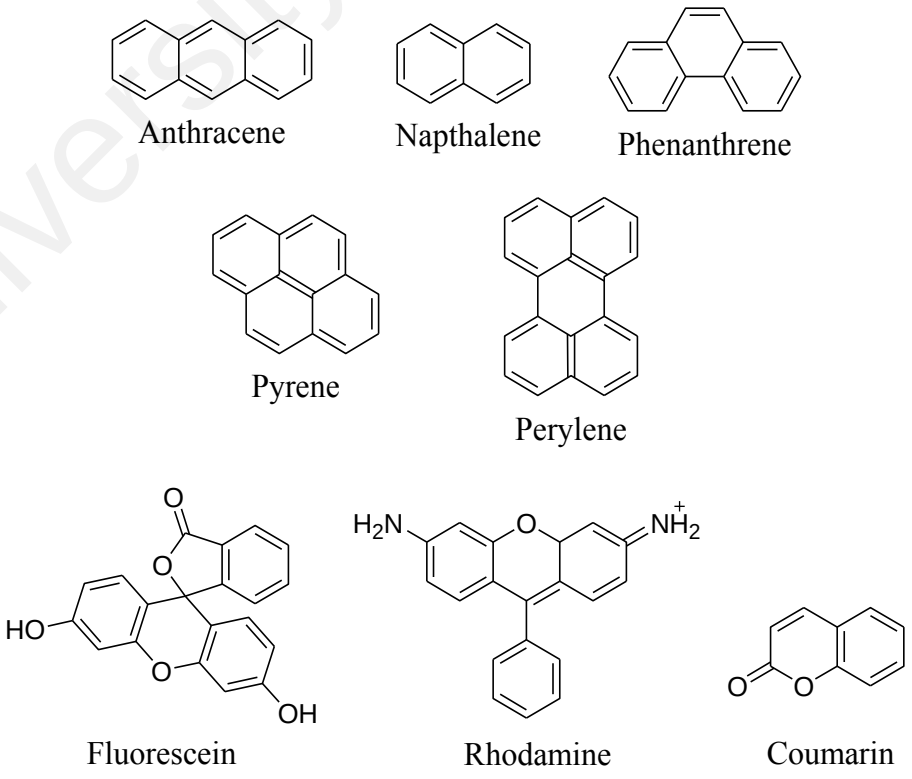

Figure 1.1: Organic compounds

Fluorescence is a property exhibited by chemical substances when irradiated with light of a short wavelength. Some of the light is absorbed and part of the energy from the absorbed light is re-radiated, usually to a longer wavelength. The term fluorescence was introduced by Sir George Gabriel Stokes, a physicist and professor of mathemathics at the University of Cambridge in the middle of nineteenth century. Stokes (1852) described the phenomenone of fluorescene in his famous 1852's paper on the change of light wavelength exhibited by fluorspar and uranium glass, materials which he viewed as having the power to convert invisible ultra-violet light into radiation of longer wavelengths that are visible (Valeur & Berberan- Santos, 2012).

Fluorescence typically occurs in aromatic molecules. One widely encountered fluorophore is quinine (**1**), which is present in tonic water. If one observes a glass of tonic water exposed to sunlight, a faint blue glow is frequently visible at the surface. This glow is most apparent when the glass is observed at a right angle relative to the direction of the sunlight, and when the dielectric constant is decreased by adding less polar solvents like alcohols. The quinine in tonic water is excited by the ultraviolet light from the sun. Upon return to the ground state the quinine emits blue light at wavelength near 450 nm (Lakowicz, 2013). The first observation of fluorescence from a quinine solution in sunlight was reported by Sir John Frederick William Herschel in 1845 (Herschel, 1845).

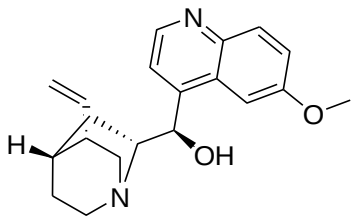

(1)

Fluorescence spectral data are generally presented as emission spectra. A fluorescence emission spectrum is a plot of the fluorescence intensity versus wavelength

(nm) or wavenumber (cm^{-1}). Emission spectra vary widely and are dependent upon the chemical structure of the fluorophore and the solvent in which it is dissolved (Lakowicz, 2013).

To account adequately for the processes of absorption and emission of light, it is necessary to assume that radiant energy can only be absorbed in definite units, or quanta. The energy, E, carried by any one quantum is proportional to its frequency of oscillation, that is

$$E = h\nu = \frac{hc}{\lambda} \text{ ergs}$$

where ν is the frequency, λ the related wavelength and h = Planck's constant (6.624 x 10-27 ergs/seconds) (Sharma & Schulman, 2000).

At room temperature most molecules occupy the lowest vibrational level of the ground electronic state, and on absorption of light they are elevated to produce excited states. Excitation can result in the molecule reaching any of the vibrational sub-levels associated with each electronic state. Since the energy is absorbed as discrete quanta, it resulted in a series of distinct absorption bands. Most compounds have broad absorption spectra except for those where rotational levels are restricted (for example, planar, aromatic compounds). Having absorbed energy and reached one of the higher vibrational levels of an excited state, the molecule rapidly loses its excess of vibrational energy by collision and falls to the lowest vibrational level of the excited state. In addition, almost all molecules occupying an electronic state higher than the second undergo internal conversion and pass from the lowest vibrational level of the upper state to a higher vibrational level of a lower excited state which has the same energy. From there the molecules again lose energy until the lowest vibrational level of the first excited state is reached (Guilbault, 1990; Sharma & Schulman, 2000).

From this level, the molecule will return to any of the vibrational levels of the ground state, emitting its energy in the form of fluorescence. If this process takes place for all the molecules that absorbed light, then the quantum efficiency of the solution will be maximum in unity. However, if any other route is followed, the quantum efficiency will be less than one and may even be almost zero (Guilbault, 1990; Sharma & Schulman, 2000).

Kasha's rule state that emission will always occur from the lowest lying electronically excited singlet state $S_{1,v=0}$ (Sauer *et al.*, 2011). The processes that occur between the absorption and emission of light are depicted by the Jablonski diagram (Figure 1.2). Jablonski diagrams are often used as the starting point for discussing light absorption and emission. It can be used in a variety of forms to illustrate various molecular processes which can occur in the excited states (Lakowicz, 2013). Hence, from this point the molecule may remain in the lowest vibrational level of the lowest excited singlet state followed by emission of visible or ultraviolet fluorescence. This fluorescence emission process was illustrated in Figure 1.2 below. The coloured circles represent the energy state of the fluorophore, whereas green depicts the normal energy level and red the maximum energy level (Sauer *et al.*, 2011).

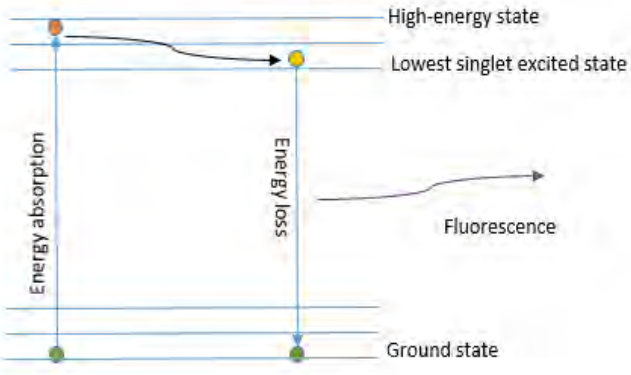

Figure 1.2: Schematic representation of an energy diagram (Jablonski diagram) (Sauer *et al.*, 2011).

The observed fluorescence is called Stokes fluorescence, in which the re-emission photons are less energetics and having a longer wavelength, this phenomenone is illustrated in Figure 1.3.

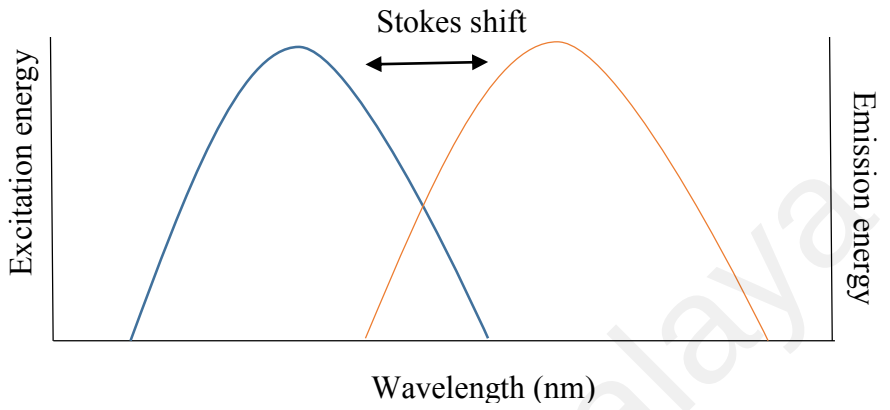

Figure 1.3: Stokes fluorescence diagram

The different in energy occur can be atttributed to the loss of vibrational excitation energy of a molecule during the excitation/emission cycle. Fluorescence cycle occurring at lower energy level with loss of photon energy called Stokes Shift (Sauer *et al.*, 2011).

In situation where the emission is at shorter wavelengths than that of the excitation, it is known as anti-Stokes fluorescence. The additional energy at re-emission photons may come from thermal energy or be associated with a molecule with many highly populated vibrational energy levels. Furthermore, when re-emission of photons have the same energy as the absorbed photons, it is called resonance fluorescene. This phenomenon does not occur in solution but only in solids and gases (Sauer *et al.*, 2011).

Phosphorescence is emission of light from the triplet excited states, in which the electron in the excited orbital has the same spin orientation as the ground-state electron (Figure 1.4). Even though it is closely related to fluorescence, it occurs at much slower pace. With transitions to the ground state forbidden and the emission rates slow (10^3 to 10^0 s^{-1}), the phosphorescence lifetimes are typically milliseconds to seconds. Even longer lifetimes are possible, as is seen in the "glow-in-the-dark" toys. Following exposure to

light, the phosphorescence substances glow for several minutes while the excited phosphors slowly return to the ground state. Phosphorescence is usually not seen in fluid solutions at room temperature. This is because there exist many deactivation processes that compete with emission, such as non-radiative decay and quenching processes (Lakowicz, 2013). In contrast to fluorescence, the re-emission of photons is decelerated by the association of excited electrons energy with a "forbidden" state. Their return to the ground state does not occur as fast as in the case of fluorescence because energy is "trapped" (Christoph, 2012).

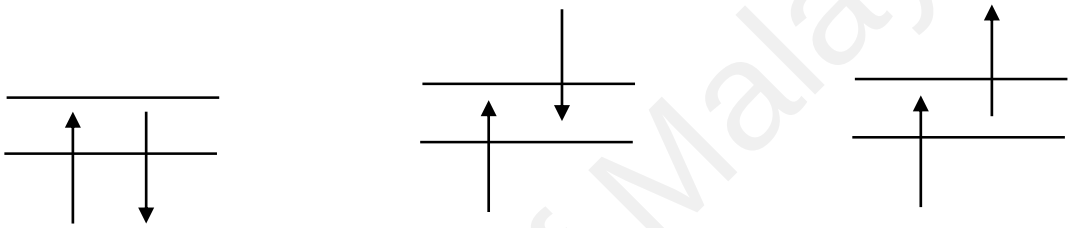

Figure 1.4: Transition diagram

Phosphorescence has been observed from a wide variety of compounds and is differentiated from fluorescence by the long-lived emission of light after extinction of the excitation source. The first analytical uses of phosphorescence were published in 1957 by Kiers *et al.* (1957). The major applications of phosphorescence are in the drug and pharmaceutical field, and in the analysis of pesticides (Moye & Winefordner, 1956; O'Donnell & Winefordner, 1975). A number of the sulphonamide class of drugs exhibit phosphorescence as do phenobarbital, cocaine, procaine, chlorpromazine and salicylic acid (Figure 1.5). Phosphorescence has been used in the detection of air and water borne pollutants, for the analysis of impurities in polycyclic aromatic hydrocarbons and in petroleum products (Williams, 1981).

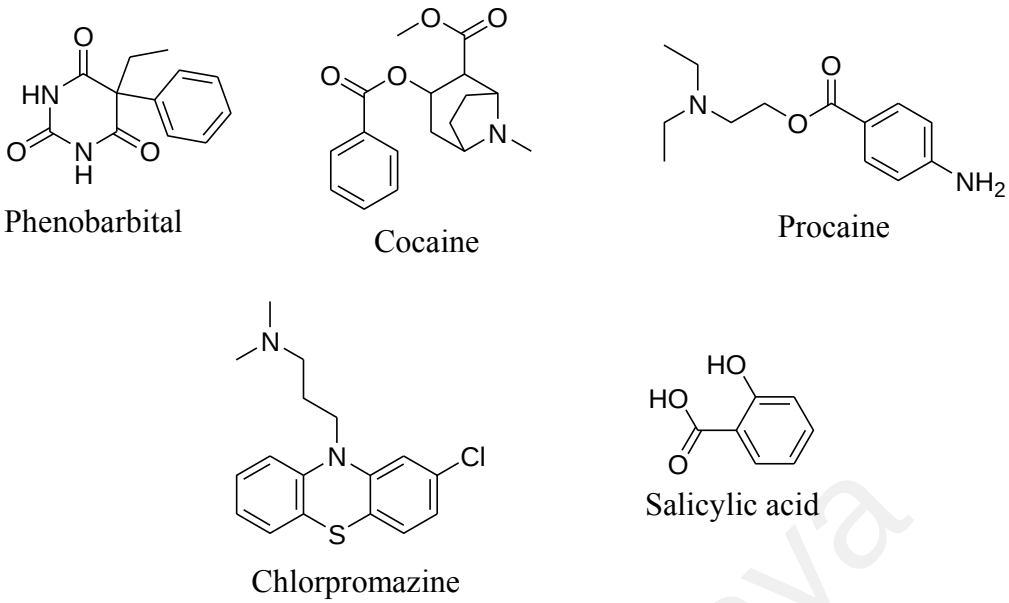

Figure 1.5: Classes of drugs

Table 1.1: Differences between fluorescence and phosphorescence

Fluorescence	Phosphorescence
When light is supplied to a sample of molecules, we immediately see the fluorescence. Fluorescence stops as soon as we take away the light source (Valeur & Berberan- Santos, 2012).	But phosphorescence tends to stay little longer even after the irradiating light source is removed (Kiers *et al.* (1957).
Fluorescence takes place when excited energy is released, and the molecule comes back to the ground state from the singlet-excited stage (Guilbault, 1990; Sharma & Schulman, 2000).	Phosphorescence takes place when a molecule is coming back to the ground state form the triplet excited state (metastable state) (Lakowicz, 2013).
A quinine solution in sunlight was first observation of fluorescence (Herschel, 1845).	Phosphorescent materials appears to 'glow in the dark', because of slow emission of light over time (Lakowicz, 2013).
The emission rates of fluorescence are typically 10^8 s^{-1} with typical lifetime of approximate 10 ns (10×10^{-9} s) (Lakowicz, 2013; Valeur & Berberan- Santos, 2012).	The phosphorescence lifetimes are typically milliseconds to seconds. (Lakowicz, 2013).

1.2 Natural products research in drug discovery

In the past thousands of years, natural products have been used in the health care and prevention of diseases. Written evidence have been provided for the use of natural sources in the ancient civilizations such as China, Indian and North Africa for curing diseases (Philipson, 2001). The Chinese Materia Medica and Indian Ayurvedic systems have records dating back to 1100 BC and 1000 BC, respectively. The earliest known records were written on clay tablets for remedies of various illnesses (Kong *et al.*, 2003).

Natural products are not only complement synthetic molecules, they also exhibit drug relevant features unsurpassable by any synthetic compound. One key feature of natural products is their enormous structural and chemical diversity. In fact, about 40% of the chemical scaffolds found in natural products are absent in today's medicinal chemistry, and therefore complementary to synthetically produced molecules. Most possibly this is one of the reasons for their historical success in drug discovery, with 45% of today's bestselling drugs originating from natural products or their derivatives (Lahlou, 2013).

All these traditional medicines are mostly derive from plants which formed the basis of the earliest medicines (Butler, 2004). Famous examples include the antimalarial drug quinine from the bark of the Cinchona species, aspirin or acetylsalicylic, derived from salicylic acid, which comes from the bark of the willow tree (*Salix alba*), and morphine, named after *Morpheus*, the Greek god of sleep and dreams (Figure 1.6) (Agosta, 1997; Kinghorn, 2001; Omprakash, 2013). Morphine from the opium poppy, *Papaver somniferum*; Atropine obtained from *Atropa belladonna*; strychnine, a central nervous system (CNS) stimulant; ziconotide, identified from a cone snail, *Conus magus*; and Taxol® obtained from the bark of the Pacific yew tree are a few examples of active components isolated from natural sources (Omprakash, 2013).

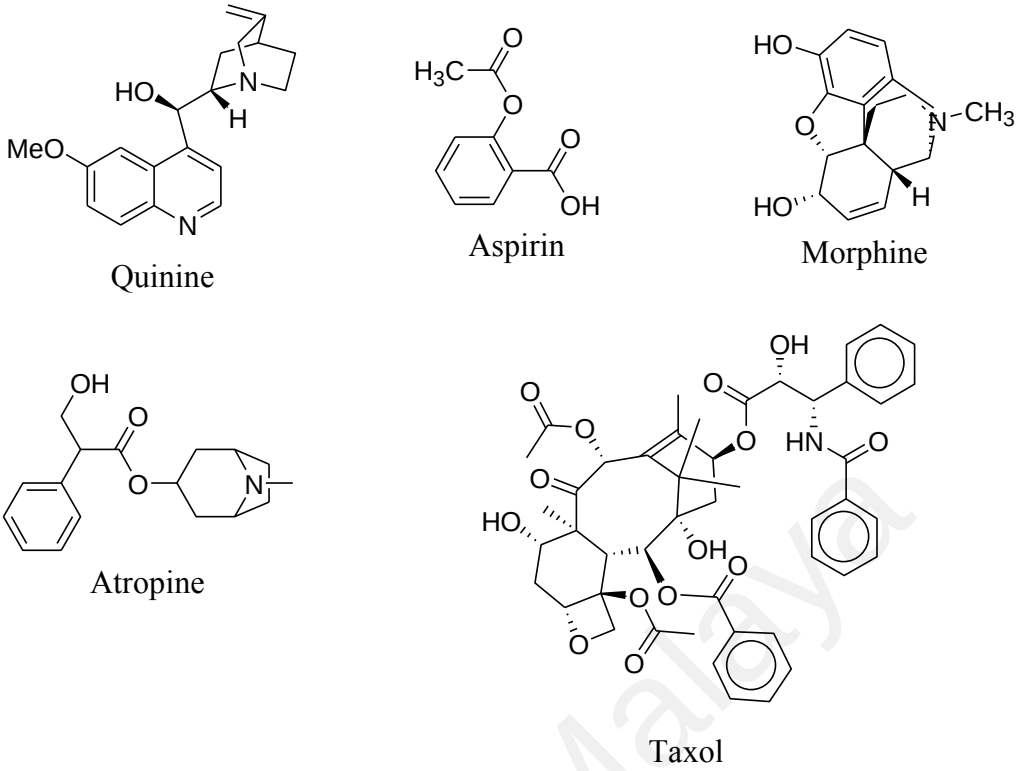

Figure 1.6: Natural products isolated from plants

The World Health Organization (WHO) Traditional Medicine Centers indicated that, of 122 compounds identified, 80% were used for the same or related ethnomedical purposes and were derived from only 94 plant species (Farnsworth *et al.,* 1985). Some relevant examples are khellin, from *Ammi visnaga* (L) Lamk., which led to the development of chromolyn (in the form of sodium chromoglycate) as a bronchodilator; galegine, from *Galega officinalis* L., which was the model for the synthesis of metformin and other bisguanidine-type antidiabetic drugs (Fabricant *et al.,* 2001); and papaverine from *Papaver somniferum* which formed the basis for verapamil used in the treatment of hypertension (Figure 1.7) (Fabricant *et al.,* 2001).

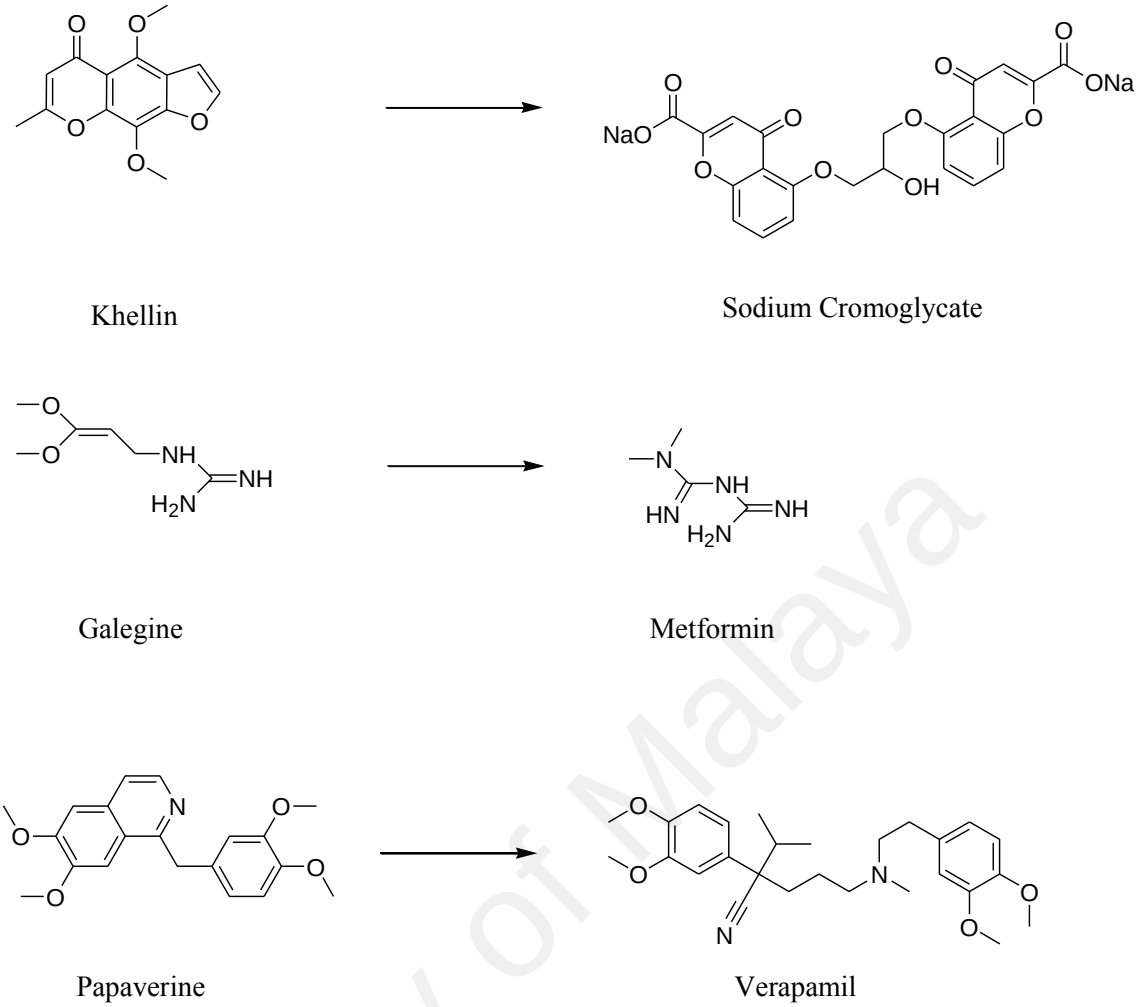

Figure 1.7: Drugs based on plant- derived pure compounds

Plants have a long history of use in the treatment of cancer (Hartwell, 1982). Of the plant-derived anticancer drugs in clinical use, some of the best known are the so-called vinblastine and vincristine (Figure 1.8). They are isolated from the Madagascar periwinkle, *Catharanthus roseus* (Gueritte *et al.,* 2005) together with the two clinically-active agents, etoposide and teniposide (Figure 1.8). Both etoposide and teniposide are semisynthetic derivatives of the natural product epipodophyllotoxin (Gueritte *et al.,* 2005; Lee *et al.,* 2012).

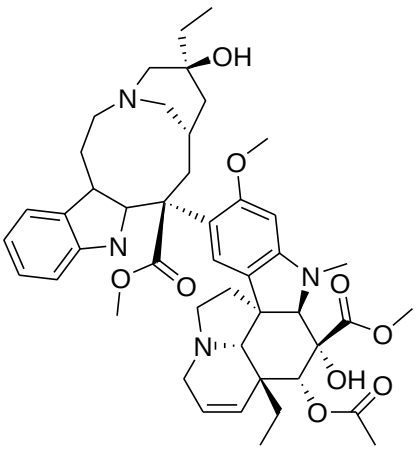

Vinblastine

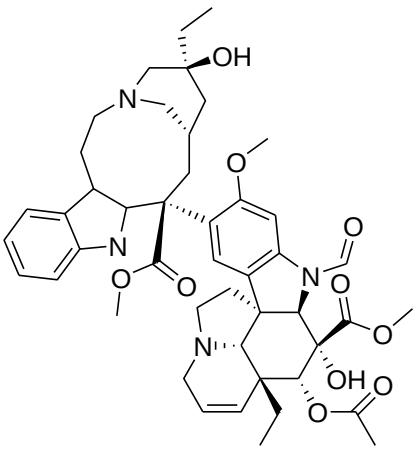

Vincristine

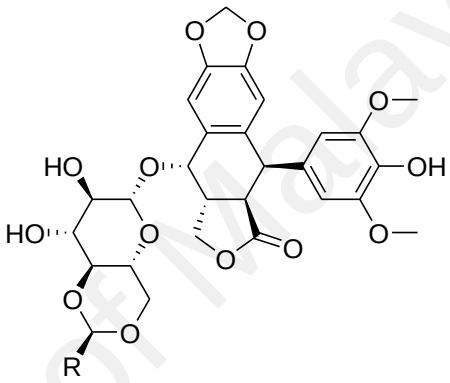

Etoposide, R = CH
Teniposide, R = a-thiazole

Figure 1.8: Plant-derived anticancer agents

1.3 Objectives

a) Photophysical properties of natural anthraquinones: The natural anthraquinones from *Morinda citrifolia* were subjected to spectroscopic analysis. The new spectroscopic information presented in this dissertation shall provide valuable information for synthetic chemists. This information will assist in designing synthetic anthraquinones with targeted properties for specific applications and serve as database for identification and characterization purposes for future studies.

b) Chemical constituents of *Boesenbergia stenophylla*: This work aimed at the study of the chemical constituents from Malayan plant species, *Boesenbergia*

stenophylla. This is the first study on *B. stenophylla* to the best of our knowledge. The objectives of this study were to isolate and characterize natural products from *Boesenbergia stenophylla* by using chromatographic and spectroscopic methods. The identified pure compounds for *Boesenbergia stenophylla* were subsequently subjected to antioxidant assays.

CHAPTER 2: LITERATURE REVIEW

2.1 Anthraquinone and photophysical properties

2.1.1 Introduction

Anthraquinones are group of functionally diverse aromatic compounds, structurally related to anthracene, with parent structure 9,10-dioxoanthracene. It has the appearance of yellow or light gray to gray-green solid crystalline powder. Its other names are 9,10-anthracene-9,10-quinone and 9,10-anthracinon, anthracene-9,10-quinone and 9,10-dihydro-9,10-dioxoanthracene (Dave & Ledwani, 2012).

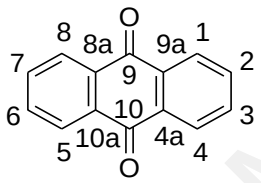

Figure 2.1: Anthraquinone structure

Anthraquinone derivatives form a most important group in the list of synthetic and natural colourants for several reasons. Anthraquinones are photosensitizers; they phototenderize cellulose materials, photosensitize the oxidation of a large number of substrates and have been suggested as photocatalysts for solar energy storage processes such as the photo-oxidation of chloride ion to chlorine and water splitting. The optical characteristics of the simpler derivatives change on chemical transformation and therefore they are widely used in analytical chemistry (Diaz, 1990).

Anthraquinone compounds, especially anthracyclines, have long been used as effective anticancer drugs. Depending on their chemical structure, anthraquinone drugs can kill tumor cells by diverse mechanisms, involving different initial intracellular targets that normally contribute to drug-induced toxicity. Anthraquinones are known as "multipotent antioxidants", as they are molecules that besides antioxidant activity possess

additional pharmacological activities such as inhibition of platelet-aggregation or display antineoplastic and anticancer activities (Zhang *et al.*, 2013).

Anthraquinones have long-standing interest for chemists both as plant and insect natural products and as important synthetic substance. The recent renaissance in anthraquinone synthesis is due, in large part, to the discovery of useful antitumor activity in the related more complex anthracycline antibiotics. Regiospecific, short, and efficient synthesis of the naturally occurring anthraquinones such as islandicin **(2a)**, digitopurpone **(2b)**, erythroglaucin **(2c)**, catenarin **(2d)**, cynodontin **(2e)**, and soranjidiol **(3)** have been achieved in 20-30% overall yields by using directed metalation of easily accessible methoxylated *N*,*N*-diethylbenzamides as the key step (De Silva *et al.*, 1979).

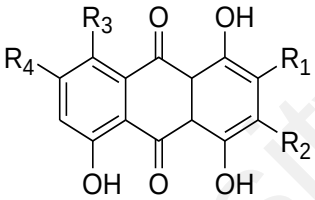

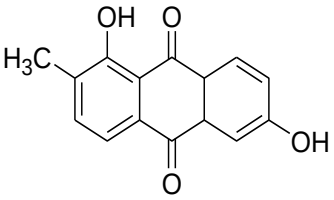

2 a, R^1 = Me; R^2 = R^3 = R^4 = H (islandicin) **(3)**

b, R^1 = R^3 = R^4 = H; R^2 = Me (digitopurpone)

c, R^1 = Me; R^2 = R^3 = H; R^4 = OMe (erythroglaucin)

d, R^1 = Me; R^2 = R^3 = H; R^4 = OH (catenarin)

e, R^1 = Me; R^2 = R^4 = H; R^3 = OH (cynodontin)

The majority of the anthraquinones which are assumed to be elaborated by the acetate-malonate pathway conform to the emodin **(4)** pattern and this is considered to arise by suitable folding and condensation of a polyketide chain derived from eight acetate units [as **5**]. Numerous variations of this basic structure exist resulting from *O*-

methylation, side-chain oxidation, chlorination, dimerization and the introduction or omission of nuclear hydroxyl groups (Thomson, 2012).

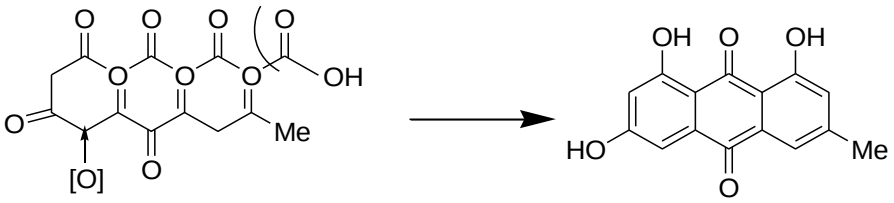

(5) **(4)**

Anthraquinones are distributed fairly widely in moluds, especially in *Aspergillus* and *Penicillium* spp; they are uncommon in higher fungi but are found more frequently in lichens. In higher plants they are located chiefly in heartwood, bark and roots (often as glycosides), occasionally in stems, seeds and fruits. The Rubiaceae accounts for half the total number (Thomson, 2012).

Anthraquinone itself has been obtained from several natural sources but was probably an artefact in all cases. It was isolated from the essential oil tobacco leaf by chromatography of a fraction and has also been detected in tannin extracts although it does not appear to be present as such in the original wood and bark. Anthraquinone was also found at a burning coal seam on Mount Pyramide by a Norwegian expedition in 1921. This mineral, hoelite,"crystallises in fine yellow needles, sitting directly on the coal, partly covered by a crust of sal-ammoniac'', and was presumably formed by oxidation of anthracene (Thomson, 2012).

Another natural sources study of anthraquinone is on *Mangifera indica* leaves extract where it is revealed the presence anthraquinone in the ethyl acetate extracts using the Borntrager's test for screening but absent in the hexane and methanol extracts (Aiyelaagbe & Osamudiamen, 2009).

2-Hydroxyanthraquinone is the simplest quinone found in chay root, or Indian madder (*O. umbellate),* and in *Galium* spp. Chay root was formerly cultivated in India for use in dyeing, and both *Galium* spp. (bedstraws) and *A. odorata* (woodruff) have been used for the same purpose. 2-Hydroxyanthraquinone is easily recognised from spectral data and colour reactions. It is best prepared from 2-aminoanthraquinone by way of the diazonium salt (Thomson, 2012).

2-acetyl-3,8-dihdroxy-6-methoxy anthraquinone or 3-acetyl-2,8-dihydroxy-6-methoxy anthraquinone **(6)** and 2-(1-hydroxyethyl)-3,8-dihdroxy-6-methoxy anthraquinone or 3-(1-hydroxyethyl)-2,8-dihydroxy-6-methoxy anthraquinone) **(7)** were produced by liquid cultures of *Fusarium oxysporum*, isolated from the roots of citrus trees affected with root rot disease. These anthraquinone compounds can be used for dyeing wool with good fastness properties and high dye uptake (Nagia & El-Mohamedy, 2007).

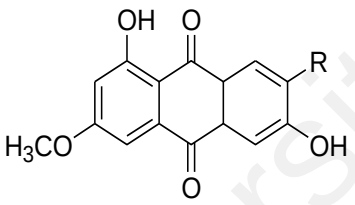

(6)

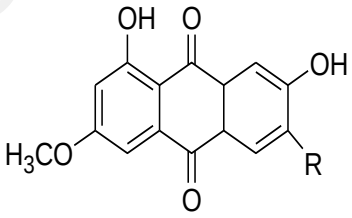

(7)

R: - $COCH_3$ **(6)**
R:-$CH(OH)CH_3$**(7)**

2.1.2 Absorption and emission properties

Anthraquinone has been combined with photosensitizers for clinical purpose, where anthraquinone is photoactive. The photoinduced intramolecular electron transfer in the porphyrin-anthraquinone dyads could accelerate the breaking up of chemical bond making these porphyrin-anthraquinone dyads used as novel anticancer drug (Tao *et al.*, 2007).

The photo and radiation chemical behaviour of quinone compounds are extremely important for understanding the effect of radiation on biological material containing quinonoid compounds. The photophysical properties of some chloro-anthraquinones and semiquinones have been previously investigated in aqueous-isopropanol-acetone mixed solvent using electron pulse radiolysis technique. The substitution of chlorine at 1, 1 and 5,1 and 8 position of the anthraquinone ring generates semiquinone free radicals. An analysis of the characteristics of the semiquinones shows that C-chloro substituents adjacent to the C-O group act as electron withdrawing groups (Rath *et al.*, 1996).

Furthermore, the photophysical properties of 1-*N*-methylamino-9,10-anthraquinone (1MAAQ) **(8)** and 1-*N*,*N*-dimethylamino-9,10-anthraquinone (1-DMAAQ) **(9)** dyes have been investigated in different solvents and solvents mixture. It is seen the relative strengths of the intramolecular hydrogen bonds present in 1-MAAQ which is also substantiated by observed deuterium isotope effect on the fluorescence decay of 1-MAAQ dye. Unlike 1-MAAQ, the 1-DMAAQ dye is seen to be unusually weak in its fluorescence (Dahiya *et al.,* 2007).

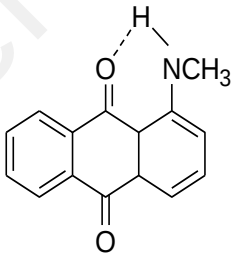

(8)

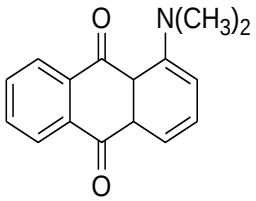

(9)

A class of anthraquinone based dyes is interesting to theoretical study as photosensitizer for dye-sensitized solar cells. It is very important to improve the performance of dye-sensitized solar cells. Based on the geometry analysis, electronic structures and spectrum properties of anthraquinone **10**, increasing the distance between

electron donor group and semiconductor surface will resulted in the reduction of electron injection rate and hence lowering the conversion efficiency (Ranjitha *et al.,* 2014).

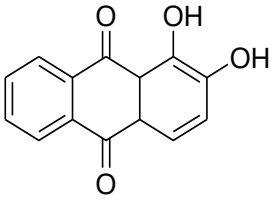

(10)

The electronic absorption spectra of anthraquinone derivatives has also been studied. The $\pi - \pi^*$ electronic absorption spectra of 1-amino- **(11)**, 1,4-diamino- **(12)**, and 1,4,5,8-tetraaminoanthraquinones **(13)** were investigated by means of the polarized absorption spectra using PVA sheets and theoretical calculations where these compounds which appear in the visible region can be assigned to the intramolecular charge-transfer transitions associated with the charge migration from the amino group to the carbonyl groups (Inoue *et al.,* 1972). The aminoanthraquinone derivatives also has been studied using picosecond fluorescence lifetimes and fluorescence quantum yields in benzene, acetonitrile, and ethanol. This paper suggests that the radiationless deactivations from charge transfer of quinones in ethanol are mainly induced through vibrational modes of the intra- and intermolecular hydrogen bonds (Inoue *et al.,* 1982).

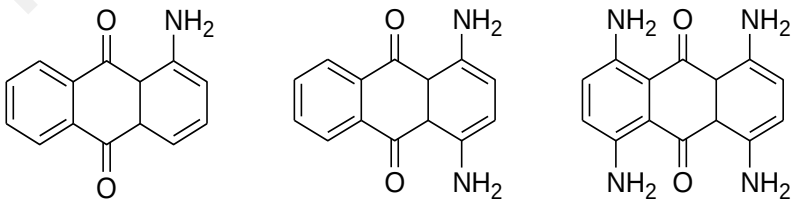

(11) **(12)** **(13)**

While, the absorption spectra of novel dye/amphiphile systems, in which the dye is a 1,5-bis-(*R*-phenylamino) anthraquinone **(14)** [R = OMe, OEt, H] and the solvents are

either organic or H_2O/organic solvent mixtures, have been investigated. It was found that an abrupt λ_{max} shift of more than 80 nm occurred for the system containing dye having R = OMe and the amphiphile (poly-bis-(2,2'-dimethyl-5,5'-disulphonate)naphthylmethane disodium salt) in pure solvents (He *et al.,* 2011).

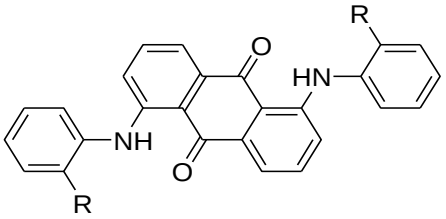

(14)

Calculations of anthraquinones electronic transition energies and oscillator strengths are carried out using the Zerner's Intermediates Neglect of Differential Overlap/Spectroscopy (ZINDO/S) semiempirical method for study on electronic absorption spectra of anthraquinone. This method has been successfully tested for the calculations of the ground and excited state properties for a wide range of organic compounds. On the basis of these calculations, the assignment of the spectra are successfully made (Khan & Khan, 2003; Marković *et al.*, 2008).

2.2 Chemical constituents of *Boesenbergia stenophylla*

2.2.1 General

Boesenbergia stenophylla R. M. Sm. belongs to the genus *Boesenbergia* and family *Zingiberacea* (Sons, 1987). In Malaysia, *B.stenophylla* is locally known as *Jerangau Merah,* Kaburo Apad (Lundayeh), or Komburuongoh Sarawak (Kulip, 2007). *B.stenophylla* is praised for its ethno-botanical importance among the various ethnic groups (Ahmad & Jantan, 2003).

The rhizome of *B. stenophylla* is used as an antidote in case of poisonings and stomach disorders, and help to cure hangovers (Kulip, 2007). Its decoction is believed to increase the libido, protect against convulsions and prevent intoxication. It is also commonly used for the preparation of tonics. A mixture of crushed rhizomes of *B. stenophylla* and *Zingiber cassumunar* is used as a poultice or lotion for rheumatic pains. The decoction of *B. stenophylla* rhizomes is also used as an antiseptic wash, and for treating to dissolve kidney stones (Ahmad & Jantan, 2003).

B. stenophylla is differentiate by the narrowly lanceolate long petioles leaves, which are rather unequal at the base, and by the prominent anther-crest and porous dehiscence (Sons, 1987). *B. stenophylla* is a perennial rhizomatous herb that can be found in the kerangas and mixed dipterocarp forest floor of highland areas of Sarawak, Malaysia, especially Bario. It usually inhabits sandy loam soil which is high in moisture content. It grows in patches but luxuriant growth can be observed under a loose forest canopy (Ahmad & Jantan, 2003).

2.2.2 Usage and compounds isolated from *Boesenbergia sp.*

Boesenbergia sp. belongs to a ginger family, *Zingiberaceae* in the order of *Zingiberales*. The *Boesenbergia* genus is synonym with *Kaempferia* genus (Sri, 2014). The *Boesenbergia* genus have 80 species distributed from India to South East Asia, in which 25 species were found in Thailand (Larsen, 2010). The *Boesenbergia sp.* also comprises about 30 species distributed from India to New Guinea (Wohlmuth, 2008). There are no native or naturalised members of this genus in Australia.

From the previous studies, the rhizome part of *Boesenbergia sp*. displayed health-benefits properties. Finger root (*Boesenbergia rotunda* (L.) Mansf. (syn. *Boesenbergia pandurata* Schltr., *Kaempferia pandurata* Roxb., *Gastrochilus panduratus* (Roxb.) Ridl.) is used as a culinary and medicinal herb in Southeast Asia. Fresh rhizomes are slightly

pungent and have a characteristic aroma. They are used for the treatment of colic, fungal infections, dry cough, rheumatism and muscular pains, and for their reputed aphrodisiac properties (Jantan *et al.*, 2001; Murakami *et al.*, 1993; Trakoontivakorn *et al.*, 2001).

In Indonesia, *B. rotunda* is typically used to prepare "jamu," a popular traditional tonic for women after childbirth as well as a beauty aid for teenage girls and to prevent leucorrhea (Eng-Chong *et al.*, 2012). In the primary health care project of Thailand, it is stated that the rhizome of this plant also used for the treatment of dyspepsia. From its biological activities, *B. rotunda* exhibited antibacterial, antifungal, anti-inflammatory, analgesic, antipyretic, antispasmodic, antitumor and insecticidal activities (Kirana *et al.*, 2007; Madaka *et al.*, 2013). The rhizomes of *B. rotunda* are commonly used as a culinary spice in Thailand and for the treatment of oral diseases, stomach discomfort, stomach pain, leucorrhoea, diuretic, dysentery, and inflammation (Hasnah *et al.*, 1995; Mahady, 2005). The methanolic extract of fresh *B. rotunda* rhizomes showed strong inhibition of tumour promoter-induced Epstein-Barr virus activation (Madaka *et al.*, 2013). The compounds from *B. rotunda* demonstrated antifeedant activities against larvae of *Spodoptera littoralis*, the Egyptian cotton leafworm (Stevenson *et al.*, 2007). Lotulung *et al.,* (2008) suggest that the antioxidant potential of the plant has been evaluated and flavonoids and phenolic derivatives found in the plant, which demonstrated inhibitory potential against lipid peroxidation, suggesting that the plant can be useful in diseases like myocardial infraction, diabetes mellitus, hepatic injury, atherosclerosis, rheumatoid arthritis, and cancer (Lotulung *et al.*, 2008; Prasad *et al.*, 2010).

Previous investigations of the chemical constituents of *B. pandurata* reported the anti-HIV, antibacterial, anti-inflammatory, analgesic, antipyretic, antitumor, antioxidant, and insecticidal activities (Eng-Chong *et al.*, 2012; Jantan *et al.*, 2001; Sri, 2014; Tewtrakul *et al.,* 2003). Compounds isolated from *B. pandurata* showed cytotoxic against

pancreatic PANC-1 cancer cell under nutrient deprived condition (Ling *et al.,* 2010; Win *et al.*, 2008). The fresh rhizomes have a characteristic aroma and are used as a flavoring agent in Thai cuisine. It also has been commonly used as self-medication by AIDS patients in southern Thailand (Eng-Chong *et al.*, 2012).

Ethanol extract *of B*. *thorelii* exert anti-allergic activity and may support the use for treatment of allergy and allergy-related diseases (Madaka *et al.*, 2013). The rhizomes of *Boesenbergia longiflora* have been traditionally used for the several treatment included inflammatory bowel disease, ulcerative colitis, aphthous ulcer and abscess by decoction with alcohol. The ethanolic extract of *B. longiflora* possesses a potent anti-inflammatory and wound healing activities (Sudsai *et al.*, 2013).

Chemical constituents that have been reported for the *Kaempferia marginata* have been evaluated using a panel of bioassays including anti-malarial, anti-tuberculous and antifungal activity (Thongnest *et al.*, 2005). *Kaempferia angustifolia*, which is locally known in Thai as *Thao Nhang Haeng*, has been used to treat abdominal illness, including dysentery and diarrhea. Cytotoxic screening indicated that most of the pure compounds tested showed significant activity showing the most potent activity against HL-60 (human promyelocytic leukemia) and MCF-7 (human breast cancer) cell lines (Madaka *et al.*, 2013; Woerdenbag *et al.*, 2004).

The *Kaempferia galanga* is a native of India, China, Taiwan, Cambodia, and other areas of southeast Asia. Since the rhizomes of this plant contain volatile oil and other important compounds of enormous medicinal values, they are very demanding to the traditional health care practitioner. The rhizome is rich in essential oils and is being used for the treatment of indigestion, cold, pectorial and abdominal pains, headache, expectorant, diuretic, carminative, stomachic, coughs, pectoral affections, asthma and hypertension. The rhizome and edible fresh leaves represent a potential food values

(Singh *et al.*, 2013). The rhizomes are stimulatory, expectorant, carminative, and diuretic. The methanol extract of the rhizome which is highly cytotoxic to *Hela* cells. Crude extracts of the rhizome of *K. galanga* with petroleum ether, acetone and methanol are screened for anti-microbial activities against two gram-positive and three gram-negative pathogenic bacteria *i.e. Bacillus sp., Pseudomonas sp., Escherichia coli, Salmonella sp.* and *Shigella sonnei.* The aqueous extracts of *K. galanga* leaves show significant anti-nociceptive and anti-inflammatory effect in rats (Singh *et al.*, 2013).

Kaempferia parviflora (Thai Ginseng) is an herb that has some historical and medicinal usage for treating metabolic ailments and improving vitality in Thailand and limited to surrounding regions. It is also reported to be an aphrodisiac compound and physical enhancer. Leaves are green with a reddish underside. It has been used as a medicinal plant in Asia (Leardkamolkarn *et al.*, 2009). They found polyphenolic flavonoids which have a wide range of biological activities, such as anti-inflammatory, anti-bacterial, anti-mutagenic, anti-oxidant, and anti-thrombotic. The compounds showed anti-bacterial and anti-fungal activities (Tewtrakul *et al.,* 2009). Hossain *et al.* (2012) reported several studies covered anti-proliferative and cytotoxic effects of the rhizome extracts of *K. parviflora*. The present study was evaluated the compound cytotoxicity on human colorectal carcinoma (HCT-15) cells.

Figure 2.2 lists the compounds isolated from the *Boesenbergia* genus and Table 2.1 shows the structures of compounds previously isolated from *Boesenbergia* genus.

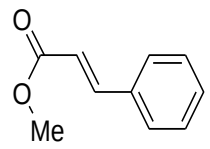

(15)

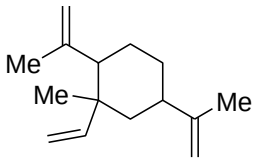

(16)

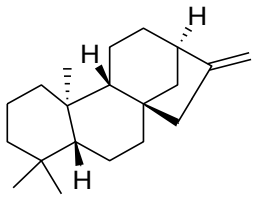

(17)

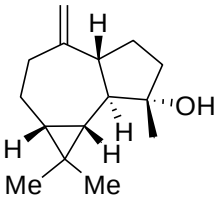

(18)

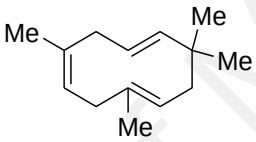

(19)

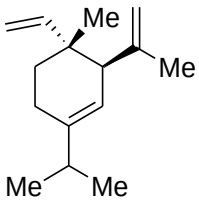

(20)

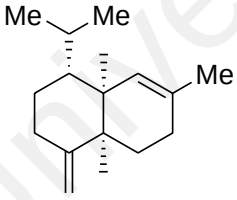

(21)

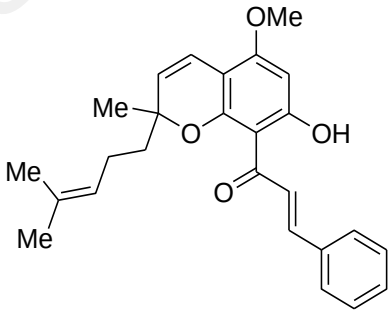

(22)

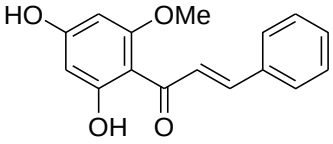

(23)

Figure 2.2: Structures of compounds isolated from the *Boesenbergia* genus

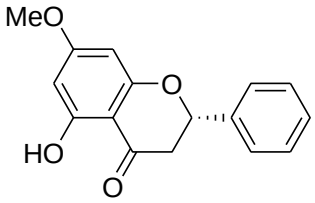

(24)

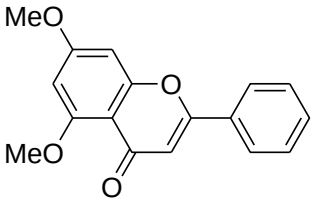

(25)

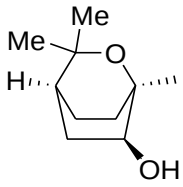

(26)

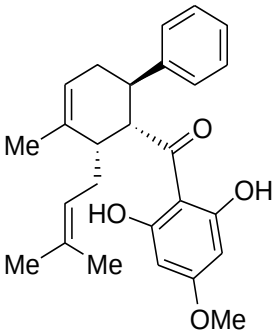

(27)

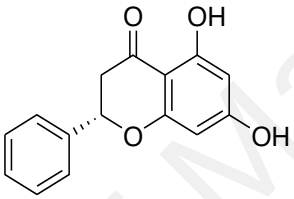

(28)

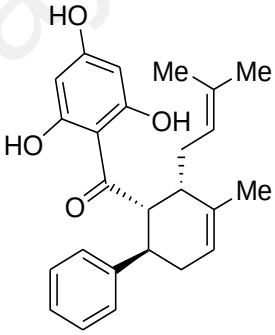

(29)

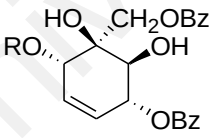

R = Ac

(30)

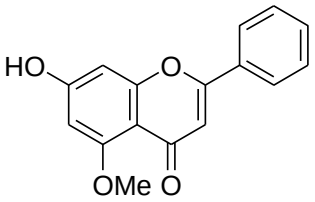

(31)

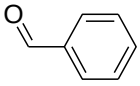

(32)

Figure 2.2, continued

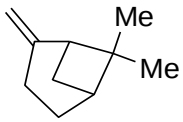

(33)

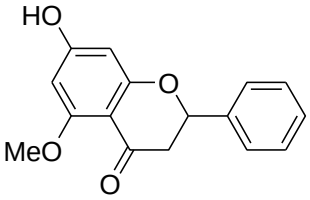

(34)

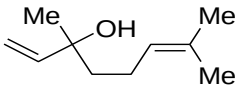

(35)

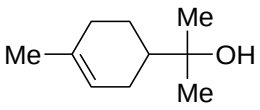

(36)

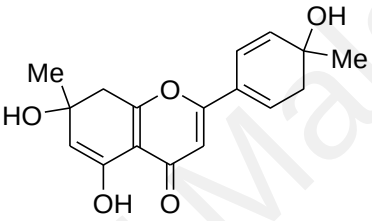

(37)

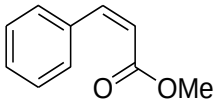

(38)

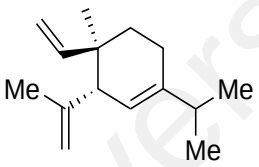

(39)

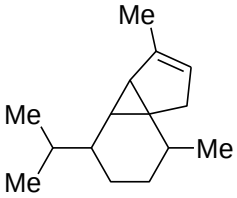

(40)

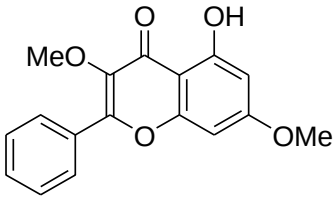

(41)

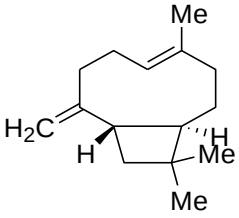

(42)

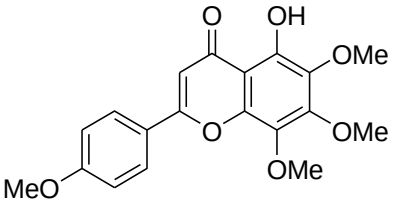

(43)

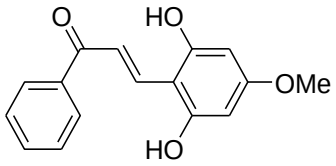

(44)

Figure 2.2, continued

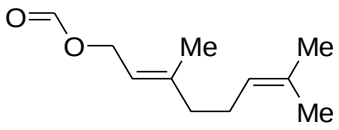

(45)

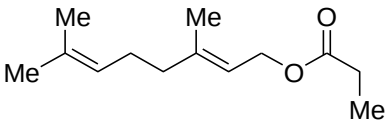

(46)

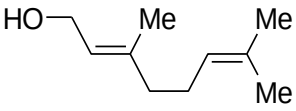

(47)

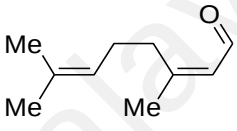

(48)

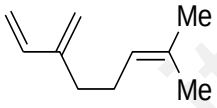

(49)

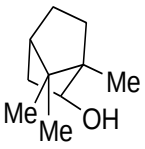

(50)

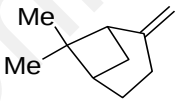

(51)

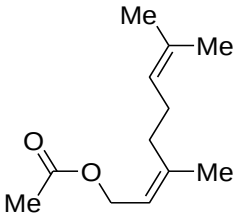

(52)

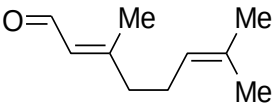

(53)

Figure 2.2, continued

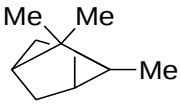

(54)

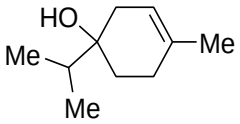

(55)

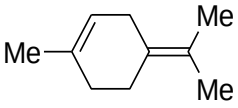

(56)

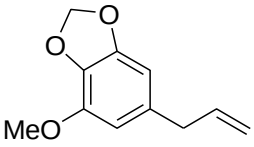

(57)

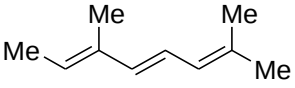

(58)

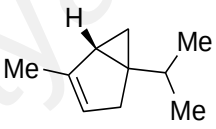

(59)

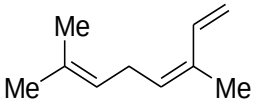

(60)

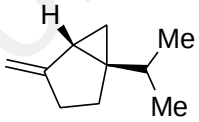

(61)

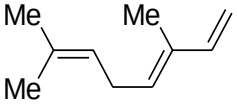

(62)

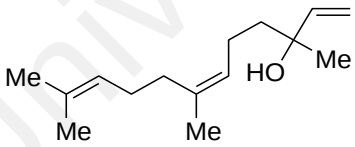

(63)

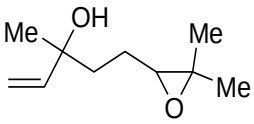

(64)

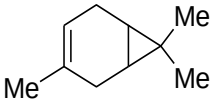

(65)

Figure 2.2, continued

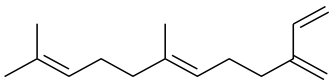

(66)

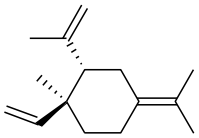

(67)

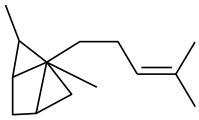

(68)

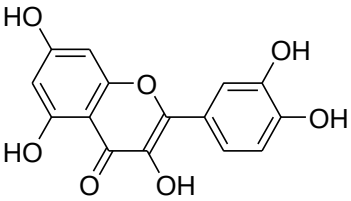

(69)

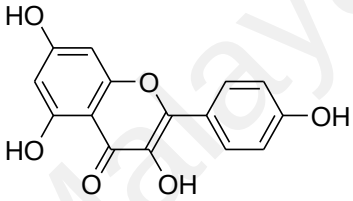

(70)

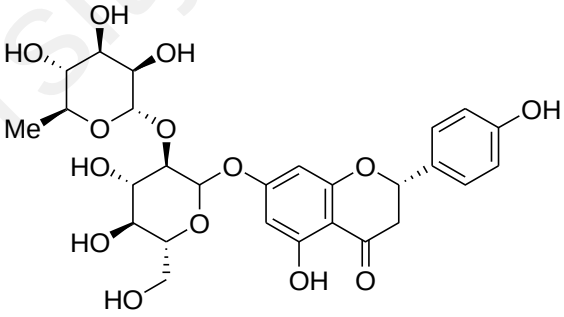

(71)

Figure 2.2, continued

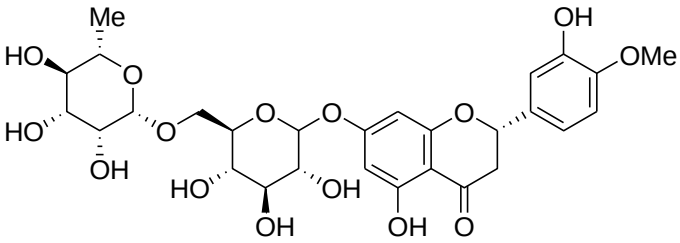

(72)

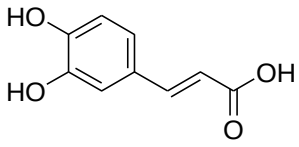

(73)

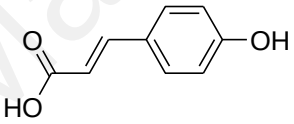

(74)

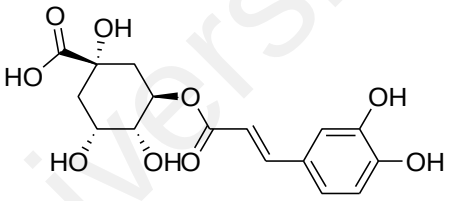

(75)

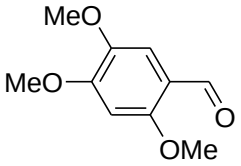

(76)

Figure 2.2, continued

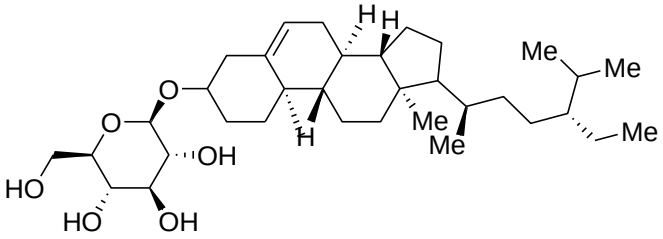

(77)

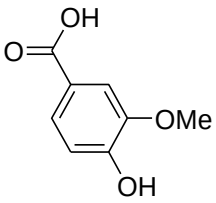

(78)

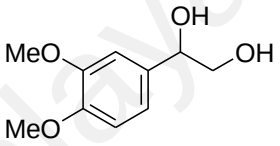

(79)

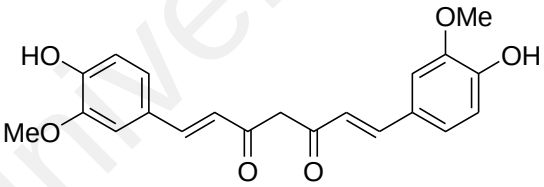

(80)

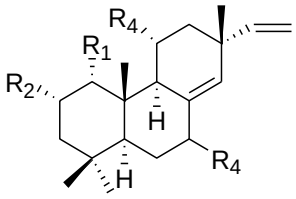

(81) $R_1 = R_2 = OH$, $R_3 = \beta$-OH, $R_4 = H$

(82) $R_1 = R_2 = R_4 = OH$, $R_3 = H$

(83) $R_1 = R_4 = OH$, $R_3 = \alpha$-OH, $R_2 = H$

(84) $R_1 = R_2 = OH$, $R_2 = R_3 = H$

(85) $R_1 = R_2 = OH$, $R_3 = O$, $R_4 = H$

Figure 2.2, continued

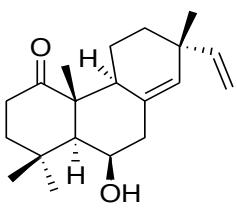

(86)

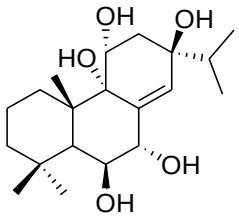

(87)

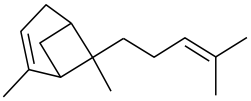

(88)

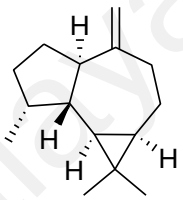

(89)

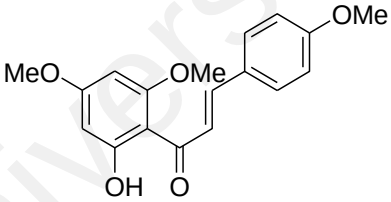

(90)

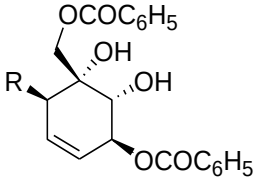

(91) R = OH

(92) R = OMe

Figure 2.2, continued

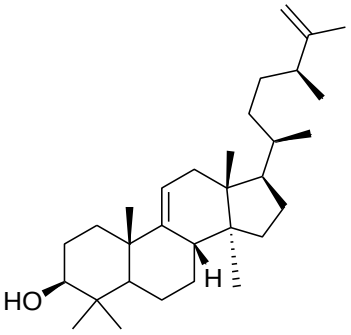

(93)

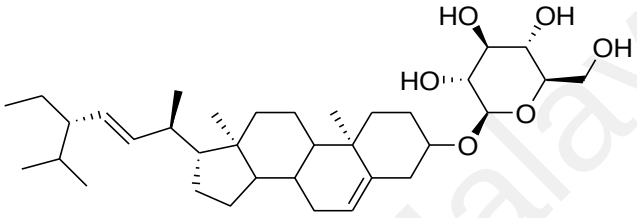

(94)

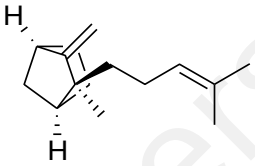

(95)

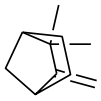

(96)

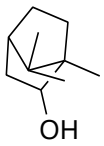

(97)

Figure 2.2, continued

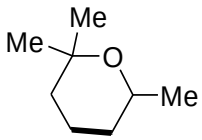

(98)

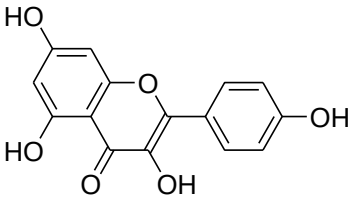

(99)

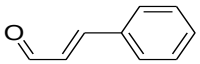

(100)

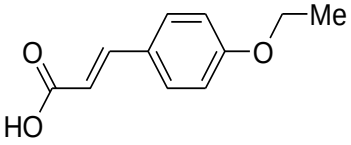

(101)

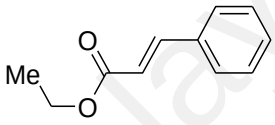

(102)

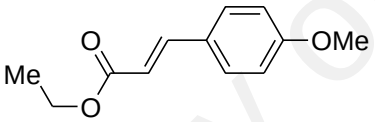

(103)

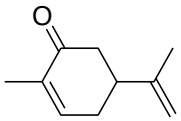

(104)

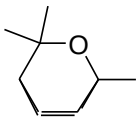

(105)

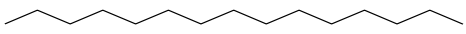

(106)

Figure 2.2, continued

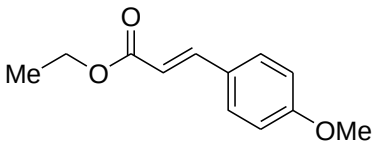

(107)

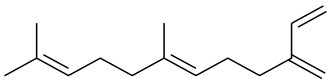

(108)

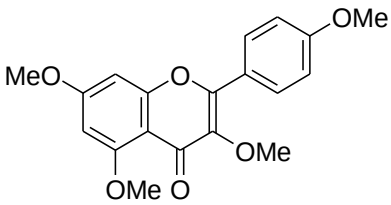

(109)

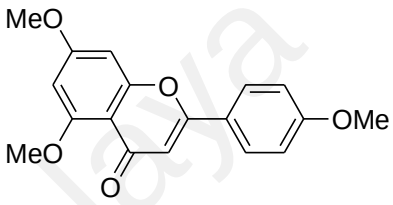

(110)

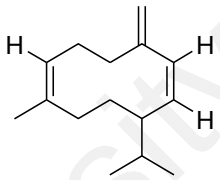

(111)

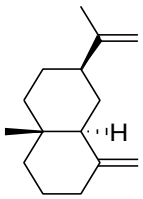

(112)

Figure 2.2, continued

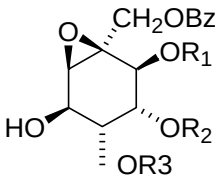

(113) $R_1 = R_3 = H_1$, $R_2 = Bz$

(114) $R_1 = R_2 = H_1$, $R_3 = Bz$

(115) $R_1 = Ac$, $R_2 = Bz$, $R_3 = H_1$

(116) $R_1 = Ac$, $R_2 = H$, $R_3 = Bz$

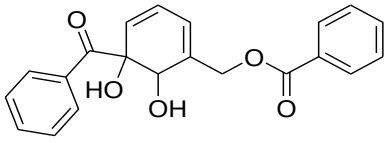

(117)

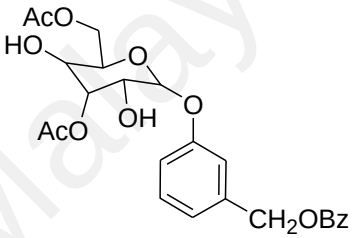

(118)

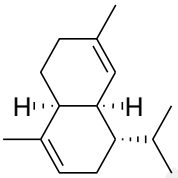

(119)

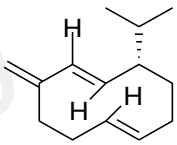

(120)

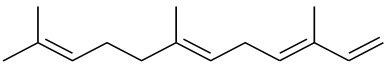

(121)

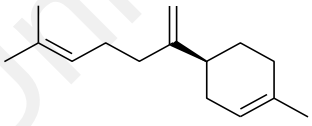

(122)

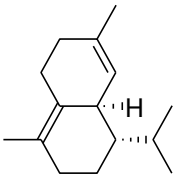

(123)

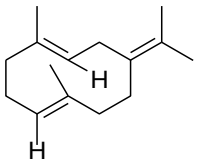

(124)

Figure 2.2, continued

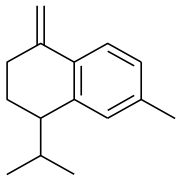

(125)

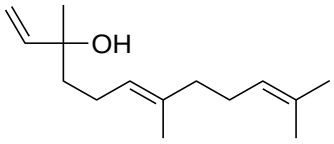

(126)

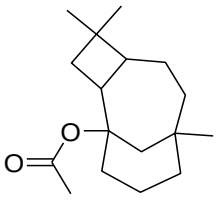

(127)

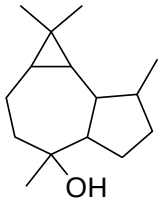

(128)

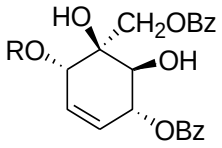

(129) R = Ac

(130) R = H

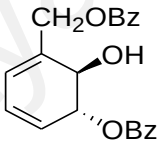

(131)

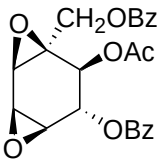

(132)

Figure 2.2, continued

Table 2.1: Compounds isolated from the *Boesenbergia* genus

Compound Number	Compound name	Sources and part	Country	Reference
(15)	Methyl (*E*)-cinnamate	*B. stenophylla,* rhizome and leaf	Malaysia	(Ahmad & Jantan, 2003)
(16)	*β*-elemene	*B. stenophylla, B. pandurata,* rhizome and leaf	Malaysia, Indonesia, Thailand	(Ahmad & Jantan, 2003; Jantan *et al.,* 2001)
(17)	Kaur-16-ene	*B. stenophylla,* rhizome and leaf	Malaysia	(Ahmad & Jantan, 2003)
(18)	Spathulenol	*B. stenophylla,* rhizome and leaf	Malaysia	(Ahmad & Jantan, 2003)
(19)	*α*-humulene	*B. stenophylla,* rhizome and leaf	Malaysia	(Ahmad & Jantan, 2003)
(20)	*α*-elemene	*B. stenophylla,* rhizome and leaf	Malaysia	(Ahmad & Jantan, 2003)
(21)	*γ*-muurolene	*B. stenophylla,* rhizome and leaf	Malaysia	(Ahmad & Jantan, 2003)
(22)	Boesenbergin	*B. pandurata,* rhizome	Indonesia	(Kirana *et al.,* 2007)
(23)	Cardamonin	*B. pandurata, B. thorelli,* rhizome	Indonesia, Thailand	(Kirana *et al.,* 2007; Madaka *et al.,* 2013)

Table 2.1, continued

Compound Number	Compound name	Sources and part	Country	Reference
(24)	Pinostrobin	*Kaempferia parviflora, B. pandurata, B. thorelli,* rhizome	Indonesia, Thailand	(Hossain *et al*., 2012; Kirana *et al*., 2007; Madaka *et al*., 2013)
(25)	5,7-dimethoxyflavone	*Kaempferia parviflora, B. pandurata,* rhizome	Indonesia	(Hossain *et al*., 2012; Kirana *et al*., 2007)
(26)	1,8-cineole	*B. pandurata,* rhizome	Indonesia	(Kirana *et al*., 2007)
(27)	Panduratin	*B. pandurata,* rhizome	Indonesia	(Kirana *et al*., 2007)
(28)	Pinocembrin	*B. rotunda, B. thorelli,* rhizome	Thailand, Malaysia, Indonesia	(Eng-Chong *et al*., 2012; Madaka *et al*., 2013)
(29)	Hydroxypanduratin	*B. thorelli,* rhizome	Thailand	(Madaka *et al*., 2013)
(30)	(-)-6-acetylzeylenol	*Kaempferia rotunda L,* rhizome	London	(Stevenson *et al*., 2007)
(31)	5-methoxy-7-hydroxy-flavone	*B. rotunda,* rhizome	Thailand, Malaysia, Indonesia	(Eng-Chong *et al*., 2012)
(32)	Benzaldehyde	*B. stenophylla,* rhizome and leaf	Malaysia	(Ahmad & Jantan, 2003)

Table 2.1, continued

Compound Number	Compound name	Sources and part	Country	Reference
(33)	B-pinene	*B. stenophylla,* rhizome and leaf	Malaysia	(Ahmad & Jantan, 2003)
(34)	Alpinetin	*B. pandurata,* rhizome and leaf	Thailand	(Tewtrakul *et al*., 2003)
(35)	Linalool	*B. stenophylla,* rhizome and leaf	Malaysia	(Ahmad & Jantan, 2003)
(36)	α- terpineol	*B. stenophylla,* rhizome and leaf	Malaysia	(Ahmad & Jantan, 2003)
(37)	4'7-dimethyl-apigenin	*B. rotunda,* rhizome	Thailand, Malaysia, Indonesia	(Eng-Chong *et al*., 2012)
(38)	Methyl (Z) - cinnamate	*B. stenophylla,* rhizome and leaf	Malaysia	(Ahmad & Jantan, 2003)
(39)	δ-elemene	*B. stenophylla,* rhizome and leaf	Malaysia	(Ahmad & Jantan, 2003)
(40)	α-cubebene	*B. stenophylla,* rhizome and leaf	Malaysia	(Ahmad & Jantan, 2003)
(41)	5-Hydroxy-3,7- dimethoxyflavone	*B. rotunda,* rhizome	Thailand, Malaysia, Indonesia	(Eng-Chong *et al*., 2012)
(42)	β-caryophyllene	*B. stenophylla,* rhizome and leaf	Malaysia	(Ahmad & Jantan, 2003)

Table 2.1, continued

Compound Number	Compound name	Sources and part	Country	Reference
(43)	3,5,7-trimethoxy-flavone 5-hydroxy-3,7,3,4- tetramethoxy-flavone	*B. rotunda,* rhizome	Thailand, Malaysia, Indonesia	(Eng-Chong *et al*., 2012)
(44)	2,6-di-hydroxy-4-methoxychalcone	*B. rotunda,* rhizome	Thailand, Malaysia, Indonesia	(Eng-Chong *et al*., 2012)
(45)	Geranyl formate	*B. pandurata,* rhizome and leaf	Malaysia, Indonesia, Thailand	(Jantan *et al*., 2001)
(46)	Geranyl propionate	*B. pandurata,* rhizome and leaf	Malaysia, Indonesia, Thailand	(Jantan *et al*., 2001)
(47)	Geraniol	*B. pandurata,* rhizome and leaf	Malaysia, Indonesia, Thailand	(Jantan *et al*., 2001)
(48)	Neral	*B. pandurata,* rhizome and leaf	Malaysia, Indonesia, Thailand	(Jantan *et al*., 2001)
(49)	Myrcene	*B. pandurata,* rhizome and leaf	Malaysia, Indonesia, Thailand	(Jantan *et al*., 2001)
(50)	Isoborneol	*B. pandurata,* rhizome and leaf	Malaysia, Indonesia, Thailand	(Jantan *et al*., 2001)
(51)	β-pinene	*B. pandurata,* rhizome and leaf	Malaysia, Indonesia, Thailand	(Jantan *et al*., 2001)
(52)	Neryl acetate	*B. pandurata,* rhizome and leaf	Malaysia, Indonesia, Thailand	(Jantan *et al*., 2001)

Table 2.1, continued

Compound Number	Compound name	Sources and part	Country	Reference
(53)	Geranial	*B. pandurata,* rhizome and leaf	Malaysia, Indonesia, Thailand	(Jantan *et al.,* 2001)
(54)	Tricyclene	*B. pandurata,* rhizome and leaf	Malaysia, Indonesia, Thailand	(Jantan *et al.,* 2001)
(55)	Terpinen-4-ol	*B. pandurata,* rhizome and leaf	Malaysia, Indonesia, Thailand	(Jantan *et al.,* 2001)
(56)	Terpinolene	*B. pandurata,* rhizome and leaf	Malaysia, Indonesia, Thailand	(Jantan *et al.,* 2001)
(57)	Myristicin	*B. pandurata,* rhizome and leaf	Malaysia, Indonesia, Thailand	(Jantan *et al.,* 2001)
(58)	Allo ocimene	*B. pandurata,* rhizome and leaf	Malaysia, Indonesia, Thailand	(Jantan *et al.,* 2001)
(59)	α-thujene	*B. pandurata,* rhizome and leaf	Malaysia, Indonesia, Thailand	(Jantan *et al.,* 2001)
(60)	(*Z*)-β-ocimene	*B. pandurata,* rhizome and leaf	Malaysia, Indonesia, Thailand	(Jantan *et al.,* 2001)
(61)	Sabinene	*B. pandurata,* rhizome and leaf	Malaysia, Indonesia, Thailand	(Jantan *et al.,* 2001)
(62)	(*E*)-β-ocimene	*B. pandurata,* rhizome and leaf	Malaysia, Indonesia, Thailand	(Jantan *et al.,* 2001)

Table 2.1, continued

Compound Number	Compound name	Sources and part	Country	Reference
(63)	(*Z*)-nerolidol	*B. pandurata,* rhizome and leaf	Malaysia, Indonesia, Thailand	(Jantan *et al.,* 2001)
(64)	*Cis*-linalool oxide	*B. pandurata,* rhizome and leaf	Malaysia, Indonesia, Thailand	(Jantan *et al.,* 2001)
(65)	3-carene	*B. pandurata,* rhizome and leaf	Malaysia, Indonesia, Thailand	(Jantan *et al.,* 2001)
(66)	(*Z*)-*β*-farnesene	*B. pandurata,* rhizome and leaf	Malaysia, Indonesia, Thailand	(Jantan *et al.,* 2001)
(67)	*γ*-elemene	*B. pandurata,* rhizome and leaf	Malaysia, Indonesia, Thailand	(Jantan *et al.,* 2001)
(68)	*α*- santalene	*B. stenophylla,* rhizome and leaf	Malaysia	(Ahmad & Jantan, 2003)
(69)	Quercetin	*B. rotunda, B. pulchella* var attenuata*, B. armeniaca,* rhizome, leaf and stems	Malaysia	(Ling *et al.,* 2010)
(70)	Kaempferol	*B. rotunda, B. pulchella* var attenuata*, B. armeniaca,* rhizome, leaf and stems	Malaysia	(Ling *et al.,* 2010)

Table 2.1, continued

Compound Number	Compound name	Sources and part	Country	Reference
(71)	Naringin	*B. rotunda, B. pulchella* var attenuata*, B. armeniaca,* rhizome, leaf and stems	Malaysia	(Ling *et al.,* 2010)
(72)	Hesperidin	*B. rotunda, B. pulchella* var attenuata*, B. armeniaca,* rhizome, leaf and stems	Malaysia	(Ling *et al.,* 2010)
(73)	Caffeic acid	*B. rotunda, B. pulchella* var attenuata*, B. armeniaca,* rhizome, leaf and stems	Malaysia	(Ling *et al.,* 2010)
(74)	*p*-coumaric acid	*B. rotunda, B. pulchella* var attenuata*, B. armeniaca,* rhizome, leaf and stems	Malaysia	(Ling *et al.,* 2010)
(75)	Chlorogenic acid	*B. rotunda, B. pulchella* var attenuata*, B. armeniaca,* rhizome, leaf and stems	Malaysia	(Ling *et al.,* 2010)

Table 2.1, continued

Compound Number	Compound name	Sources and part	Country	Reference
(76)	Asaronaldehyde	*B. thorelli,* rhizome	Thailand	(Madaka *et al.,* 2013)
(77)	*β*-sitosterol-*D*-glucoside	*B. thorelli,* rhizome	Thailand	(Madaka *et al.,* 2013)
(78)	Protocatechuic acid methyl ester	*B. thorelli,* rhizome	Thailand	(Madaka *et al.,* 2013)
(79)	2-hydroxy-1-(3, 4-dimethoxyphenyl) ethanols	*B. thorelli,* rhizome	Thailand	(Madaka *et al.,* 2013)
(80)	Diarylheptanoids	*B. thorelli,* rhizome	Thailand	(Madaka *et al.,* 2013)
(81)	(1*R*,2*S*,5*S*,7*S*,9*R*,10*S*,13*R*)-1,2,7-trihydroxypimara-8(14),15-diene	*Kaempferia marginata,* rhizome	Thailand	(Thongnest *et al.,* 2005)
(82)	(1*R*,2*S*,5*S*,*9S*,10*S*,11*R*,13*R*)-1,2,11-trihydroxypimara-8(14),15-diene	*Kaempferia marginata,* rhizome	Thailand	(Thongnest *et al.,* 2005)
(83)	(1*S*,5*S*,7*R*,9*R*,10*S*,11*R*,13*R*)-1,7,11-trihydroxypimara-8(14),15-diene	*Kaempferia marginata,* rhizome	Thailand	(Thongnest *et al.,* 2005)
(84)	(1*S*,5*S*,9*S*,10*S*,11*R*,13*R*)-1,11-dihydroxypimara-8(14),15-diene	*Kaempferia marginata,* rhizome	Thailand	(Thongnest *et al.,* 2005)
(85)	(1*R*,2*S*,5*S*,7*S*,9*R*,10*S*,13*R*)-1,2-dihydroxypimara-8(14),15-diene-7-one	*Kaempferia marginata,* rhizome	Thailand	(Thongnest *et al.,* 2005)

Table 2.1, continued

Compound Number	Compound name	Sources and part	Country	Reference
(86)	(5*S*, 6*R*,9*S*,10*S*,13*R*)-6-hydroxypimara-8(14),15-diene-1-one	*Kaempferia marginata,* rhizome	Thailand	(Thongnest *et al.,* 2005)
(87)	Kaempfolienol	*Kaempferia galanga* L., rhizome	Thailand	(Singh *et al.,* 2013)
(88)	*α-trans*-Bergamotene	*B. stenophylla,* rhizome and leaf	Malaysia	(Ahmad & Jantan, 2003)
(89)	Aromadendrene	Rhizome and leaf	Malaysia	(Ahmad & Jantan, 2003)
(90)	2′-hydroxy-4,4′,6′-trimethoxychalcone	*Kaempferia galanga* L., rhizome	Thailand	(Singh *et al.,* 2013)
(91)	Zeylenol	*Kaempferia rotunda* L., *Kaempferia angustifolta* rhizome	Thailand	(Singh *et al.,* 2013; Woerdenbag *et al.,* 2004)
(92)	6-methylzeylenol	*Kaempferia galanga* L., rhizome	Thailand	(Singh *et al.,* 2013)
(93)	(24*S*)-24-methyl-lanosta-9(11), 25-dien-3*β*-ol	*Kaempferia galanga* L., rhizome	Thailand	(Singh *et al.,* 2013)
(94)	*β*-sitosterol-3-*O*-*β*-*D*-glucopyranoside	*Kaempferia galanga* L., rhizome	Thailand	(Singh *et al.,* 2013)

Table 2.1, continued

Compound Number	Compound name	Sources and part	Country	Reference
(95)	*epi*- *β*- santalene	*B. stenophylla,* rhizome and leaf	Malaysia	(Ahmad & Jantan, 2003)
(96)	Camphene	*Kaempferia galanga* L., rhizome	Thailand	(Singh *et al.,* 2013)
(97)	Borneol	*Kaempferia rotunda* L., rhizome	London, Thailand	(Stevenson *et al.,* 2007)
(98)	Cineol	*Kaempferia galanga* L., rhizome	Thailand	(Singh *et al.,* 2013)
(99)	Kaempferide	*Kaempferia galanga* L., rhizome	Thailand	(Singh *et al.,* 2013)
(100)	Cinnamaldehyde	*Kaempferia galanga* L., rhizome	Thailand	(Singh *et al.,* 2013)
(101)	*p*-metho-xycinnamic acid	*Kaempferia galanga* L., rhizome	Thailand	(Singh *et al.,* 2013)
(102)	Ethyl cinnamate	*Kaempferia galanga* L., rhizome	Thailand	(Singh *et al.,* 2013)
(103)	Ethyl pmethoxycinnamate	*Kaempferia galanga* L., rhizome	Thailand	(Singh *et al.,* 2013)
(104)	Carvon	*Kaempferia galanga* L., rhizome	Thailand	(Singh *et al.,* 2013)

Table 2.1, continued

Compound Number	Compound name	Sources and part	Country	Reference
(105)	Eucalyptol	*Kaempferia galanga* L., rhizome	Thailand	(Singh *et al.,* 2013)
(106)	Pentadecane	*Kaempferia galanga* L., rhizome	Thailand	(Singh *et al.,* 2013)
(107)	Ethyl *p*-methoxy-trans-cinnamate	*Kaempferia galanga* L., rhizome	Thailand	(Singh *et al.,* 2013)
(108)	(*E*)- *β*-Farnesene	*B. stenophylla,* rhizome and leaf	Malaysia	(Ahmad & Jantan, 2003)
(109)	3,5,7,4′-tetramethoxyflavone	*Kaempferia parviflora,* rhizome	Indonesia	(Hossain *et al.,* 2012)
(110)	5,7,4′-trimethoxyflavone	*Kaempferia parviflora,* rhizome	Indonesia	(Hossain *et al.,* 2012)
(111)	Germacrene *D*	*B. stenophylla,* rhizome and leaf	Malaysia	(Ahmad & Jantan, 2003)
(112)	*β*-Selinene	*B. stenophylla,* rhizome and leaf	Malaysia	(Ahmad & Jantan, 2003)
(113)	(-)-3-benzoyl-1-benzoloxymethyl-1,6-epoxycyclohexane-2,3,4,5-tetrol	*Kaempferia rotunda* L., rhizome	London	(Stevenson *et al.,* 2007)
(114)	4-benzoyl-1-benzoyloxymethyl-1,6-epoxycyclohexan-2,3,4,5-tetrol	*Kaempferia rotunda* L., rhizome	London	(Stevenson *et al.,* 2007)

Table 2.1, continued

Compound Number	Compound name	Sources and part	Country	Reference
(115)	2-acetyl-3-benzoyl-1-benzoyloxymethyl-1,6-epoxycyclohexan-2,3,4,5-tetrol	*Kaempferia rotunda* L., rhizome	London	(Stevenson *et al.,* 2007)
(116)	2-acetyl-4-benzoyl-1-benzoyloxymethyl-1,6-epoxycyclohexan-2,3,4,5-tetrol	*Kaempferia rotunda* L., rhizome	London	(Stevenson *et al.,* 2007)
(117)	3-benzoyl-1-benzoyloxy-methylcyclohexa-4,6dien-2,3-diol	*Kaempferia rotunda* L., rhizome	London	(Stevenson *et al.,* 2007)
(118)	Triacylated derivative of salicin	*Kaempferia rotunda* L., rhizome	London	(Stevenson *et al.,* 2007)
(119)	*α*-Muurolene	*B. stenophylla*, rhizome and leaf	Malaysia	(Ahmad & Jantan, 2003)
(120)	Germacrene *A*	*B. stenophylla*, rhizome and leaf	Malaysia	(Ahmad & Jantan, 2003)
(121)	(*E,E*)- *α*- Farnesene	*B. stenophylla*, rhizome and leaf	Malaysia	(Ahmad & Jantan, 2003)
(122)	*β*-Bisabolene	*B. stenophylla*, rhizome and leaf	Malaysia	(Ahmad & Jantan, 2003)
(123)	*δ*- Cadinene	*B. stenophylla*, rhizome and leaf	Malaysia	(Ahmad & Jantan, 2003)
(124)	Germacrene *B*	*B. stenophylla*, rhizome and leaf	Malaysia	(Ahmad & Jantan, 2003)

Table 2.1, continued

Compound Number	Compound name	Sources and part	Country	Reference
(125)	*β*-Calacorene	*B. stenophylla*, rhizome and leaf	Malaysia	(Ahmad & Jantan, 2003)
(126)	(*E)*-Nerolidol	*B. stenophylla*, rhizome and leaf	Malaysia	(Ahmad & Jantan, 2003)
(127)	Caryophyllene alcohol	*B. stenophylla*, rhizome and leaf	Malaysia	(Ahmad & Jantan, 2003)
(128)	Globulol	*B. stenophylla*, rhizome and leaf	Malaysia	(Ahmad & Jantan, 2003)
(129)	(-)-6-acetylzeylenol	*Kaempferia rotunda* L., rhizome	London	(Stevenson *et al.,* 2007)
(130)	(-)-Zeylenol	*Kaempferia rotunda* L., rhizome	London	(Stevenson *et al.,* 2007)
(131)	(-)-1,6-desoxypipoxide	*Kaempferia parviflora, Kaempferia galanga* L., *Kaempferia rotunda* L., rhizome	London, Thailand	(Leardkamolkarn *et al.,* 2009; Singh *et al.,* 2013; Stevenson *et al.,* 2007)
(132)	Crotepoxide	*Kaempferia galanga* L., *Kaempferia angustifolta* rhizome	London, Thailand	(Mahady, 2005; Singh *et al.,* 2013; Woerdenbag *et al.,* 2004)

2.3 Antioxidant assay – Ferric reducing antioxidant power (FRAP)

Antioxidant compounds can be found in food such as whole grains, fruits and vegetables. It plays an important role as a health protecting factor. Antioxidant definition has been defined as substances that have the ability to trap free radicals that will oxidize nucleic acid, proteins that can initiate degenerative diseases such as cancer and heart disease. Thus, antioxidant can inhibit the oxidative mechanisms that lead to degenerative diseases. Several epidemiological studies suggest that a high intake of food rich in natural antioxidants increases the antioxidant capacity of the plasma and reduces the risk of some, but not all, cancers, heart diseases, and stroke (Hassimotto *et al.*, 2005).

Lim *et al.* (2007) states that, the most abundant antioxidants in fruits are polyphenols and Vitamin C, Vitamins A, B and E and carotenoids are present to a lesser extent in some fruits. Clinical and research evidence on the effects of vitamin C on cancer and cardiovascular disease were also well discussed in a recent review (Li & Schellhorn, 2007). Well-known natural antioxidants, such as vitamin E (α-tocopherol), vitamin C, and polyphenols/flavonoids, have been investigated for their possible use to prevent various diseases (Núñez-Sellés, 2005). Vitamin E therapy is reportedly effective in decreasing oxidative stress and the levels of erythrocyte osmotic fragility in patients on dialysis (Uzum *et al.*, 2006). One review reports that vitamin E therapy had beneficial effects on patients with diabetes (Moon & Shibamoto, 2009). There are a number of clinical studies suggesting that the antioxidants in fruits, vegetables, tea and red wine are the main factors for the observed efficacy of these foods in reducing the incidence of chronic diseases including heart disease and some cancers (Aruna *et al.*, 2007).

Antioxidant has the ability to trap highly reactive free radicals and oxygen species which are present in biological systems. These free radicals may oxidize nucleic acids, proteins, lipids or DNA and can initiate degenerative disease such as heart disease and

cancer. Antioxidant compounds such as phenolic acids, polyphenols and flavonoids scavenge free radicals such as peroxide, hydroperoxide or lipid peroxyl and thus inhibit the oxidative mechanisms that lead to degenerative diseases (Aruna *et al.*, 2007). It is well known that oxidation damages on various biological substances may subsequently cause diseases such as cancer, liver disease, Alzheimer's disease, premature ageing, arthritis, inflammation, diabetes, Parkinson's disease and atherosclerosis (Moon & Shibamoto, 2009).

On the basis of the chemical reactions involved, major antioxidant capacity assays can be roughly divided into two categories. First is the hydrogen atom transfer (HAT) reaction based assays and second is the single electron transfer (ET) reaction based assays. The ET-based assays involve one redox reaction with the oxidant (also as the probe for monitoring the reaction) as an indicator of the reaction endpoint. Most HAT-based assays monitor competitive reaction kinetics, and the quantitation is derived from the kinetic curves. HAT-based methods generally are composed of a synthetic free radical generator, an oxidizable molecular probe, and an antioxidant. HAT- and ET-based assays are intended to measure the radical (or oxidant) scavenging capacity, instead of the preventive antioxidant capacity of a sample. Because the relative reaction rates of antioxidants (or substrates) against oxidants, particularly peroxyl radicals, are the key parameters for sacrificial antioxidant capacity, we will analyze autoxidation and its inhibition kinetics before in-depth analysis of the individual assays (Huang *et al.,* 2005).

Antioxidant capacities have several assay that have been frequently used to estimate antioxidant capacities in fresh fruits and vegetables and their products and foods for clinical studies including 2,2-azinobis(3-ethyl-benzothiazoline-6-sulfonic acid) (ABTS) **(133)**, 2,2- diphenyl-1-picrylhydrazyl (DPPH) **(134)**, ferric reducing antioxidant power (FRAP), and the oxygen radical absorption capacity (ORAC) assay.

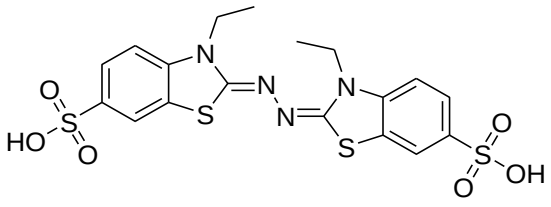

(133)

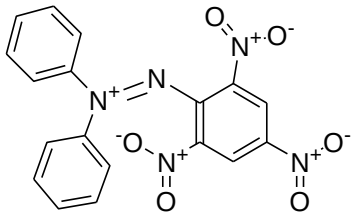

(134)

FRAP assay is commonly used to study the antioxidant capacity of plant materials. The antioxidant capacity of fruits extracts is determined by the ability of the antioxidants in these extracts to reduce ferric iron to ferrous in FRAP reagent, which consists of 2,4,6-tris(1-pyridyl)-5-triazine (TPTZ) prepared in sodium acetate buffer, pH 3.6. The reduction of ferric iron in FRAP reagent will result in the formation of a blue product (ferrous – TPTZ complex) whose absorbance can be read at 593 nm (Alothman *et al.*, 2009; Antolovich *et al.*, 2002).

The FRAP assay also takes advantage of electron-transfer reactions. Herein a ferric salt, Fe (III) $(TPTZ)_2Cl_3$(TPTZ = 2,4,6-tripyridyl-*s*-triazine) **(135)**, is used as an oxidant. The redox potential of Fe (III) salt (~0.70 V) is comparable to that of ABTS•- (0.68 V). Therefore, essentially, there is not much difference between TEAC assay and the FRAP assay except TEAC is carried out at neutral pH and FRAP assay under acidic (pH 3.6) conditions.

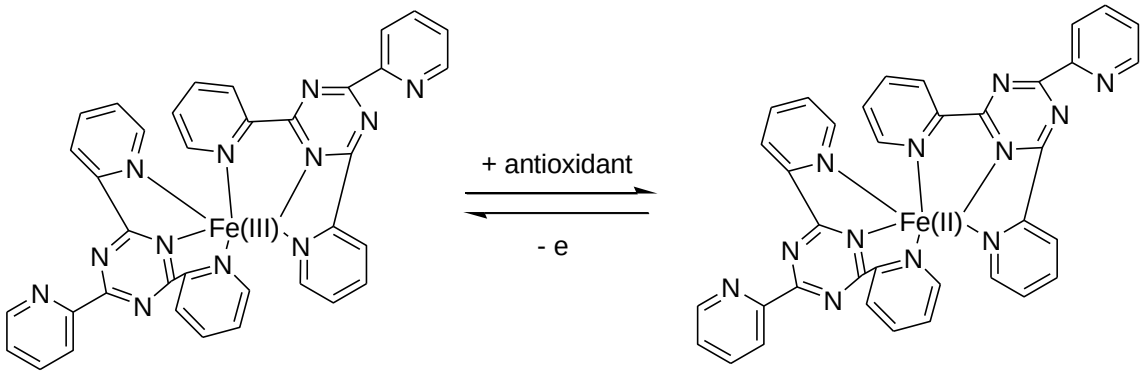

(135) Ferrous tripyridyltriazine (Fe^{2+}-TPTZ)

Figure 2.3: Formation of (Fe^{2+}-TPTZ) complex from (Fe^{3+}-TPTZ) complex by antioxidant

Guo *et al.* (2003) states that there are many different antioxidants contained in fruits and it is very difficult to measure each antioxidant component separately. Therefore, several methods have been developed to evaluate the total antioxidant activity of fruits or other plants and animal tissues. FRAP method was originally applied to plasma but has been extended to other biological fluids, foods, plant extracts, juices, *etc* (Antolovich *et al.*, 2002). FRAP method claim to be simple and rapid and both manual and automated procedures have been described. It provides instead a very useful 'total' antioxidant concentration, without measurement and summation of the concentration of all antioxidants involved (Antolovich *et al.*, 2002).

FRAP assay treats the antioxidants in the samples as reductants in a redox-linked colorimetric reaction. The procedure of FRAP assay is relatively simple and easy to be standardized. One possible disadvantage with FRAP assay is the fact that this assay does not react fast with some antioxidants, such as glutathione. However, we consider that FRAP assay is still suitable for assessment of antioxidant activity of fruit samples because only limited amounts of plant glutathione are absorbed by humans (Guo *et al.*, 2003; Prior

et al., 2005). Thaipong *et al*. (2006) affirms that the FRAP technique showed high reproducibility, was simple, rapidly performed and showed the highest correlation with both ascorbic acid and total phenolics compared to the other methods.

Comparative study of antioxidant properties over 30 plants extract were investigated using DPPH and ABTS radical scavenging capacity assay, oxygen radical absorbance capacity (ORAC) assay, superoxide dismutase (SOD) assay, and ferric reducing antioxidant potential (FRAP) assay. The result show that he highest correlations were found between ABTS and FRAP (Dudonné *et al.*, 2009). The FRAP assay is a simple and reproducible method which can be applied not only to the study of the antioxidant activity of plasma or antioxidants in food extracts and beverages, but also to the study of the antioxidant efficiency of pure dietary antioxidants (Pulido *et al.*, 2000).

CHAPTER 3: RESULTS AND DISCUSSION

3.1 Photophysical study of anthraquinones

Ten anthraquinones have been isolated from the root bark of *Morinda citrifolia,* which was collected from Kuala Lipis, Pahang on June 2013 (Nur Atiqah, 2016). It was categorized into two groups for photophysical studies for better discussion purpose. In the first group (**AQ1**-**AQ5**) the substituent group bear different types of electron withdrawing and electron donating, namely -CHO, -Me, -OH and -OMe. While in the second group (**AQ6** - **AQ10**), only electron donating substituent group is present, *i.e.* -Me, -OMe and/or -OH. The structures of the **AQ1-AQ10** are summarized below.

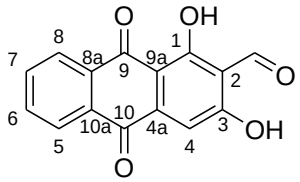

AQ1

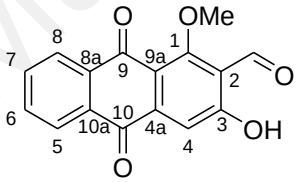

AQ2

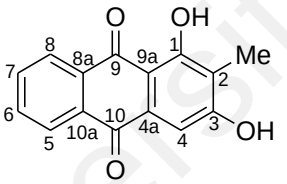

AQ3

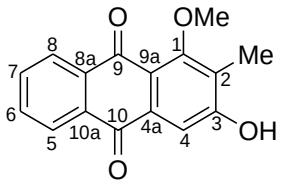

AQ4

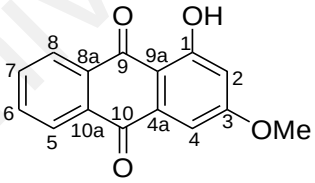

AQ5

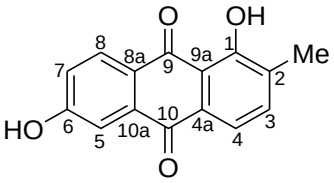

AQ6

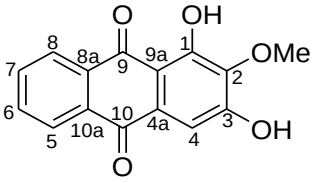

AQ7

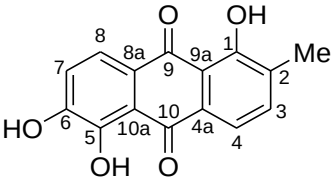

AQ8

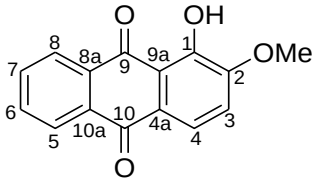

AQ9

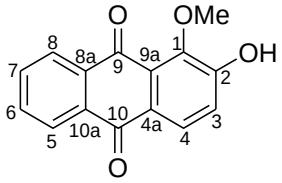

AQ10

3.1.1 Photophysical study of anthraquinones

3.1.1.1 Absorption and emission of anthraquinone AQ1-AQ5

The absorption spectra of natural anthraquinones **AQ1**–**AQ5** isolated from *M. citrifolia* are displayed in Figure 3.1 and Table 3.1. Anthraquinones **AQ1**–**AQ5** have shown absorption signals in the range of 200–300 nm. This suggests presence of $\pi \rightarrow \pi^*$ transition of fused aromatic rings and quinone backbones, with relatively small shifting but high dependence on substituent groups (Allen *et al.*, 1995; Diaz, 1990, 1991; Langdon-Jones & Pope, 2014). Besides that, anthraquinones have revealed longer wavelengths with weaker intensities within the 350–450 nm region, which were assigned to the $n \rightarrow \pi^*$ transition (Anouar *et al.*, 2014; Peter & Sumner, 1953). Nevertheless, the $n \rightarrow \pi^*$ transition is weak for anthraquinone **AQ5** as indicated by disappearance of absorption within this range.

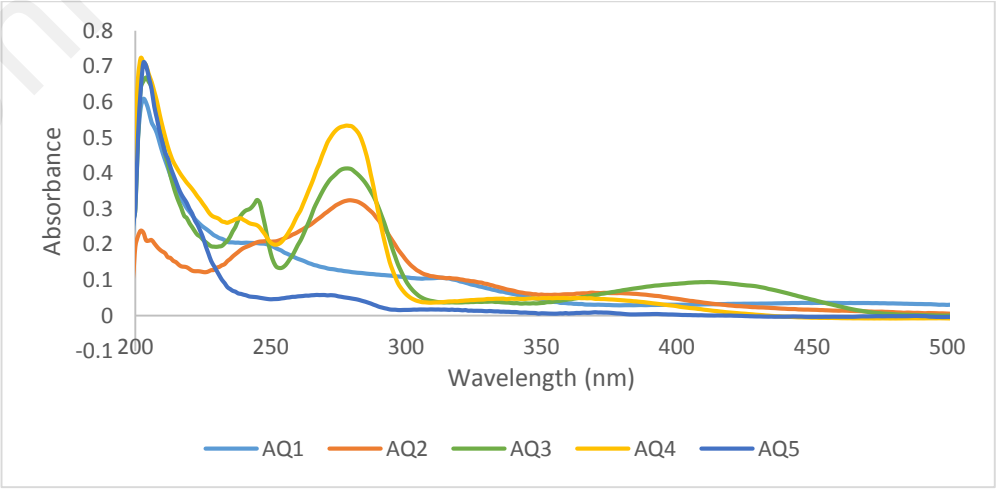

Figure 3.1: UV-visible absorption of anthraquinones **AQ1-AQ5**

Table 3.1: Absorbance and their coefficient of anthraquinones **AQ1** – **AQ5**

No	λ_{max} (nm)	Intensity	ε, (M cm^{-1})
AQ1	241	0.39	2749.26
	313	0.20	1434.98
	365	0.06	442.56
	387	0.06	402.33
	419	0.06	442.56
	456	0.07	482.80
AQ2	203	0.23	1642.92
	248	0.21	1475.63
	279	0.32	2284.39
	316	0.10	737.88
	369	0.06	446.78
AQ3	204	0.60	4248.97
	245	0.29	2064.99
	278	0.37	2626.67
	412	0.09	601.05
AQ4	205	1.32	9285.23
	239	0.77	5452.83
	278	1.64	11566.84
	360	0.18	1300.46
AQ5	203	0.64	4517.61
	267	0.05	370.04
	309	0.02	111.37

Signals appear to be broader when an aldehyde substituent group is present at C2 position as exemplified in anthraquinones **AQ1** and **AQ2**. Furthermore, two distinctive but narrower peaks are observed when C2-CHO substituent is replaced by a methyl group as illustrated by anthraquinones **AQ3** and **AQ4**. This can be attributed as electron

donation effect of methyl group, which resulted in higher π conjugation in aromatic rings (Figure 3.2).

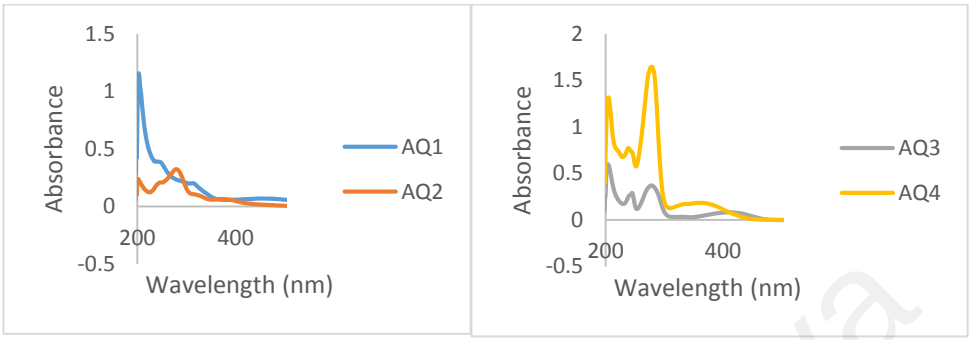

Figure 3.2: Anthraquinone **AQ1** and **AQ2** displayed broader absorbance than that of **AQ3** and **AQ4**

Experimental absorption data were then used as a guideline to measure emission wavelengths. Emission wavelengths and quantum yields of natural anthraquinones **AQ1**–**AQ5** were measured in the same solvent system (Figure 3.3 and Table 3.2). Anthraquinone **AQ1** that gave the brightest emission also displayed the highest quantum yield value (0.01036), followed by compounds **AQ4** (0.00140), **AQ3** (0.00053), and **AQ2** (0.00047). In addition, all anthraquinones have an emission wavelength lower than 450 nm except anthraquinone **AQ1**. Anthraquinone **AQ1** has the highest red shifted emission wavelength at 479 nm followed by anthraquinone **AQ3** at 426 nm (Figure 3.4). Besides that, the emissions' bathochromic shift of anthraquinones **AQ1** and **AQ3** can be ascribed to low-lying $S_{n,*}$ transitions influenced by 1-OH and 3-OH substituent groups and adjacent C9-carbonyl group (Figure 3.5). The three other anthraquinones, **AQ2**, **AQ4**, and **AQ5**, have shown blue shifted emissions at 314, 354, and 321 nm, respectively. Blue shifting emission wavelengths of these anthraquinones are correlated to $S_{\pi,*}$ transition attributed to presence of weaker electron donating 1-OMe or 3-OMe substituent groups.

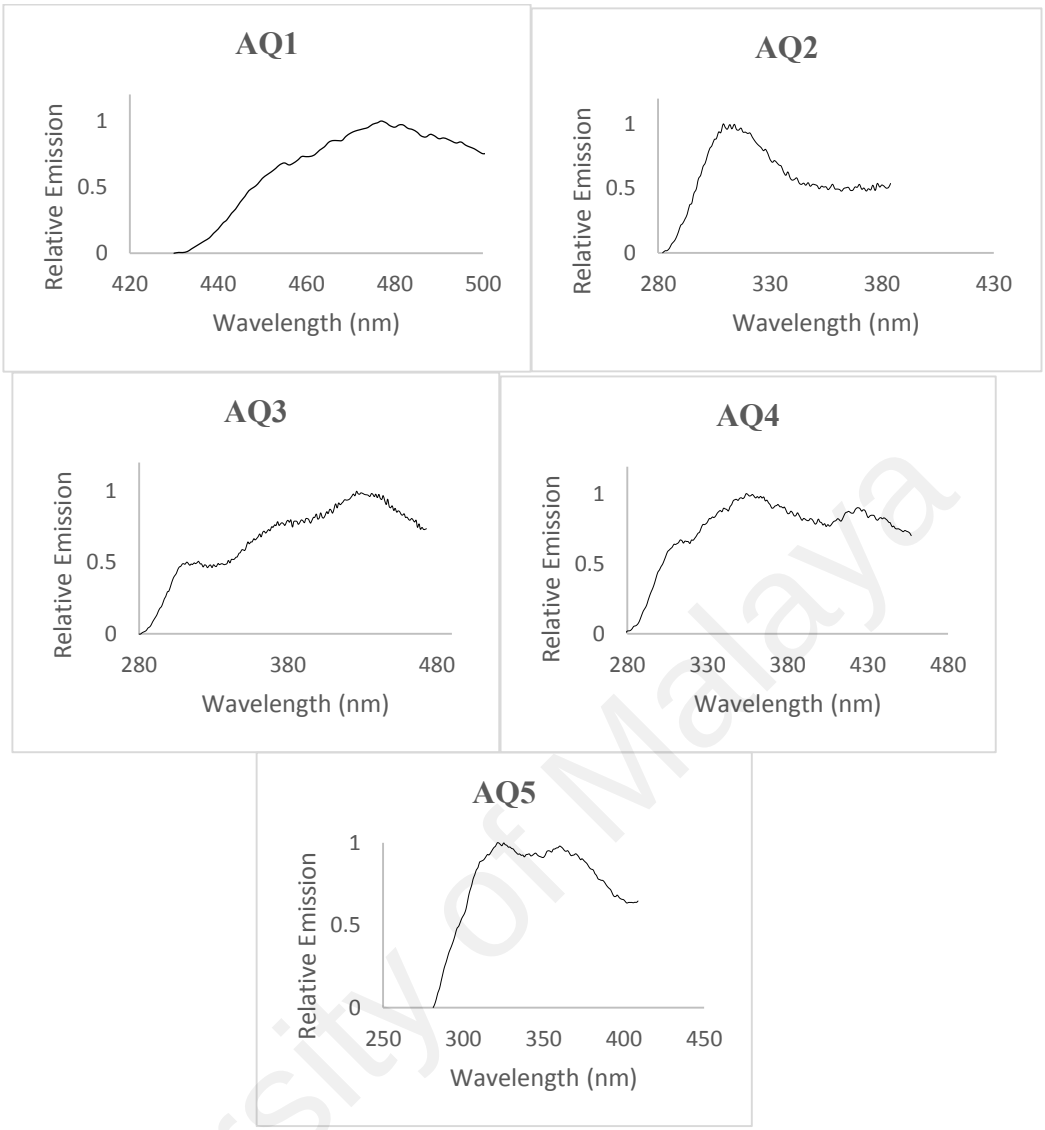

Figure 3.3: Fluorescene spectra of anthraquinones **AQ1-AQ5**

Table 3.2: Excitation, emission, Stokes shift and quantum yield of anthraquinones **AQ1 – AQ5**

Compound	Excitation (nm)	Emission (nm)	Intensity	Stokes Shift (nm)	Quantum Yield	Concentration (mol/L)
AQ1	419	479	17.13	60	0.01036	7.46×10^{-5}
AQ2	248	314	53.40	66	0.00047	1.49×10^{-4}
AQ3	245	426	127.62	181	0.00053	1.49×10^{-4}
AQ4	239	354	57.85	115	0.00140	1.49×10^{-4}
AQ5	267	321	256.26	54	n.d.	1.49×10^{-4}

n.d. - Not determined

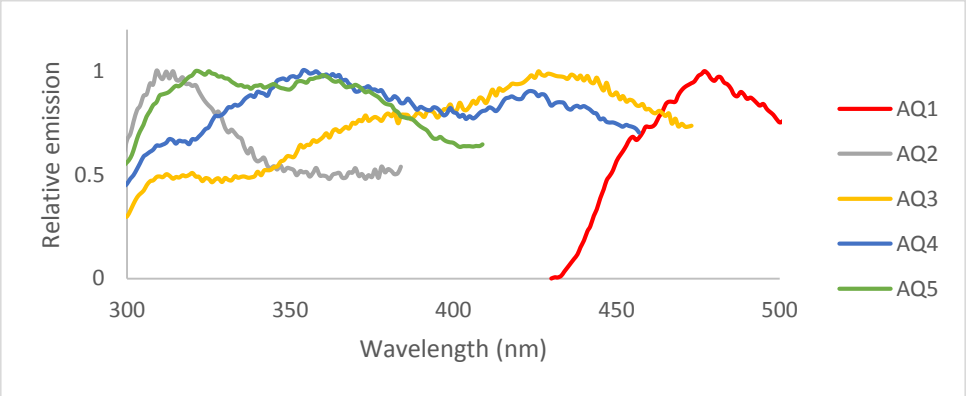

Figure 3.4: Normalized fluorescene spectra of anthraquinones **AQ1-AQ5**

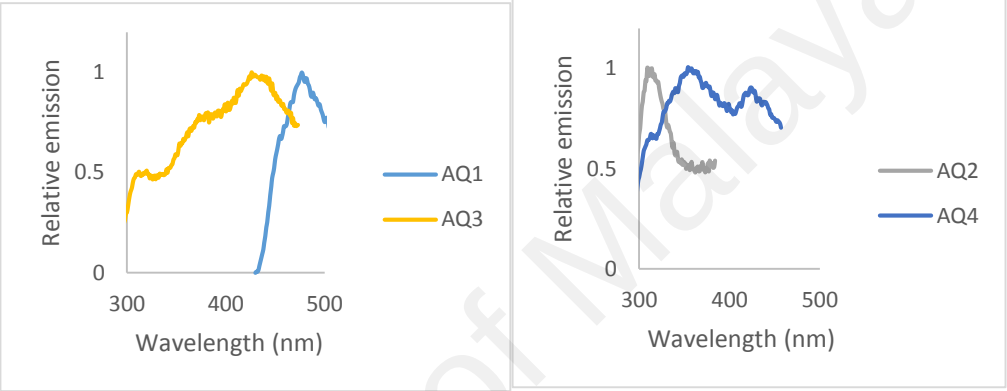

Figure 3.5: The emissions of anthraquinone **AQ1** and **AQ3** displayed bathochromic shifting while anthraquinone **AQ2** and **AQ4** showed hypsochromic shifting

.

3.1.1.2 Absorption and emission of anthraquinone AQ6-AQ10

Absorption spectra of the other five anthraquinones **AQ6-AQ10** isolated from *M. citrifolia* are displayed in Figure 3.6 and Table 3.3. Anthraquinones **AQ6-AQ10** have shown absorption signals in the range of 200 - 400 nm, which is also observed in **AQ1 – AQ5**. The observation suggested the presence of $\pi \rightarrow \pi^*$ transition, attributed to the electronic transitions of fused aromatic rings and quinone backbones (Diaz, 1990). However, **AQ6 – AQ10** showed stronger intensities within 350-450 nm region as compared to **AQ1 – AQ5** in the absorption spectral, which was also assigned to the $n \rightarrow \pi^*$ transition (Anouar *et al.,* 2014).

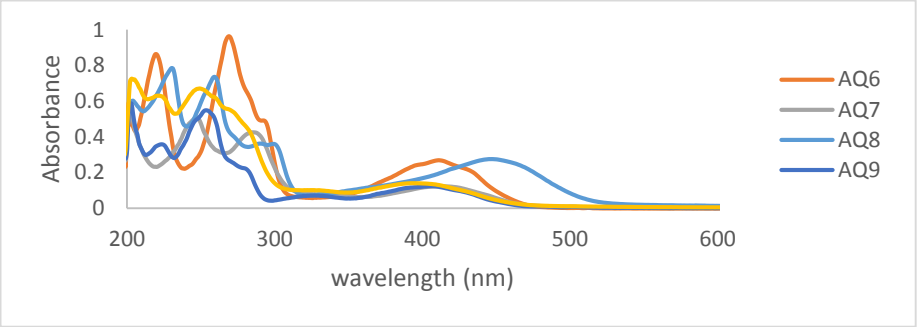

Figure 3.6: UV-visible absorption of anthraquinones **AQ6 – AQ10**

Table 3.3: Absorbance and their coefficient of anthraquinones **AQ6 – AQ10**

No	λ_{max} (nm)	Intensity (a.u)	ε, (M cm^{-1})
AQ6	201	0.53	3740.23
	219	0.78	5478.41
	269	0.87	6122.07
	411	0.24	1705.99
AQ7	202	0.51	3572.72
	247	0.49	3439.18
	285	0.41	2869.54
	415	0.12	827.06
AQ8	204	0.58	4073.51
	230	0.75	5305.61
	259	0.71	4975.78
	290	0.35	2446.88
	447	0.26	1863.47
AQ9	202	0.53	3723.99
	223	0.32	2274.25
	253	0.49	3485.15
	327	0.06	447.99
	406	0.11	783.95
AQ10	203	0.65	4609.65
	222	0.57	4004.38
	249	0.60	4261.28
	394	0.13	890.34

Absorption maxima appear to be higher and sharper when the number of hydroxy substituent is more than one as exemplified in anthraquinone **AQ6** and **AQ7** (Gierschner *et al.,* 2012). Furthermore, two distinctive peaks are observed when two hydroxy substituent is present as observed in anthraquinone **AQ6** and **AQ7** (Gierschner *et al.,* 2012). This observation can be attributed to the electron donation effect of the hydroxy group, which resulted in higher π conjugation in the aromatic backbone of **AQ6** and **AQ7** (Figure 3.7).

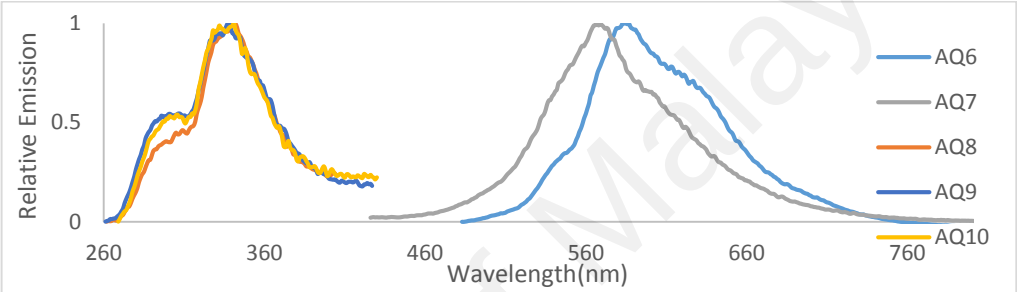

Figure 3.7: Normalized fluorescence spectra indicate relatively large emission shifting for anthraquinones **AQ6** and **AQ7**

Experimental absorption data obtained in the studies were then used as a guideline to measure emission wavelengths. Emission wavelengths of natural anthraquinones **AQ6-AQ10** were measured in the methanol, similar as **AQ1-AQ5** (Figure 3.8). **AQ6** gave the brightest emission followed by compounds **AQ7**, **AQ8, AQ10** and **AQ9**. **AQ6** and **AQ7** showed the highest red shifted emission at 585 and 567 nm, respectively, followed by **AQ8, AQ10** and **AQ9** at 342, 341 and 338 nm, respectively (Figure 3.9). Besides that, the emission bathochromic shift of **AQ6** and **AQ7** can be ascribed to the influence of two hydroxy substituent group present in the structure (Gierschner *et al.,* 2012). Two other anthraquinones, **AQ9** and **AQ10** have shown blue shifted emission (Figure 3.9). Blue shifting emission of **AQ9** and **AQ10** are correlated to the hypsochromic phenomenon that is attributed to the presence of only one hydroxy group. The mesomeric effect of the

hydroxy group extended the π-conjugation in the frontier orbitals in **AQ9** and **AQ10** (Gierschner *et al.,* 2012).

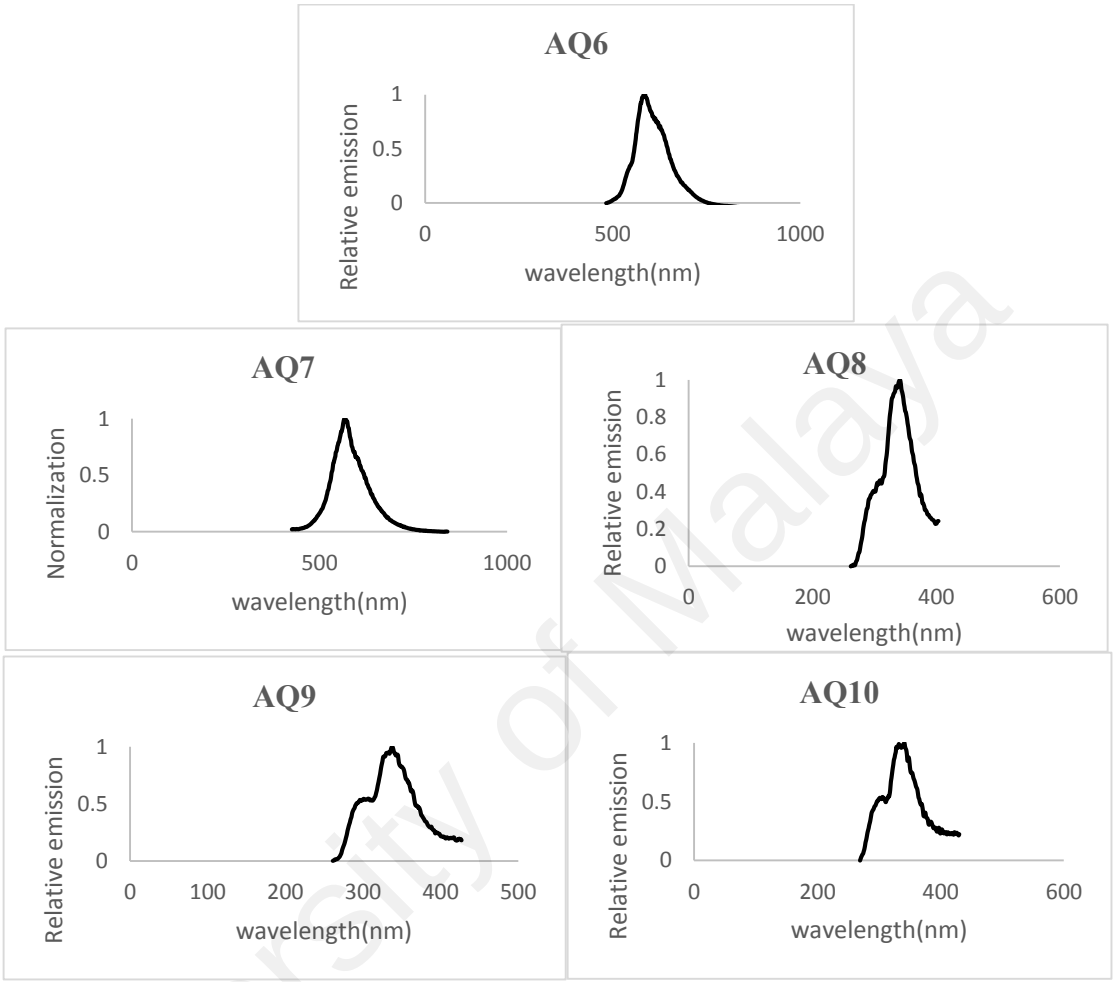

Figure 3.8: Fluorescence spectra of anthraquinones **AQ6- AQ10**

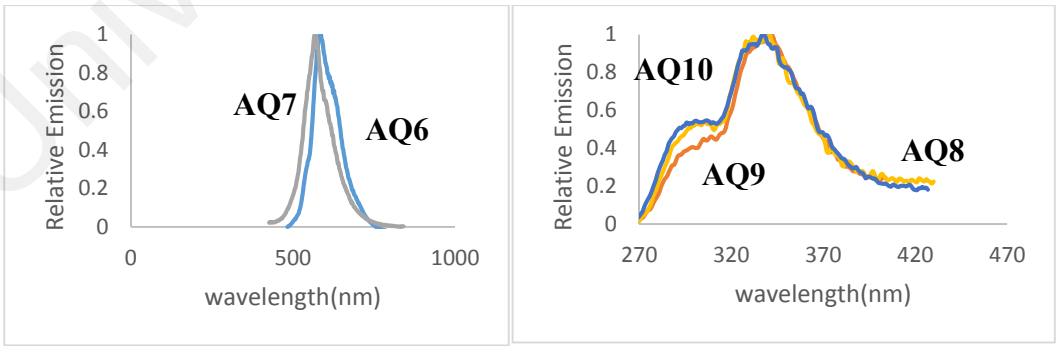

Figure 3.9: The emissions of anthraquinones **AQ6** and **AQ7** displayed bathochromic shifting while anthraquinones **AQ8**, **AQ9** and **AQ10** showed hypsochromic shifting

3.1.1.3 Substituent effect of anthraquinone AQ1-AQ5

The observed higher absorption and emission maxima of compounds **AQ1** (456 and 479 nm, respectively), **AQ2** (369 and 314 nm, respectively), and **AQ3** (412 and 426 nm, respectively) can be attributed to intra-hydrogen bonding between 1-OH and C9 carbonyl groups and/or 2-CHO and 3-OH groups. This results in formation of additional quasi-aromatic ring due to perturbation in the quinone core structure (Figure 3.10) (Flom & Barbara, 1985; Lakowicz, 2006).

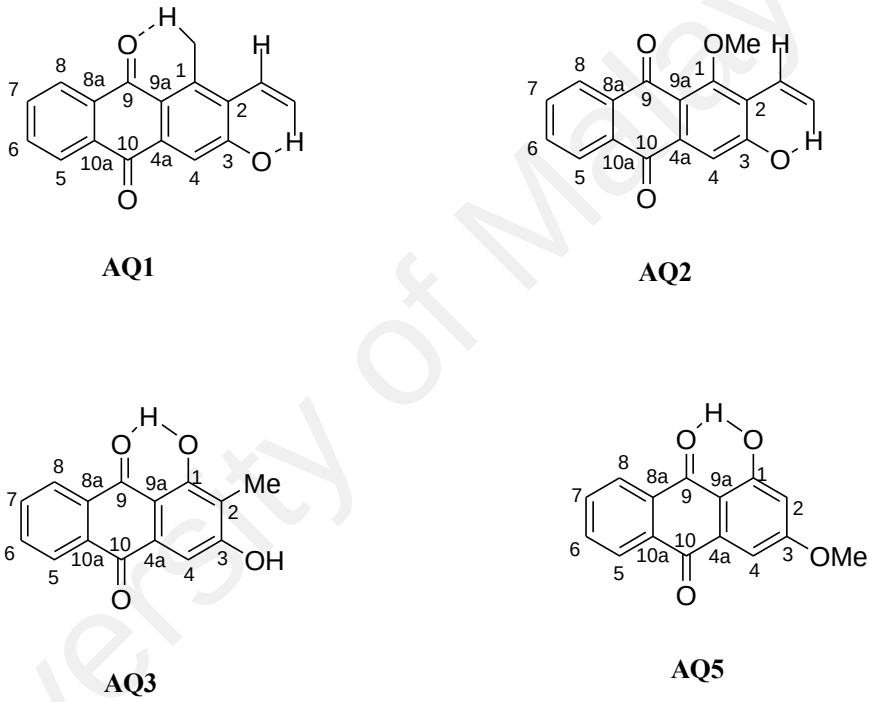

Figure 3.10: Proposed intramolecular proton transfer indicated by shifting of transitions

On the other hand, observation of ^{1}H NMR signal for hydroxy substituents at $\delta_{1\text{-}OH}$ 14.05 (**AQ1**) and $\delta_{1\text{-}OH}$ 13.11 (**AQ3**) provides supportive evidence for intrahydrogen bonding between 1-OH and C9 carbonyl groups in anthraquinones **AQ1** and **AQ3** (Table 3.4). Furthermore, formation of intramolecular hydrogen bonding between 2-CHO and 3-OH groups in compounds **AQ1** and **AQ2** is supported by ^{1}H NMR spectroscopy data. Low field signals of hydroxy substituents at $\delta_{3\text{-}OH}$ 12.67 for anthraquinone **AQ1** and $\delta_{3\text{-}OH}$ 12.28 for anthraquinone **AQ2** were noted (Table 3.4).

Besides that, additional electron transfer between 1-OH and C9 carbonyl and 2-CHO and 3-OH groups in anthraquinone **AQ1** contributed to the increase of delocalization effect. This resulted in the lowest energy difference between ground and exited states. Hence, compound **AQ1** displayed the longest absorption (456 nm) and emission maxima (479 nm), and quantum yield (0.01036). On the other hand, only one intramolecular hydrogen bonding between 1-OH and C9 carbonyl groups is present in anthraquinone **AQ3**, which displayed a shorter emission maxima at 426 nm. In contrast, intramolecular hydrogen bonding between 3-OH and 2-CHO groups in anthraquinone **AQ2** resulted in a much shorter emission maxima at 314 nm (Wcisło *et al.,* 2013).

This observation indicates that quasi aromatic rings formed by intramolecular hydrogen bonding between 1-OH and C9 carbonyl groups resulted in higher perturbation in the quinone core structure. It also extended the π-electron system of conjugated heterocyclic ring and disturbed π-electron's mobility. Hence, this resulted in lower fluorescence intensity (Weisstuch & Testa, 1970) compared to that of quasi aromatic rings formed from intramolecular hydrogen bonding between 3-OH and 2-CHO groups.

Anthraquinone **AQ4**, which possess an electron-donating 2-Me group did not undergo intrahydrogen bonding and displayed a lower absorption maxima at 360 nm in comparison to anthraquinone **AQ2** (369 nm).

Steric hindrance between substituent groups and other parts of the molecule has been indicated in previous studies to play a role in determining spatial configuration adopted by the system and hence caused shifting of absorption bands (Diaz, 1990; Langdon-Jones & Pope, 2014). Absorption maxima of 1,3-di-substituted anthraquinone **AQ5** is observed at 309 nm whereas values for 1,2,3-tri-substituted anthraquinones **AQ1**–**AQ4** were 456, 369, 412, and 360 nm, respectively. Steric hindrance has the least effect on di-substituted anthraquinone **AQ5,** which allowed it to adopt a more planar spatial

configuration promoting better hydrogen bonding between C9 carbonyl and 1-OH substituent. This observation is further corroborated with ^{1}H NMR spectroscopy in which a strong signal was observed for 1-OH substituent of anthraquinone **AQ5** at $\delta_{1\text{-OH}}$ 13.33.

The quasi aromatic ring formed from intramolecular hydrogen bonding between 1-OH and C9 carbonyl groups is present in both compounds **AQ3** and **AQ5**. Nonetheless, an electron donating substituent, *i.e.* 2-Me group exists in compound **AQ3** that contributed to bathochromic shift of emission maxima (426 nm) and a larger Stokes shift (181 nm) compared to anthraquinone **AQ5** (321 nm and 54 nm, respectively).

Luminescence properties are characterized by the presence of substitution groups (electron withdrawing or electron donating) and formation of intramolecular hydrogen bonding. Hence, absence of phosphorescence activities in anthraquinones **AQ1**–**AQ5** indicate that intramolecular hydrogen bonding caused by substituents in these structures contributed to the effect of intramolecular charge transfer, which weakened the central quinoid structure (Figure 3.10) (Anouar *et al.,* 2014).

Table 3.4: ^{1}H NMR of anthraquinones **AQ1-AQ5**

Position	AQ1	AQ2	AQ3	AQ4	AQ5
2	-	-	-	-	6.26 s
4	7.33 s	7.68 s	7.16 s	7.40 s	7.53 s
5	8.29 dd (8,1)	8.25 dd (8,1)	8.15 dd (8)	8.12 dd (8,1)	8.33 m
6	7.84 m	7.78 td (8,1)	7.69 td (8)	7.65 td (8,1)	7.85 m
7	7.84 m	7.83 td (8,1)	7.73 td (8)	7.72 td (8,1)	7.85 m
8	8.32 dd (8,1)	8.30 dd (8,1)	8.22 dd (8)	8.21 dd (8,1)	8.33 m
1-OH	14.05 s		13.11 s	-	13.33 s
3-OH	12.67 s	12.28 s	-	-	-
2-CHO	10.50 s	10.47 s	-	-	-
1-OMe	-	4.13 s	-	3.84 s	-
2-Me	-	-	2.14 s	2.21 s	-
3-OMe	-	-	-	-	3.42 s

3.1.1.4 Substituent effect of anthraquinone AQ6-AQ10

The observed higher absorption and emission of compounds **AQ6** (269 and 585 nm, respectively), **AQ7** (285 and 567 nm, respectively), **AQ8** (230, 342 nm, respectively) and **AQ9** (223, 338 nm, respectively) can be attributed to intrahydrogen bonding between 1-OH and C9 carbonyl groups, similar as **AQ1** - **AQ5**. This resulted in the formation of additional quasi-aromatic ring due to perturbation in the quinone core structure (Figure 3.11) (Flom & Barbara 1985; Lakowicz, 2006). However, intrahydrogen bonding is not form in compound **AQ10** since the substitution at C1 is OMe rather than OH as the case in **AQ6**-**AQ7**.

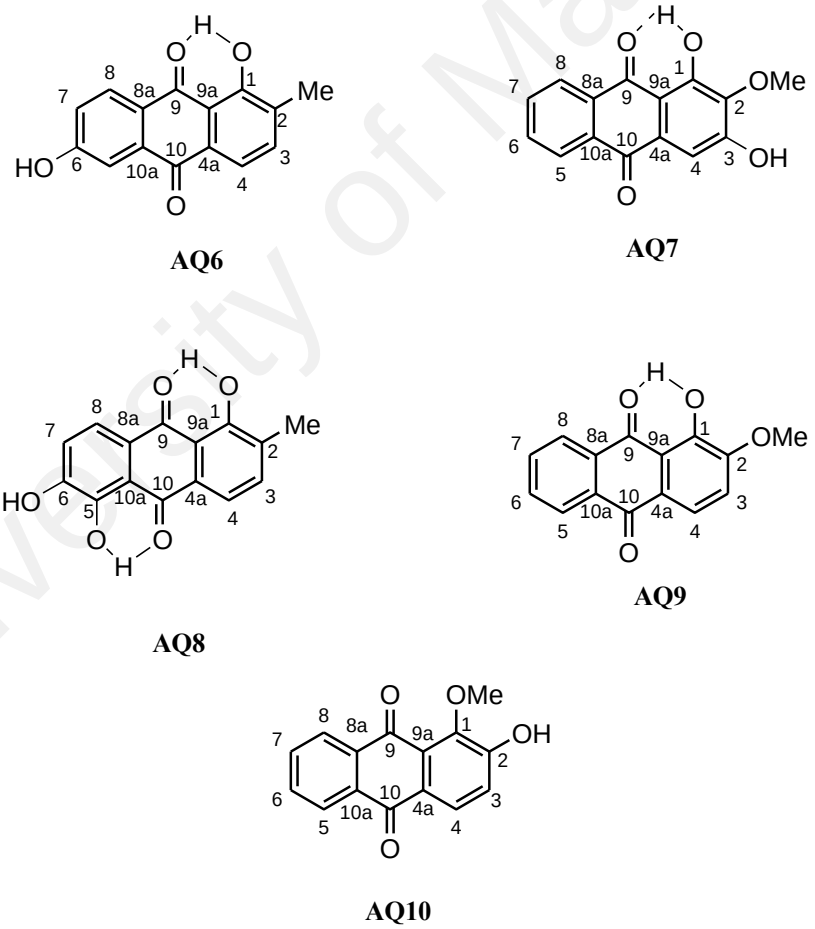

Figure 3.11: Proposed intramolecular proton transfer indicated by shifting of transitions

Compound **AQ6** – **AQ9** displayed higher absorption maxima when compared to **AQ10**. This observation indicates that the importance of 1-OH group. The observation is further corroborated with ^{1}H NMR spectroscopy in which a strong deshielded signal was observed for 1-OH for anthraquinones **AQ6**, **AQ7** and **AQ9**, at $\delta_{1\text{-OH}}$ 13.12, 14.81 and 13.03, respectively, (Table 3.5), suggesting that 1-OH is strongly bonded to the nearby C9 carbonyl group through intrahydrogen bonding.

The absence of 1-OH group induces a significant blue shift in the emission maxima; for instance compound **AQ6** (possessing 1-OH group) emission maxima is observed at 585 nm, while compound **AQ10** (does not possess 1-OH group) emission maxima is 341 nm. The experimental data also showed that 1-OH substituted anthraquinones, *i.e.* **AQ6** – **AQ9**, the maximum wavelength is greater than that of 2-OH substituted anthraquinone (**AQ10**). This can be rationalized by the charge transfer stabilization in C1 is greater than that in C2 (Diaz, 1990).

The presence of more than one hydroxy substituents in **AQ6** (C1 and C6) and **AQ7** (C1 and C3) and **AQ8** (C1, C5 and C6) enhances the fluorescence properties, in which the number of quasi aromatic ring formed due to intramolecular hydrogen bonding increases (Dahiya *et al.,* 2006). Hence, this resulted in the observation of higher fluorescence intensity in **AQ6**, **AQ7** and **AQ8** when compared to **AQ9** and **AQ10** (Peters & Sumner, 1953; Yoshida & Takabayashi 1968). This phenomenon was also observed in **AQ1** and **AQ3**, which possessed two hydroxy substituents in the structure and displayed enhanced the fluorescence properties when compared to that of **AQ2**, **AQ4** and **AQ5**.

Anthraquinone **AQ10**, which possess an electron-donating 1-OMe group is unable to form intrahydrogen bonding with the C9 carbonyl group and displayed the lowest absorption maxima at 222 nm in comparison to anthraquinone **AQ8** and **AQ9** (230 and 223 nm respectively).

Table 3.5: ^{1}H NMR of anthraquinones **AQ6-AQ10**

Position	AQ6	AQ7	AQ8	AQ9	AQ10
3	7.43 d (8)	-	7.45 d (8)	7.79 d (8)	7.36 d (9)
4	7.63 d (8)	7.40 s	7.68 d (8)	7.86 m	8.14 d (9)
5	7.50 (s)	8.28 dd (8,1)	-	8.32 m	8.27 m
6	-	7.82 m	-	7.82 m	7.78 m
7	7.12 d (8)	7.82 m	7.13 d (8)	7.82 m	7.78 m
8	8.13 d (8)	8.34 dd (8,1)	7.75 d (8)	8.32 m	8.27 m
1-OH	13.12 s	14.81 s	-	13.03 s	-
2-Me	2.30 s	-	2.32 s	-	-
3-OH	-	12.63 s	-	-	-
2-OMe	-	4.08 s	-	4.86 s	-
1-OMe	-	-	-	-	4.04 s
2-OH	-	-	-	-	13.02 s

3.2 Chemical constituents of *Boesenbergia stenophylla*

Four compounds have been isolated from the roots of *B. stenophylla*. The roots *Boesenbergia stenophylla* were obtained from Alor Setar, Malaysia on September 2012. Antioxidant capacity of these compounds have also been evaluated by using the Ferric reducing antioxidant power (FRAP) assay. The structures of the isolated compounds are summarized below.

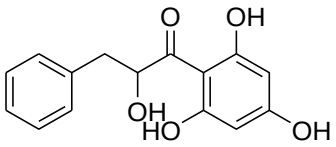

2-hydroxy-3-phenyl-1-(2,4,6-trihydroxy-phenyl)-propan-1-one (**BS1**) (New)

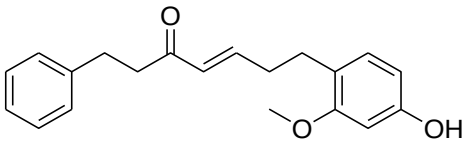

7-(2”-Methoxy-4”-hydroxyphenyl)-1-phenyl-hept-4-en-3-one (**BS2**) (New)

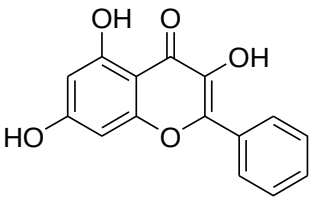

3,5,7-trihydroxy-flavone (**BS3**)

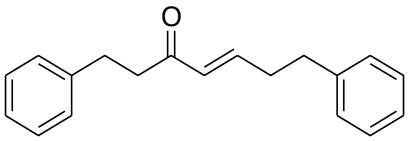

1,7-diphenylhept-4-en-3-one (**BS4**)

3.2.1 BS1: 2-hydroxy-3-phenyl-1-(2,4,6-trihydroxy-phenyl)-propan-1-one (New)

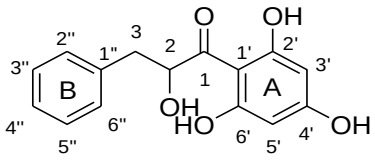

BS1 was isolated as light yellow oil with molecular formula $C_{15}H_{14}O_5$ as determined by HREIMS *m/z* 257.0802 $[M+H-H_2O]^+$ (calculated for $C_{15}H_{14}O_5 + H - H_2O$, 257.0808) and *m/z* 255.0689 $[M-H-H_2O]^-$ (calculated for $C_{15}H_{14}O_5 - H - H_2O$, 255.0663). The UV spectrum showed two absorption maxima at 203, 294, and 341 nm. The IR spectrum indicated the presence of hydroxy (3227 cm^{-1}) and carbonyl (1644 cm^{-1}) functional groups.

The ^1H NMR (Figure 3.13 and Table 3.6) displayed ten resolved proton signals and one hydroxy signal (δ_H 12.04). Of the ten proton signal, five signals were observed as multiplet (δ_H 7.44), two signals were observed as singlet (δ_H 6.00), and three signals were observed as doublet of doublet (δ_H 5.42, 3.09 and 2.83).

The ^{13}C NMR spectrum (Figure 3.14 and Table 3.6) showed the presence one *sp3* tertiary carbon signal at δ_C 79.4; one *sp3* secondary carbon signal at δ_C 43.5; seven *sp2* tertiary carbon signal at δ_C 129.0, 129.0, 128.8, 126.3, 126.3, 95.7, 95.7; and six *sp2* tertiary carbon signal at δ_C 195.9, 164.8, 164.5, 164.5, 138.4, 103.3. The carbon signal at δ_C 79.4 (C(2)) indicated the presence of a hydroxy methine function, the carbon signal at δ_C 195.9 (C(1)) indicated the presence of a carbonyl function, while the aromatic carbon

signals at δ_C 164.5 (C(2')), 164.8 (C(4')) and 164.5 (C(6')) indicated the presence of phenolic functions.

The HMBC spectrum (Figure 3.12, 3.15 and Table 3.6) showed J^3 correlations from C(1) to H(3), C(1'') to H(2), C(1'') to H(3''), C(1'') to H(5''), C(2'') to H(4''), C(3'') to H(5''), C(4'') to H(2''), C(4'') H(6''), C(5'') to H(3''), and C(6'') to H(4''); and J^2 correlations from C(2) to H(3) and C(1'') to H(3) thereby confirming ring A and its connectivity with the aliphatic chain. The observation of HMBC J^3 correlations from C(1') to H(3'), C(1') to H(5'), CC(3') to H(5'), and C(5') to H(3'); and J^2 correlations from C(2' to H(3'), C(4') to H(3'), C(4') to H(5') and C(6') to H(5') thereby confirming the ring B is connected with ring A through the aliphatic chain. This is the first report of **BS1**.

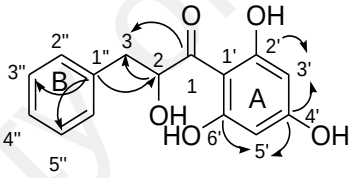

Figure 3.12: Selected HMBC correlations of **BS1**

Table 3.6: The NMR ($CDCl_3$, 600 MHz) data of **BS1** (2-hydroxy-3-phenyl-1-(2,4,6-trihydroxy-phenyl)-propan-1-one)

Position	δ_H	δ_C	HMBC
1	-	195.9	3
2	5.42 dd (13.0, 3.0)	79.4	3
3	2.83 dd (17.2, 3.0)	43.5	-
	3.09 dd (17.2, 13.0)	43.5	-
1'	-	103.3	3', 5'
2'	-	164.5	3'
3'	6.00 s	95.7	5'
4'	-	164.8	3', 5'
5'	6.00 s	95.7	3'
6'	-	164.5	5'
1"	-	138.4	2, 3, 3'', 5''
2"	7.44 m	129.0	4''
3"	7.44 m	126.3	5''
4"	7.40 m	128.8	2'', 6''
5"	7.44 m	126.3	3''
6"	7.44 m	129.0	4''
2'-OH	12.04 s	-	-

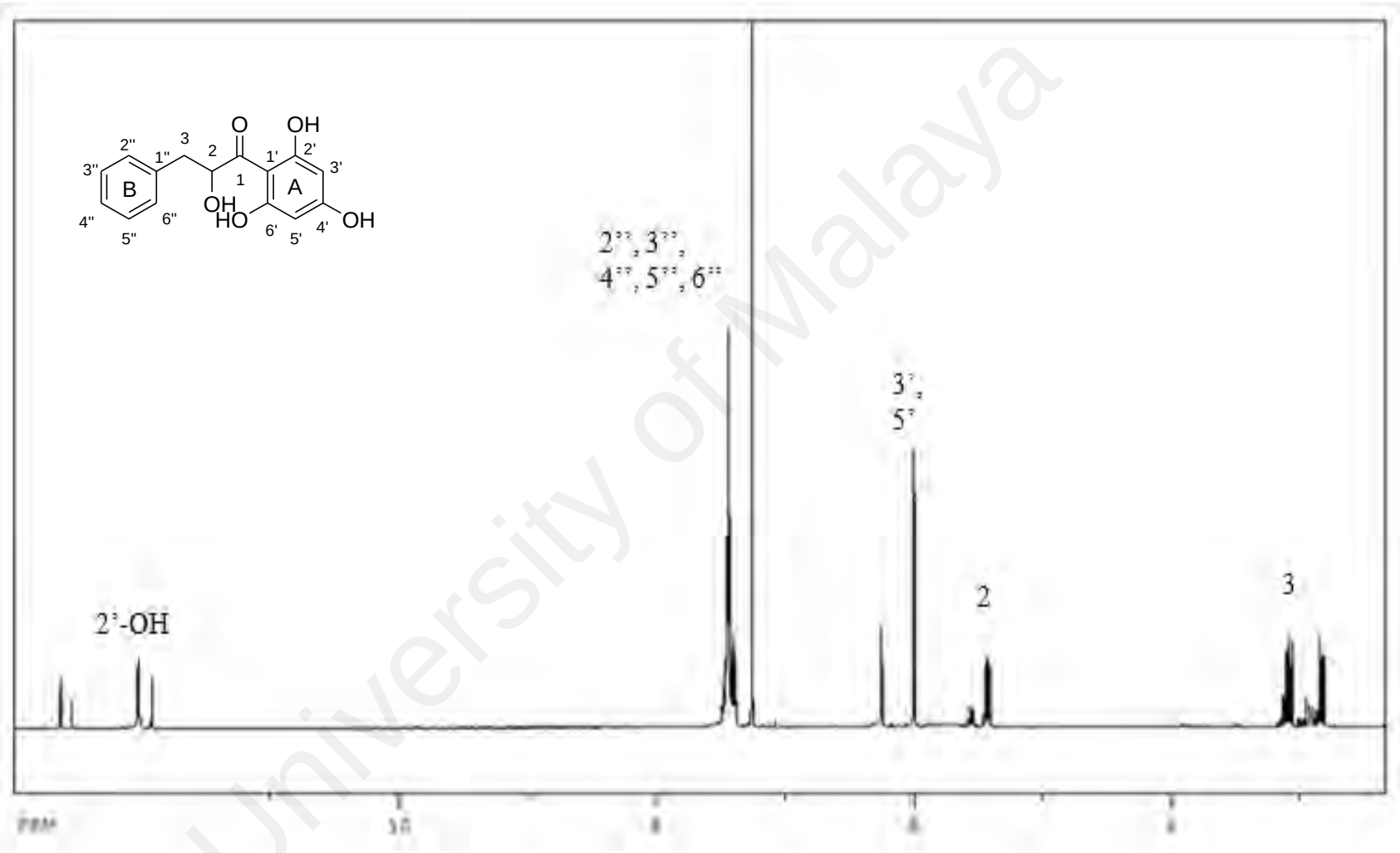

Figure 3.13: ^{1}H NMR spectrum ($CDCl_3$, 600 MHz) of **BS1** (2-hydroxy-3-phenyl-1-(2,4,6-trihydroxy-phenyl)-propan-1-one)

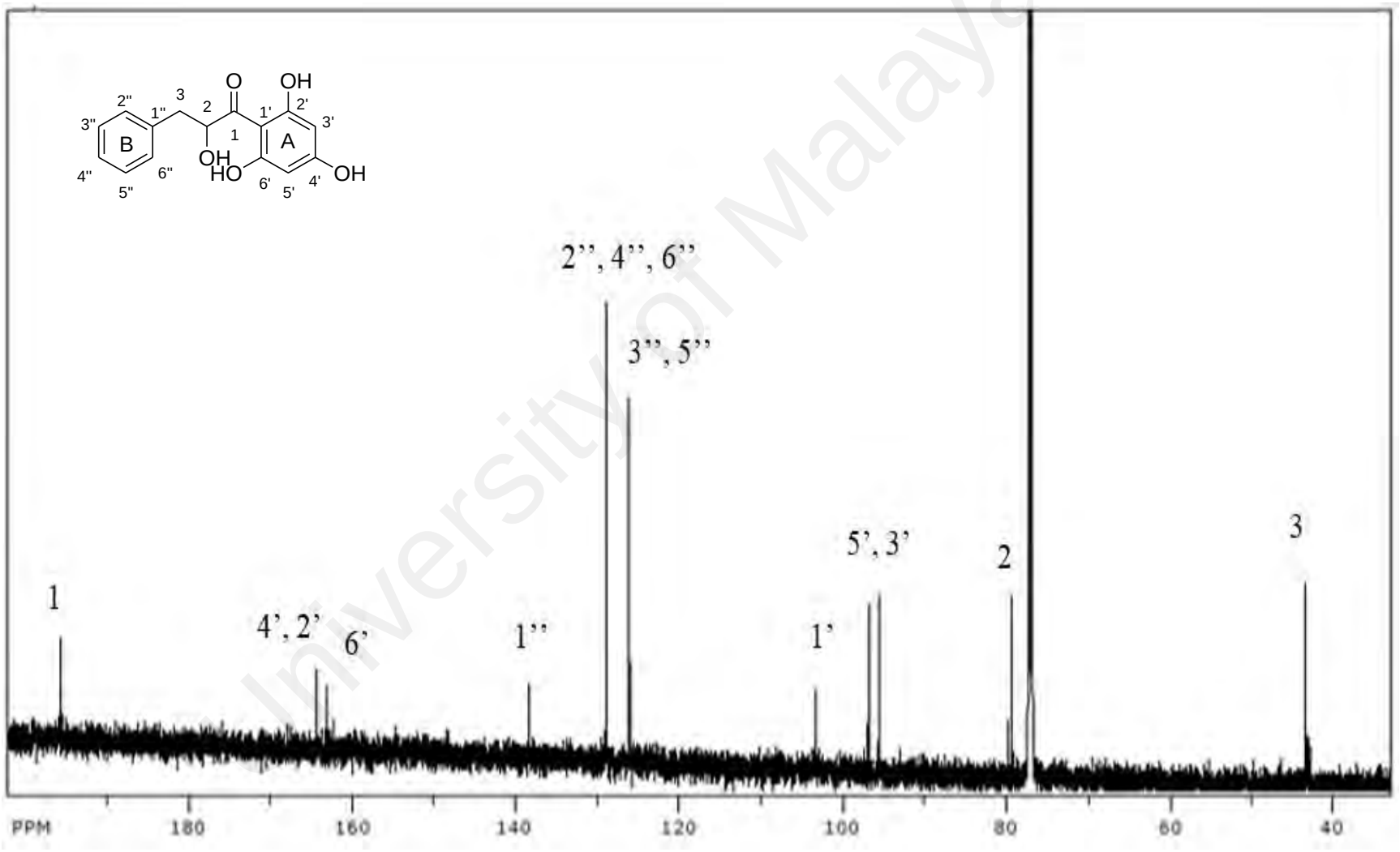

Figure 3.14: ^{13}C NMR spectrum ($CDCl_3$, 150 MHz) of **BS1** (2-hydroxy-3-phenyl-1-(2,4,6-trihydroxy-phenyl)-propan-1-one)

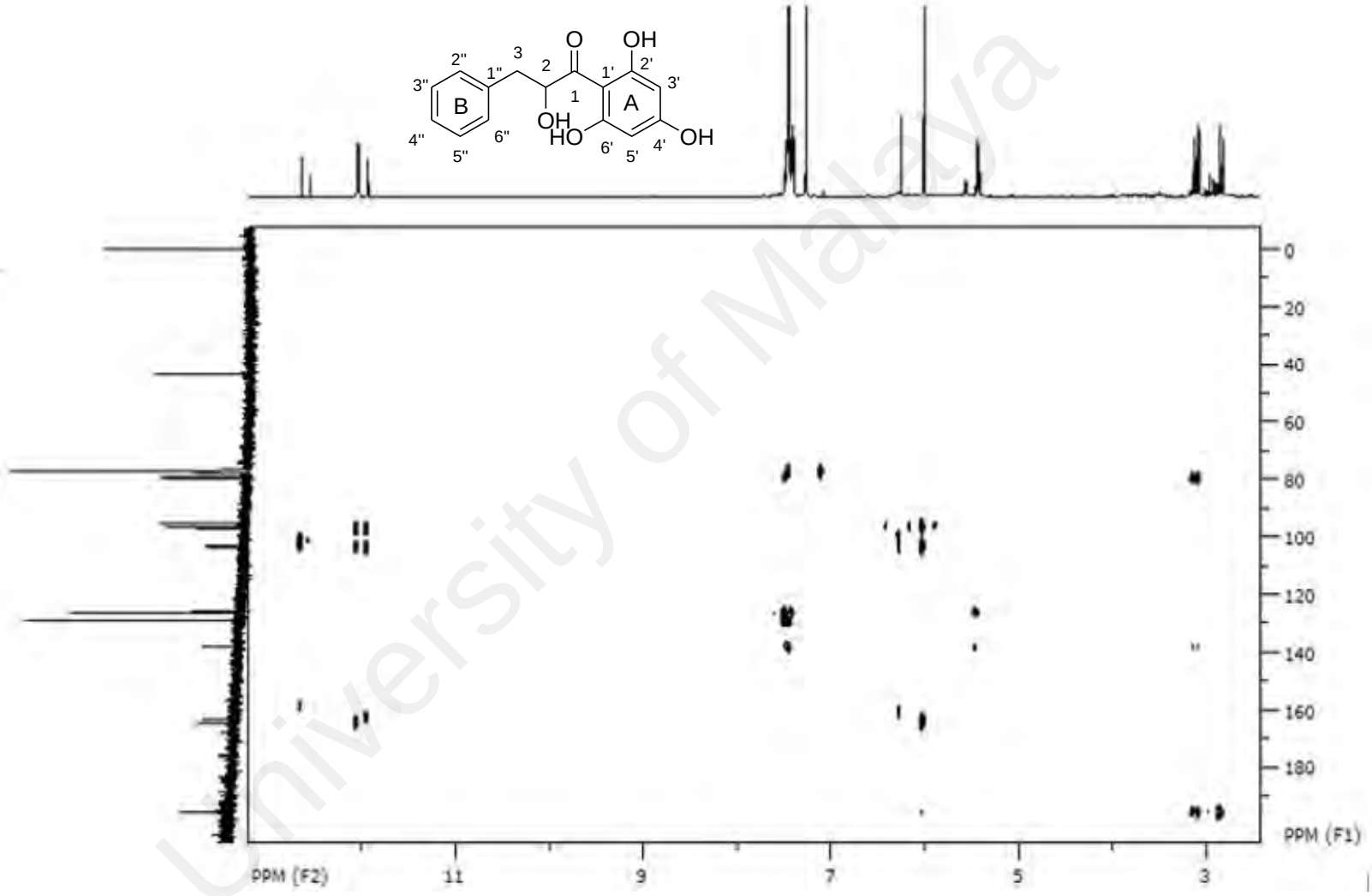

Figure 3.15: HMBC spectrum ($CDCl_3$, 150 MHz) of **BS1** (2-hydroxy-3-phenyl-1-(2,4,6-trihydroxy-phenyl)-propan-1-one)

3.2.2 BS2: 7-(2”-Methoxy-4”-hydroxyphenyl)-1-phenyl-hept-4-en-3-one (New)

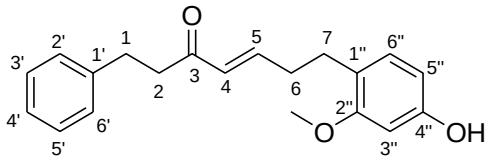

BS2 was isolated as brownish oil with molecular formula $C_{20}H_{22}O_3$ as determined by HREISM with *m/z* 309.1752 $[M-H]^-$ (calculated for $C_{20}H_{22}O_3$ - H, 309.1728) and *m/z* 293.1808 $[M-OH]^-$ (calculated for $C_{20}H_{22}O_3$ - OH, 293.1779). The UV spectrum showed absorption maxima at 371, 282, and 224 nm. The IR spectrum indicated the presence of hydroxy (3422 cm^{-1}) and carbonyl functional group (1656 cm^{-1}).

The ^1H NMR spectrum (Figure 3.17 and Table 3.7) displayed fifteen resolved proton signals, and a methoxy signal (δ_H 3.85). Of the fifteen resolved proton signals, two signals were observed overalappped at at δ_H 7.27 (one as doublet (d) and another as triplet (t)), two sets of overlapping doublet (d) at at δ_H 7.19 and one triplet (t) at δ_H 7.19, two multiplets (m) at δ_H 6.83, two multiplets (m) at δ_H 6.65, a multiplet (m) at δ_H 6.11, and four triplets at δ_H 2.92, 2.84, 2.69 and 2.49.

The ^{13}C NMR spectrum (Figure 3.18 and Table 3.7) showed the presence of four *sp3* secondary carbon signals at δ_C 41.9, 34.6, 34.3, and 30.2; ten *sp2* tertiary carbon signals at δ_C 146.6, 130.8, 128.6, 128.5, 128.5, 126.2, 121.0, 120.6, 114.5 and 111.5; five *sp2* quartenary carbon signals at δ_C 199.6, 144.1, 141.4, 132.7, and 56.0; and one sp^3 primary carbon signal at δ_C 146.6. The carbon signal at δ_C 146.6 was assigned to the quaternary C(2’’) aromatic carbon attached to a methoxy group and carbon signal at δ_C 199.6 is assigned to the C(3) carbonyl carbon. The carbon signal at δ_C 144.1 indicated the presence of a hydroxy substituent at the aromatic carbon C(4’’) and the carbon signals at δ_C 130.8 and 114.5 are assigned to the double bond C(4)=C(5).

The HMBC spectrum (Figure 3.16, 3.19 and Table 3.7) showed J^2 correlations from C(1') to H(1) and C(2') to H(3'); and J^3 correlations from C(1) to H(6'), C(1') to H(2), C(1') to H(2'), C(1') to H(3'), C(1') to H(5'), C(2') to H(6'), C(2') to H(4'), C(3') to H(5'), C(5') to H(3'), and C(6') to H(2') thereby confirming the aliphatic chain and its connectivity with the B ring. The observation of HMBC J^3 correlations from C(3) to H(5), C(4) to H(5), C(6) to H(4), C(7) to H(5), and C(5'') to H(3''); and J^2 correlations from C(6) to H(5), C(7) to H(6), C(1'') to H(7), C(1'') to H(6''), C(4'') to H(3'') and C(4'') to H(5''), thereby confirming the A ring and its connectivity with the aliphatic chain. This is the first report of **BS2**.

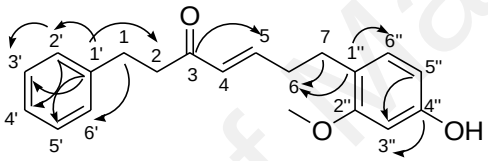

Figure 3.16: Selected HMBC correlations of **BS2**

Table 3.7: The NMR ($CDCl_3$, 600 MHz) data of **BS2** (7-(2''-Methoxy-4''-hydroxyphenyl)-1-phenyl-hept-4-en-3-one)

Position	δ_H	δ_C	HMBC
1	2.92 t (7.5)	41.9	6'
2	2.84 t (7.5)	30.2	-
3	-	199.6	5
4	6.11 br (7.0)	130.8	6
5	6.83 m	114.5	-
6	2.49 q (7.5)	34.6	4, 5
7	2.69 t (7.5)	34.3	5, 6
1'	-	141.4	2', 5', 3', 1, 2
2'	7.19 d (7.0)	128.5	4', 6'
3'	7.27 d (7.0)	120.6	5'
4'	7.19 t (7.0)	126.2	2'
5'	7.27 t (7.0)	128.6	3'
6'	7.19 d (7.0)	128.5	2'
1"	-	132.7	6, 7, 6''
2"	-	56.02	-
3"	6.65 m	111.5	-
4"	-	144.1	3''
5"	6.65 m	121.0	3''
6"	6.83 m	146.6	-
2"-OMe	3.85 s	146.6	-
4"-OH	-	-	-

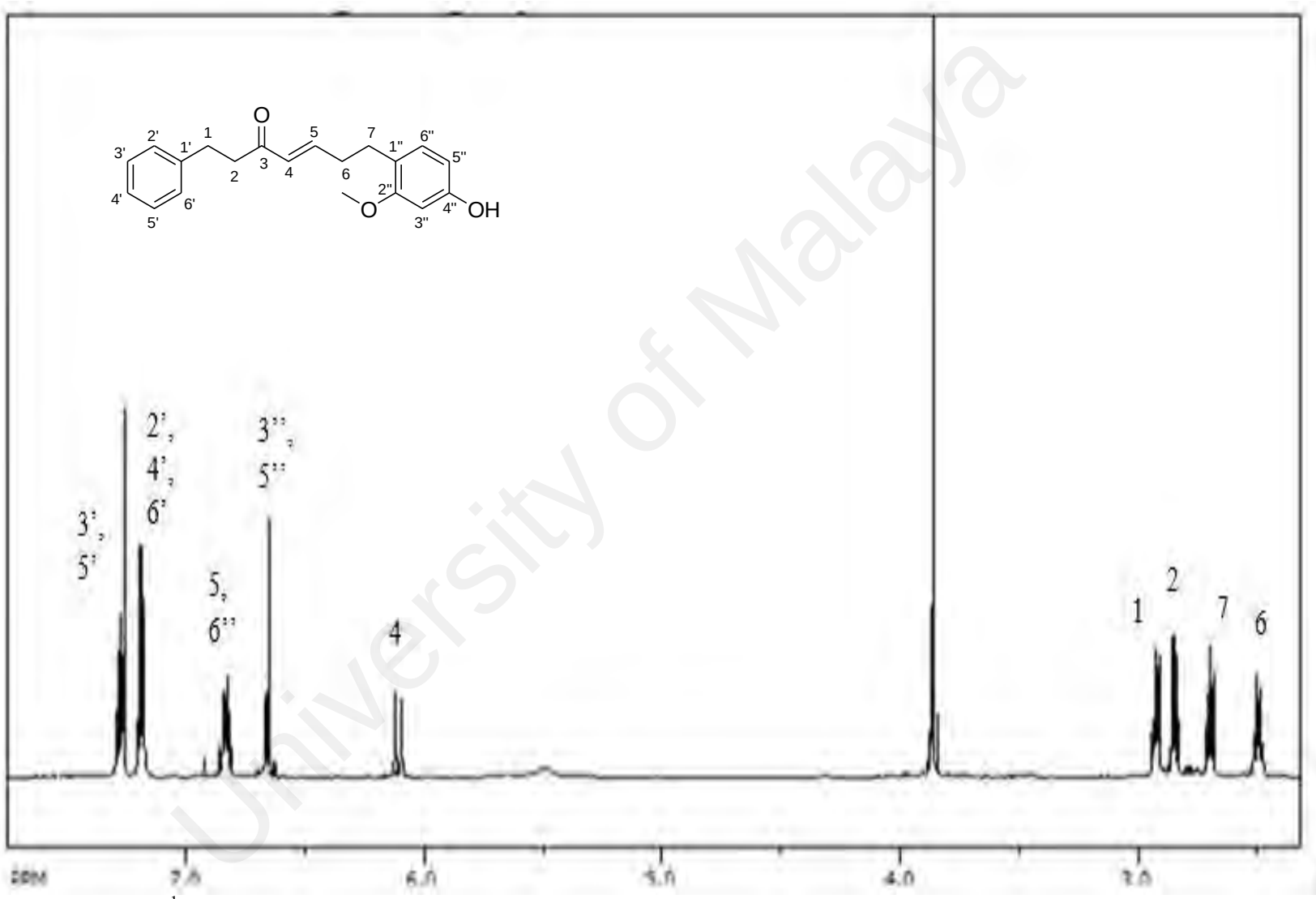

Figure 3.17: ^{1}H NMR spectrum ($CDCl_3$, 600 MHz) of **BS2** (7-(2”-Methoxy-4”-hydroxyphenyl)-1-phenyl-hept-4-en-3-one)

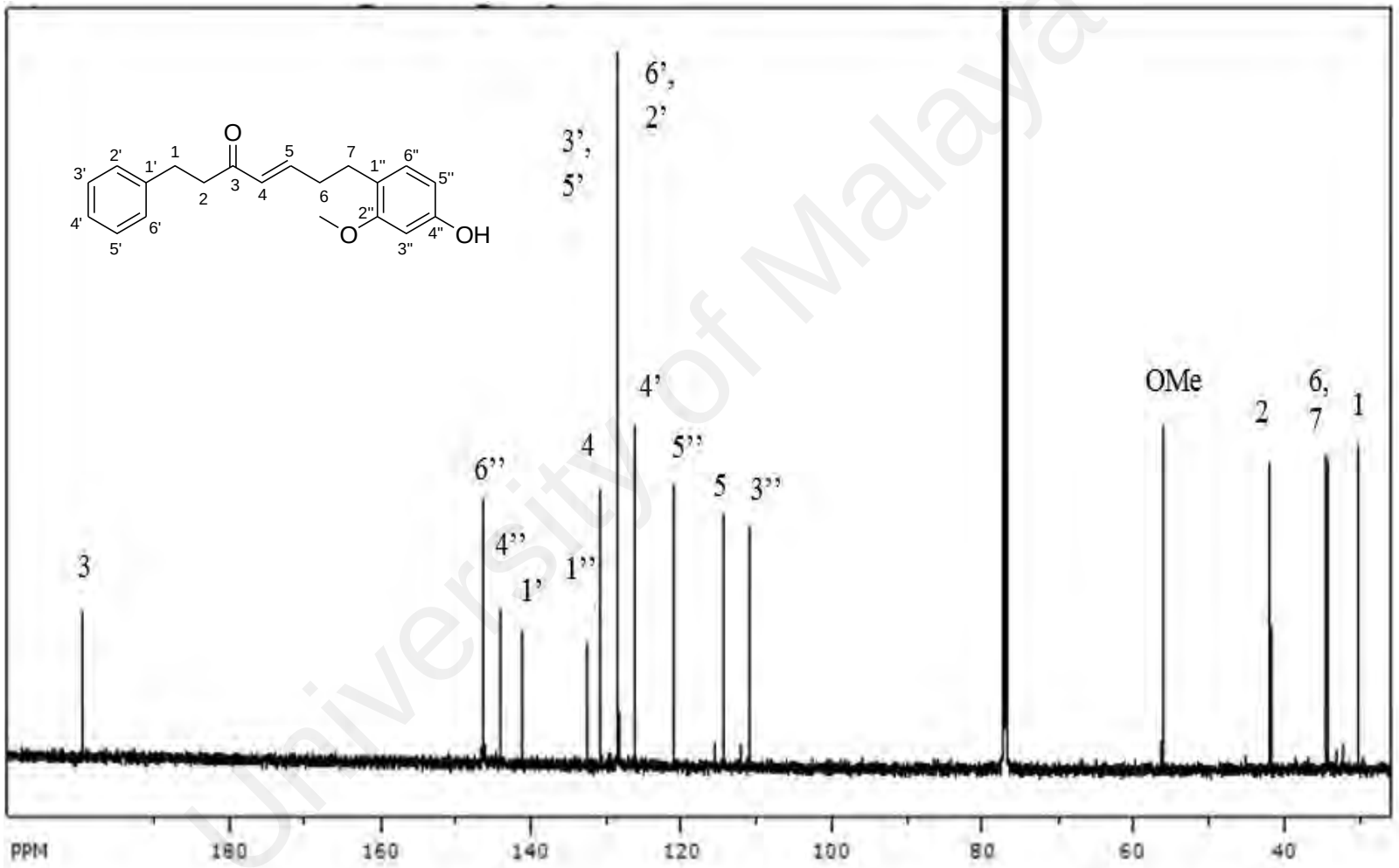

Figure 3.18: ^{13}C NMR spectrum ($CDCl_3$, 150 MHz) of **BS2** (7-(2”-Methoxy-4”-hydroxyphenyl)-1-phenyl-hept-4-en-3-one)

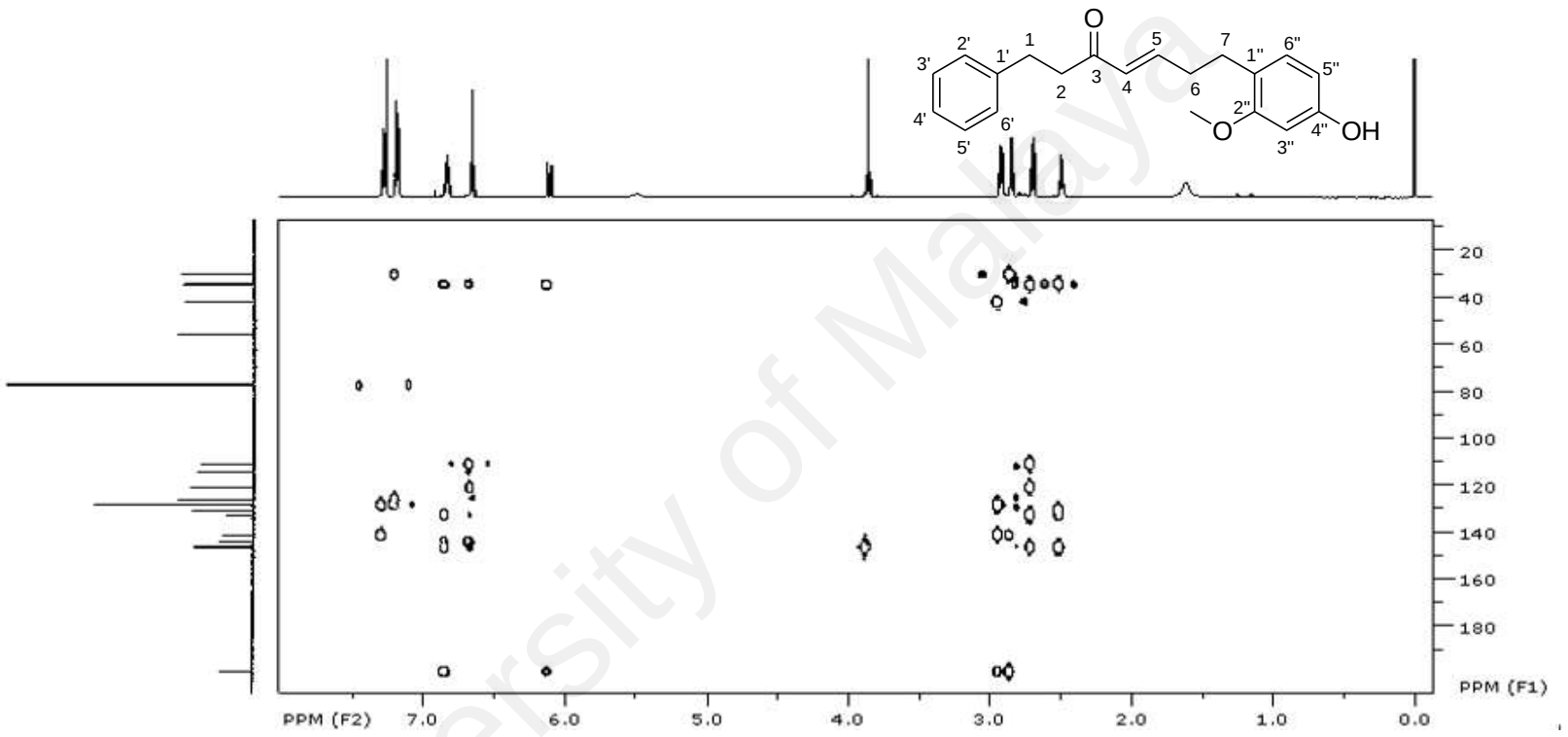

Figure 3.19: HMBC spectrum ($CDCl_3$, 150 MHz) of **BS2** (7-(2"-Methoxy-4"-hydroxyphenyl)-1-phenyl-hept-4-en-3-one)

3.2.3 BS3: 3,5,7-trihydroxy-flavone

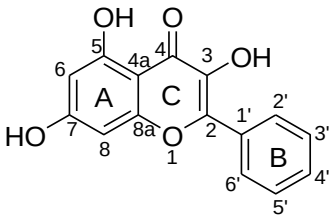

BS3 was isolated as light yellow oil with molecular formula $C_{15}H_{10}O_5$ as determined by HREIMS *m/z* 269.0481 $[M-H]^-$ (calculated for $C_{15}H_{10}O_5$ - H, 271.0). The UV spectrum showed two absorption maxima at 213, 269, 318 and 367 nm. The IR spectrum indicated the presence of hydroxy (3352 cm^{-1}), carbonyl (1599 cm^{-1}) and ether (1220 cm^{-1}) functional groups.

The ^1H NMR spectrum (Figure 3.21 and Table 3.8) displayed seven resolved aromatic proton signals. Of the seven resolved aromatic proton signals, two signals were observed as singlet at δ_H 5.61 and δ_H 5.40, two doublets overlapped at δ_H 7.38 and one doublet at δ_H 6.69, and two triplets at δ_H 6.69 and 6.64.

The ^{13}C NMR (Figure 3.22 and Table 3.8) showed the presence of seven *sp2* tertiary carbon signals at δ_C 121.6, 120.1, 120.1, 119.4, 119.4, 90.1 and 84.6; and six *sp2* quartenary carbon signals at δ_C 158.2, 156.5, 153.1, 137.7, 123.2 and 94.9. The carbon signals at δ_C 158.2 (C(5)) and δ_C 156.5 (C(7)) suggests that these quaternary carbons are located adjacent to an oxygen atom.

The HMBC experiment (Figure 3.20, 3.23 and Table 3.8) showed J^3 correlations from C(4a) to H(6), C(4a) to H(8), C(6) to H(8); and J^2 correlations from C(5) to H(6), C(7) to H(6) and C(8a) to H(8) thereby connecting the ring A and C together. The observation of HMBC J^3 correlations from C(2) to H(2'), C(2) to H(6'), C(1') to H(3'),

C(1') to H(5'), C(2') to H(6'), C(4') to H(6'), C(5') to H(3'), C(6') to H(2'); and J^2 correlations from C(1') to H(2'), C(1') to H(6'), C(3') to H(2'), C(5') to H(6') and C(6') to H(5') thereby confirming ring C and its connectivity with ring B.

BS3 is a known flavonol and the experimental data were in agreement with the reported data (Deep & Siddqui, 2012; Wollenweber *et al.,* 2003).

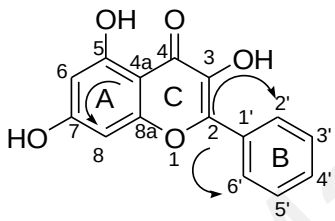

Figure 3.20: Selected HMBC correlations of **BS3**

Table 3.8: The NMR ($CDCl_3$, 600 MHz) data of **BS3** (3,5,7-trihydroxy-flavone)

Position	δ_H	δ_C	HMBC
1	-	-	-
2	-	137.7	2', 6'
3	-	n.d.[a]	-
4	-	n.d.[a]	-
4a	-	94.9	6, 8
5	-	158.2	6
6	5.40 s	84.6	8
7	-	156.5	-
8	5.61 s	90.1	-
8a	-	153.1	8
1'	-	123.2	2', 3', 5', 6'
2'	7.38 d (8.0)	119.4	6'
3'	6.69 d (8.0)	120.1	2'
4'	6.64 t (8.0)	121.6	6'
5'	6.69 t (8.0)	120.1	3' ,6'
6'	7.38 d (8.0)	119.4	5'

[a] n.d. Not detectable

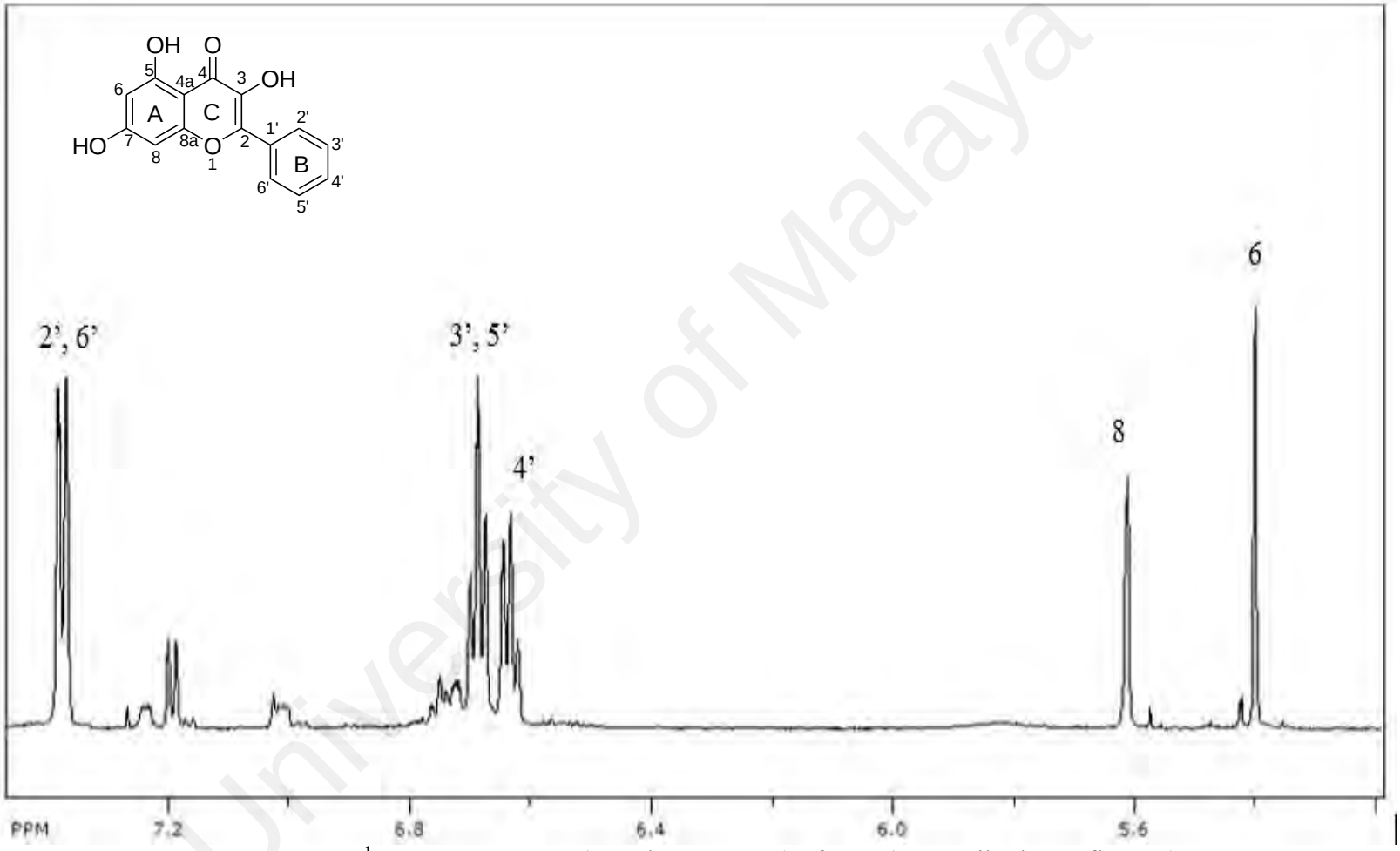

Figure 3.21: ^{1}H NMR spectrum ($CDCl_3$, 600 MHz) of **BS3** (3,5,7-trihydroxy-flavone)

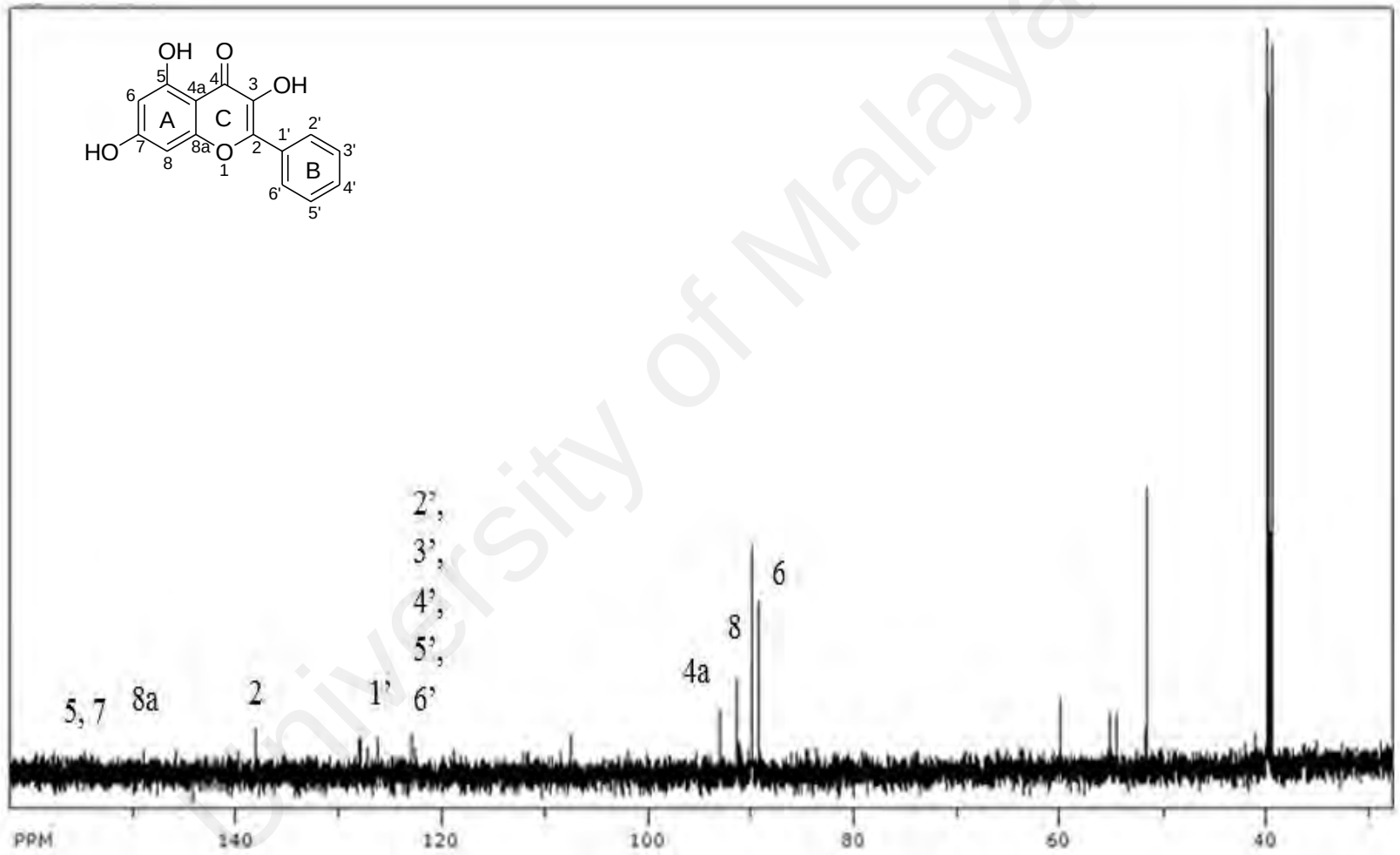

Figure 3.22: ^{13}C NMR spectrum ($CDCl_3$, 150 MHz) of **BS3** (3,5,7-trihydroxy-flavone)

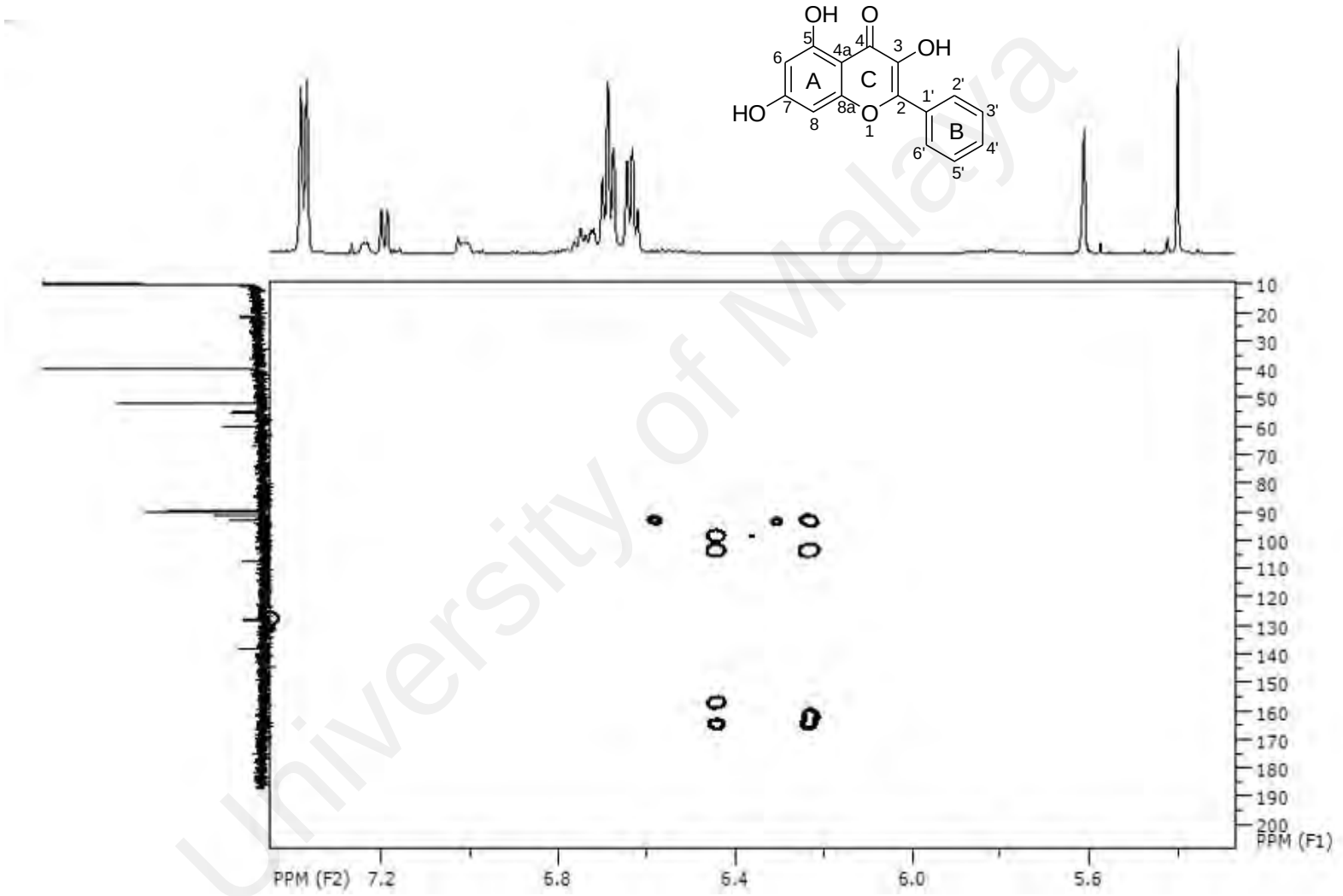

Figure 3.23: HMBC spectrum ($CDCl_3$, 150 MHz) of **BS3** (3,5,7-trihydroxy-flavone)

3.2.4 BS4: 1,7-diphenylhept-4-en-3-one

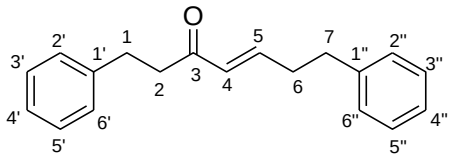

BS4 was isolated as light yellow oil with molecular formula $C_{19}H_{20}O_4$ as determined by HREIMS *m/z* 283.1791 $[M+H+H_2O]^+$ (calculated for $C_{19}H_{20}O + H + H_2O$, 283.1698). The UV spectrum showed absorption maxima at 280, 245, 210 nm. The IR spectrum indicated the presence of conjugated carbonyl group (1719 cm^{-1}), and the aromatic ring (1458 cm^{-1}).

The ^1H NMR spectrum (Figure 3.25 and Table 3.9) displayed sixteen proton signals. Of the sixteen proton signals, one signal were observed as doublet of doublet of doublet at δ_H 2.53, three signals were observed as triplet at δ_H 2.92, 2.84, and 2.76, two signals were observed as doublet of triplet at δ_H 6.84 and 6.11, and two clusters of multiplets at δ_H 7.28 (integrate for three protons) and δ_H 7.19 (integrate for four protons).

The ^{13}C NMR spectrum (Figure 3.26 and Table 3.9) showed the presence four *sp3* secondary carbon signals at δ_C 41.9, 34.6, 34.3, 30.2; ten *sp2* tertiary carbon signal at δ_C 128.7, 128.7, 128.5, 128.5, 128.5, 128.5, 128.2, 126.7, 126.7, 126.6; two *sp2* tertiary carbon signals at δ_C 146.4 and 130.9; and three sp^2 quaternary carbon signals at δ_C 199.6, 141.4 and 140.8. The carbon signal at δ_C 199.6 (C(3)) indicated the presence of carbonyl function while the carbon signal at δ_C 130.9 (C(4)) and 146.4 (C(5)) indicate the presence of double bond C(4)=C(5) function.

The HMBC spectrum (Figure 3.24, 3.27 and Table 3.9) showed J^2 correlations from C(3) to H(4), C(1') to H(1) and C(1'') to H(7); and J^3 correlations from C(1) to H(2'), C(1) to H(6'), C(2) to H(4), C(3) to H(1), C(3) to H(5), C(4) to H(6), C(6) to H(4), C(1') to H(3'), C(1') to H(5'), C(2') to H(6'), C(2') to H(4'), C(1'') to H(5''), C(1'') to

H(3’’), C(2’’) to H(6’’), C(3’’) to H(5’’), C(4’’) to H(2’’), C(5’’) to H(3’’),and C(6’’) to C(4’’) thereby confirming both ring connected with the aliphatic chain.

BS4 is a known diarylheptanoid and the experimental data were in agreement with the reported data (An *et al.*, 2006; Itokawa *et al.*, 1981; Sun *et al.*, 2008; Wu *et al.*, 2015; Yasukawa *et al.*, 2008).

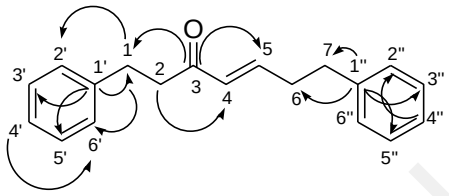

Figure 3.24: Selected HMBC correlations of **BS4** (1,7-diphenylhept-4-en-3-one)

Table 3.9: The NMR ($CDCl_3$, 600 MHz) data of **BS4** (1,7-diphenylhept-4-en-3-one)

Position	δ_H	δ_C	HMBC
1	2.92 t (7.5)	30.2	2’, 6’
2	2.84 t (7.5)	41.9	4
3	-	199.6	1, 4, 5
4	6.11 dt (15.0, 1.0)	130.9	6
5	6.84 dt (15.0, 7.0)	146.4	-
6	2.53 ddd (15.0, 7.0, 1.0)	34.3	4
7	2.76 t (7.0)	34.6	-
1'	-	141.4	1, 5’
2'	7.19 m	126.7	6’, 4’
3'	7.28 m	128.5	5’
4'	7.19 m	126.6	2’, 6’
5'	7.28 m	128.5	3’
6'	7.19 m	126.7	2’
1"	-	140.8	6, 7, 3’’, 5’’
2"	7.19 m	128.7	6’’
3"	7.28 m	128.5	5’’
4"	7.19 m	128.2	2’’, 6’’
5"	7.28 m	128.5	3’’
6"	7.19 m	128.7	2’’, 4’’

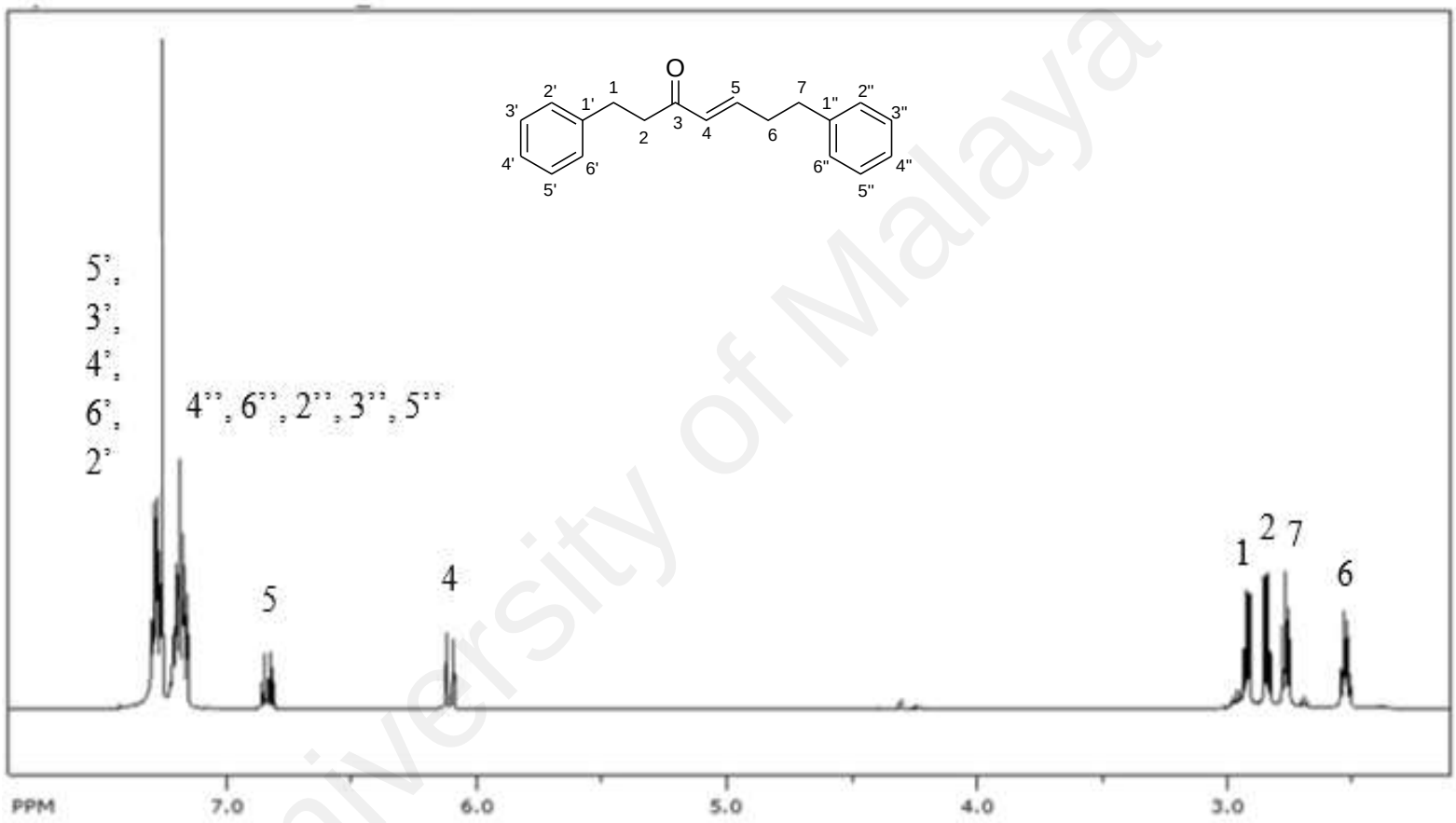

Figure 3.25: ^{1}H NMR spectrum ($CDCl_3$, 600 MHz) of **BS4** (1,7-diphenylhept-4-en-3-one)

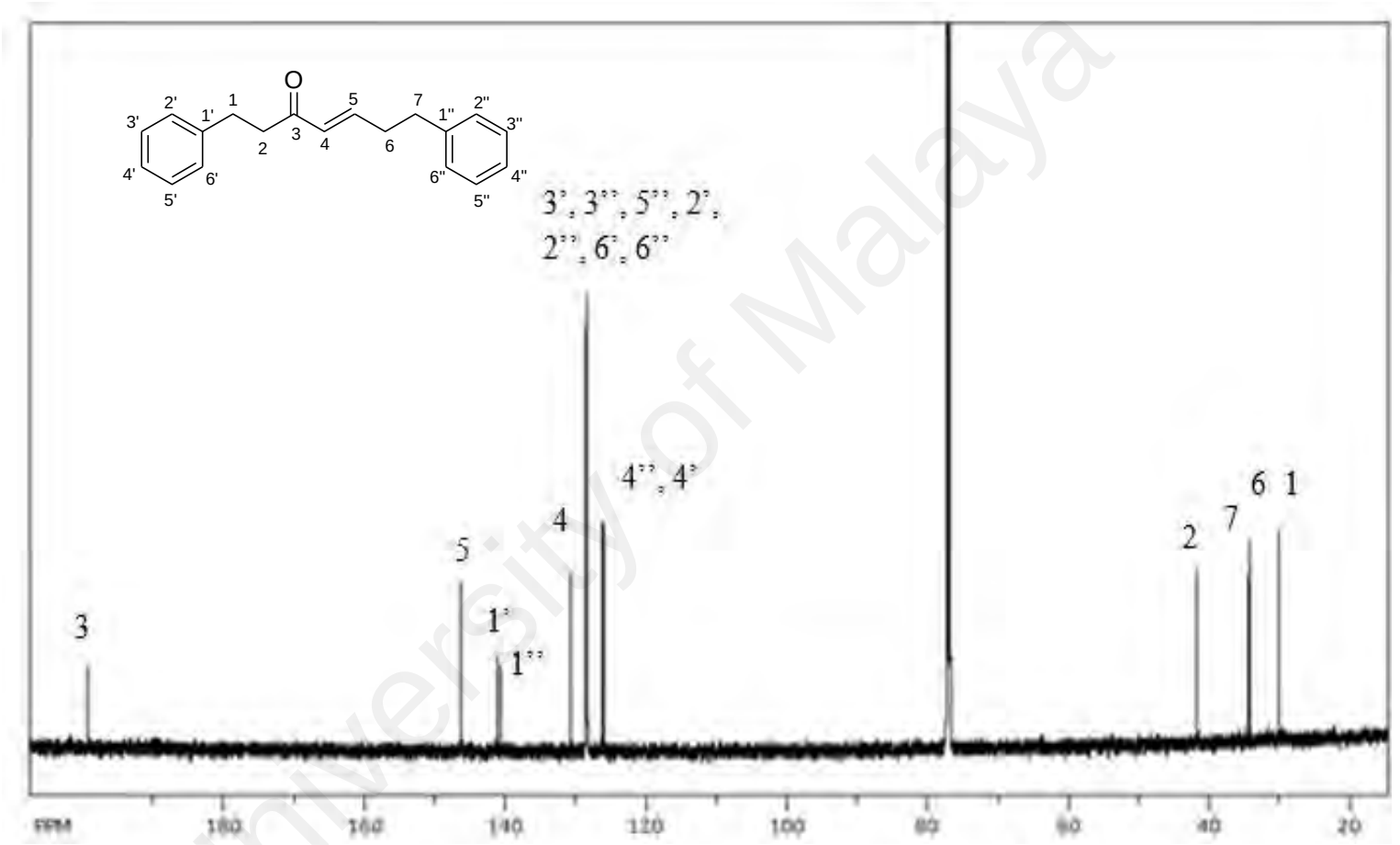

Figure 3.26: ^{13}C NMR spectrum ($CDCl_3$, 150 MHz) of **BS4** (1,7-diphenylhept-4-en-3-one)

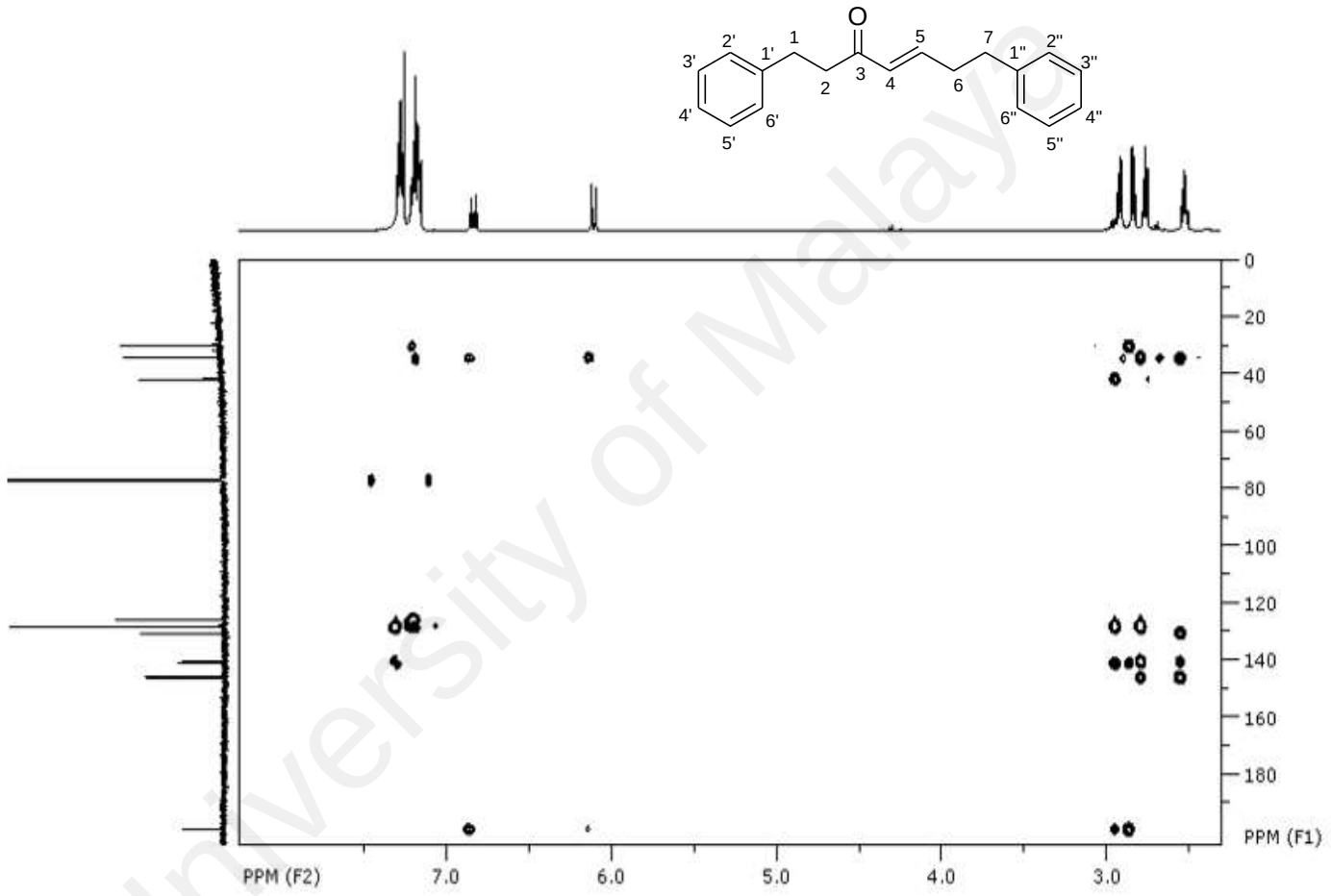

Figure 3.27: HMBC spectrum ($CDCl_3$, 150 MHz) of **BS4** (1,7-diphenylhept-4-en-3-one)

3.2.5 Antioxidant assay – Ferric reducing antioxidant power

Measurement of reducing ability of the antioxidant property was performed using FRAP method as described by Benzie & Strain (1996). The principle of this method is based on the reduction of a ferric-tripyridyl-triazine complex to its ferrous, colored form in the presence antioxidants, measuring the ability to reduce Fe^{3+} to Fe^{2+}. Fe^{2+} is measured spectrophotometrically via determination of its colored complex 2,4,6-tris(2pyridyl)-*s*-triazine (TPTZ), which has a high absorbance at 593 nm. Since the antioxidant activity of a substance is usually correlated directly to its reducing capacity, FRAP assay provides a reliable method to study the antioxidant activity of various compound (Benzie & Strain, 1996). This method has been frequently used for a rapid evaluation of the total antioxidant capacity of plant extracts containing flavonoids (Luximon-Ramma *et al.,* 2002). **BS1 - BS4**, ascorbic acid and caffeic acid were subjected to FRAP assay. Ascorbic acid and caffeic acid were used as standards and positive controls.

In this assay, the results revealed that a good linearity of ferrous sulfate ($FeSO_4$) was obtained within the range of 2–24 µg/mL (R^2 = 0.9984) (Figure 3.28).

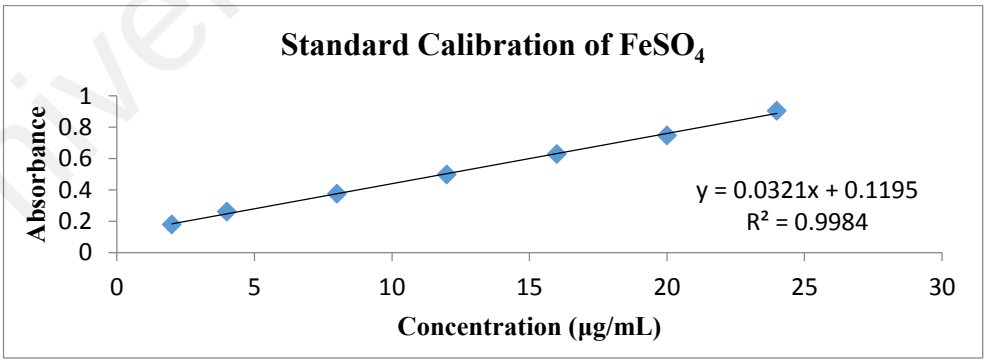

Figure 3.28: $FeSO_4$ standard curve. Standard equation: y= 0.0321x + 0.1195; R^2 = 0.9984

Caffeic acid (4.74 ± 0.02 mmol/g) had the strongest FRAP activities. Second is **BS2** (3.68 ± 0.03 mmol/g), third is **BS3** (2.23 ± 0.06 mmol/g) and fourth is ascorbic acid (4.26 ± 0.11 mmol/g) (Table 3.10). Compound **BS1** and **BS4** does not show significant antioxidant activity in comparison with ascorbic acid and caffeic acid (Babu *et al.*, 2013; Garrido *et al.*, 2012; Lu *et al.*, 2014).

Table 3.10: Ferric reducing antioxidant capacity of **BS1**, **BS2**, **BS3**, **BS4**, ascorbic acid and caffeic acid

Sample (12 μg/mL)	Antioxidant capacity (mmol/g)	Standard deviation
BS1	n. a.[a]	n. a.[a]
BS2	3.68	0.03
BS3	2.23	0.06
BS4	n. a.[a]	n. a.[a]
Ascorbic acid	4.26	0.11
Caffeic acid	4.74	0.02

[a] n. a. Not available

BS1 is a member of the chalcone group. Chalcones are flavonoids with open C-ring (Figure 3.29) and hence electron delocalize poorer than other ring-C intact flavonoids. However, the structure of chalcones allows for greater geometrical flexibility which is important for ligand-binding affinity. In a 2007 study, Kozlowski *et al.* demonstrated the importance of the α,β-double bond (Figure 3.29) in chalcone structure where the absence of this double bond would decreased the antioxidant activity. In **BS1** (Figure 3.30), the absent of α,β-double bond could be a reason for the lack of antioxidant activity. The presence of the OH substituent group (location and number are important criteria for increament the antioxidant activity in chalcones (Kozlowski *et al.*, 2007; Lien *et al.*, 1998). However, in **BS1**, the number nor the location of the OH substituent did not give any significant contribution to the antioxidant activity.

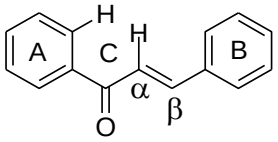

Figure 3.29: α,β-Double bond of chalcone with opened C-ring

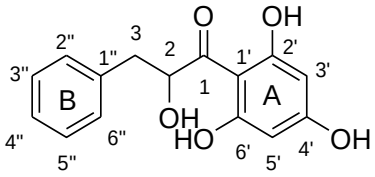

Figure 3.30: Structure of **BS1**

BS3 is known as galangin. Previous report showed that caffeic acid has higher FRAP activity in comparison with galangin. The antioxidant capacity of caffeic acid and galangin is 1.813 μmol/mg and 0.161 μmol/mg, respectively. The FRAP data of these compounds were expressed as μmol of Myricetin-3-*O*-glucoside equivalents per mg of dried sample (Csepregi *et al.,* 2016). Our result shows similar antioxidant trend in agreement with previous studies, *i.e.* caffeic acid value (4.74 ± 0.02 mmol/g) is higher than **BS3** (2.23 ± 0.06 mmol/g). The values obtained were expressed as mmol/g of ferrous equivalent Fe (II) per gram of dried sample.

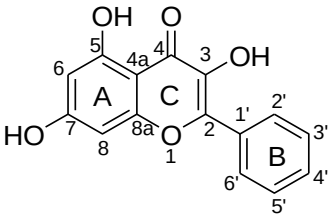

Figure 3.31: Structure of **BS3**

Both compound **BS2** and **BS4** (Figure 3.32) possess similar structures. However, **BS2** (new compound) show higher antioxidant activity when compared to **BS4** (known compound). **BS4** has never been evaluated for the antioxidant activity before. The antioxidant activity of **BS2** may be attributed to the phenolic and methoxy functionality (Bairwa *et al.*, 2014; Somparn *et al.*, 2007) present in the structure, in agreement with

previous report which stated that the antioxidant activity increased proportionally to the polyphenol contents and appears to be the trend in many plant species (Oktay *et al.,* 2003).

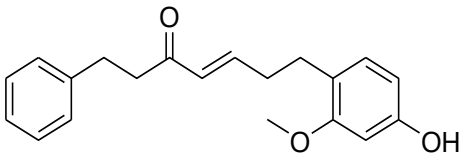

BS2

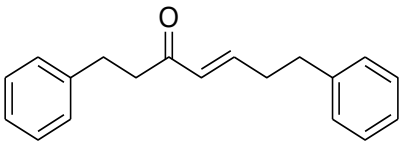

BS4

Figure 3.32: Structures of **BS2** and **BS4**

CHAPTER 4: EXPERIMENTAL

4.1 Photophysical studies of anthraquinones

4.1.1 General

The absorption spectra were recorded between 190 and 1100 nm on Cary 60 UV-Vis spectrometer, Agilent Technology using methanol as solvent. Emission spectra were obtained from the Horiba Scientific Fluoromax-4 spectrofluorometer (HORIBA Instruments Incorporated, Edison, USA) at 25 °C at 5 nm slit width for both excitation and emission measurements. **AQ1-AQ10** was obtained from *Morinda citrifolia,* which was collected from Kuala Lipis, Pahang on June 2013 (Nur Atiqah, 2016). Concentration 1.42 x 10^{-4} M of anthraquinones **AQ1-AQ10** were used in the experiments. The NMR spectra data were obtained from the 600 MHz Bruker AVANCE III with chemical shifts (δ) expressed in ppm and TMS as an internal standard in $CDCl_3$ or CD_3OD. The coupling constants (*J*) are reported in Hz. The ESI-MS data were obtained from the Agilent 6490 Triple Quad (Agilent Technologies, Santa Clara, CA, USA) mass-spectrometer equipped with Agilent 1290 Infinity u-HPLC system. The HRESIMS data were obtained from the Agilent 6530 Q-TOF (Agilent Technologies, Santa Clara, CA, USA) mass-spectrometer equipped with Agilent 1290 Infinity u-HPLC system. The IR measurement was carried out on the Perkin-Elmer RX1 FT-IR (Perkin Elmer, Waltham, MA, USA) spectrophotometer using NaCl cell.

4.1.2 Fluorescence measurement of anthraquinone

4.1.2.1 Absorption data

The molar absorptivity (Table 4.1) of the solution in methanol were calculated by applying this on equation (1)

$$A = \epsilon lc \qquad (1)$$

where A is the absorbance, ϵ is the molar absorptivity of the solution, l is the length of solution the light passes through (cm) and c is the concentration of solution (mol dm^{-3}). The length of solution the light passes through used is 1.0 cm. Concentration between 1.42 x 10^{-4} M of anthraquinones **AQ1-AQ10** were used in the experiments.

Table 4.1: Absorbance and their coefficient of anthraquinones **AQ1** – **AQ10**

Entry	λ_{max} (nm)	Intensity (a.u)	ε, (M cm^{-1})
AQ1	241	0.39	2749.26
	313	0.20	1434.98
	365	0.06	442.56
	387	0.06	402.33
	419	0.06	442.56
	456	0.07	482.80
AQ2	203	0.23	1642.92
	248	0.21	1475.63
	279	0.32	2284.39
	316	0.10	737.88
	369	0.06	446.78
AQ3	204	0.60	4248.97
	245	0.29	2064.99
	278	0.37	2626.67
	412	0.09	601.05
AQ4	205	1.32	9285.23
	239	0.77	5452.83
	278	1.64	11566.84
	360	0.18	1300.46
AQ5	203	0.64	4517.61
	267	0.05	370.04
	309	0.02	111.37
AQ6	201	0.53	3740.23
	219	0.78	5478.41

Table 4.1, continued

Entry	λ_{max} (nm)	Intensity (a.u)	ε, (M cm^{-1})
	269	0.87	6122.07
	411	0.24	1705.99
AQ7	202	0.51	3572.72
	247	0.49	3439.18
	285	0.41	2869.54
	415	0.12	827.06
AQ8	204	0.58	4073.51
	230	0.75	5305.61
	259	0.71	4975.78
	290	0.35	2446.88
	447	0.26	1863.47
AQ9	202	0.53	3723.99
	223	0.32	2274.25
	253	0.49	3485.15
	327	0.06	447.99
	406	0.11	783.95
AQ10	203	0.65	4609.65
	222	0.57	4004.38
	249	0.60	4261.28
	394	0.13	890.34

4.1.2.2 Emission data

Table 4.2: Emission of anthraquinones **AQ1 – AQ10**

Entry	λ_{max} (nm)	Intensity (a.u)
AQ1	307	14.28
	469	15.04
	472	12.80
	471	13.38
	479	17.13

Table 4.2, continued

Entry	λ_{max} (nm)	Intensity (a.u)
	479	13.97
AQ2	314	53.40
	307	42.19
	424	24.70
	431	30.84
AQ3	426	127.62
	309	61.18
	472	23.50
AQ4	354	57.85
	326	18.72
	443	27.99
AQ5	321	256.26
	403	174.70
AQ6	586	295.30
	583	410.06
	585	640.62
	583	430.79
AQ7	558	643.59
	567	721.61
	559	304.16
AQ8	342	112.79
	438	44.28
	323	38.53
	612	100.03
AQ9	338	242.61
	356	73.20
	572	67.98
	577	119.34

Table 4.2, continued

Entry	λ_{max} (nm)	Intensity (a.u)
AQ10	341	176.68
	430	61.15
	583	76.91

4.1.2.3 Stokes shift data

Stokes shift (Table 4.3) describes the difference in wavelength between the maximum of the excitation spectrum (shorter wavelength, higher energy), and the maximum of the emission spectrum (longer wavelength, lower energy) where examination of the Jablonski diagram (Figure 1.2) reveals that the energy of the emission is typically less than that of absorption. This phenomenon was first observed by Sir. G. G. Stokes in 1852 at the University of Cambridge (Demasa & Crosby, 1968).

Table 4.3: Absorbance, emission and Stokes shift of anthraquinones **AQ1** – **AQ10**

Entry	Excitation(nm)	Emission (nm)	Stokes shift
AQ1	241	307	66
	313	469	156
	365	472	107
	387	471	84
	419	479	60
	456	479	23
AQ2	203	n.d.[a]	n.a.[b]
	248	314	66
	279	307	28
	316	424	108
	369	431	62
AQ3	204	n.d.[a]	n.a.[b]
	245	426	181
	278	309	31
	412	472	60

Table 4.3, continued

Entry	Excitation(nm)	Emission (nm)	Stokes shift
AQ4	205	n.d.[a]	n.a.[b]
	239	354	115
	278	326	48
	360	443	83
AQ5	203	n.d.[a]	n.a.[b]
	267	321	54
	309	403	94
AQ6	201	586	385
	219	583	364
	269	585	316
	411	583	172
AQ7	202	n.d.[a]	n.a.[b]
	247	558	311
	285	567	282
	415	559	144
AQ8	204	n.d.[a]	n.a.[b]
	230	342	112
	259	438	179
	290	323	33
	447	612	165
AQ9	202	n.d.[a]	n.a.[b]
	223	338	115
	253	356	103
	327	572	245
	406	577	171
AQ10	203	n.d.[a]	n.a.[b]
	222	341	119
	249	430	181
	394	583	189

[a] n.d. Not detected. [b] n.a. Not available

4.1.2.4 Quantum yield

Quantum yield is the number of emitted photons relative to the number of absorbed photons. Substances with the largest quantum yields, approaching unity, display the brightest emissions (Demasa & Crosby, 1968).

The fluorescence quantum yields of the anthraquinones in methanol were measured relative to quinine sulphate ($\Phi_F = 0.55$ in 0.1 N aqueous H_2SO_4 as standards (Demasa & Crosby, 1968); where $y = 6679.5x + 32.851$; $r^2 = 0.997$) using equation (2). The fluorescence quantum yield of quinine sulphate (Figure 4.1) was assumed to be 0.55 (Demasa & Crosby, 1968). A refractive index correction was applied by multiplying the integrated fluorescence intensity of each sample by the square of the refractive index of the solvent by applying the equation

$$Ø_{sample} = Ø_{Reference} \left(\frac{m_{sample}}{m_{Reference}}\right) \left(\frac{Refractive\ index^2{}_{sample}}{Refractive\ index^2{}_{Reference}}\right) \qquad (2)$$

where m is the integrated fluorescence intensity of each sample and the refractive index of reference used is 1.346.

For each compound, the stock solutions were prepared at concentration that gave an absorbance of 0.1 at the excitation wavelength. For anthraquinones **AQ1** – **AQ4**, a concentration of 2 μM was prepared and 10 μM concentration was prepared for quinine sulphate. Stock solutions were diluted up to five times to enable maximum fluorescent emission intensity to fit within the spectrofluorophotometer's measurement range. All measurement were conducted in methanol except for quinine sulphate (in 0.1 N aqueous H_2SO_4), in order to generate data that could be compared directly with the literature data (Ritter *et al.,*1988).

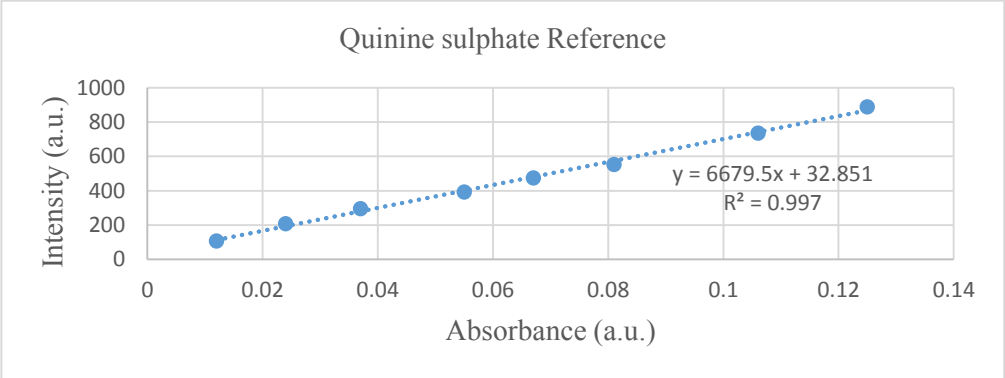

Figure 4.1: Quinine sulphate reference

Table 4.4: Quinine sulphate reference

Concentration (μM)	Absorption (a.u.)	λ (nm)	Intensity (a.u.)	Emission Wavelength (nm)
1	0.012	349.00	106.72	451.96
2	0.024	344.00	207.27	458.93
3	0.037	348.00	294.61	458.03
4	0.055	348.00	391.76	456.06
5	0.067	347.00	474.52	453.93
6	0.081	347.00	552.32	456.96
8	0.106	344.00	734.62	451.96
10	0.125	347.00	887.52	458.93

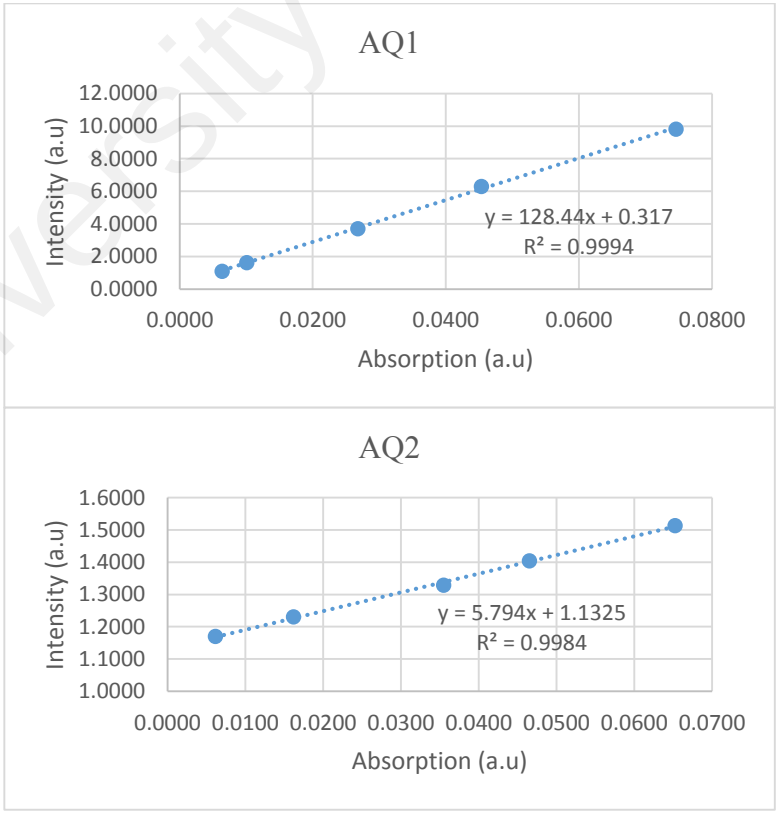

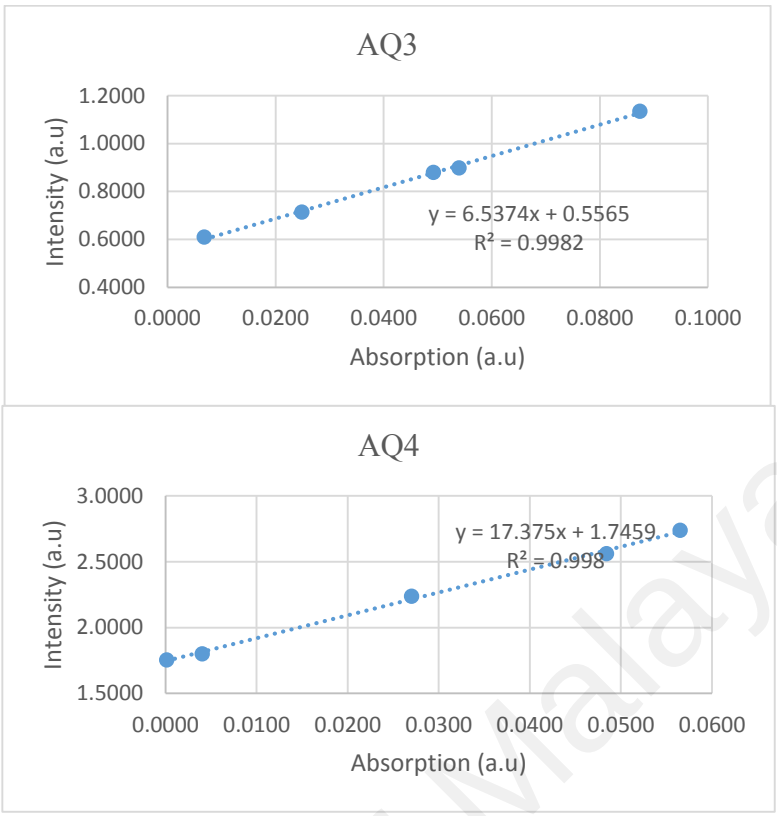

Figure 4.2: Quantum yield of anthraquinones **AQ1 – AQ4**

Table 4.5: Quantum yield data of anthraquinones **AQ1– AQ4**

	Concentration (M)	**Absorption (a.u.)**	**λ (nm)**	**Intensity (a.u.)**	**Emission Wavelength (nm)**	
AQ1	$5.94x10^{-4}$	0.075	419.98	9.8220	476.96	
	$2.98x10^{-4}$	0.045	419.98	6.2899	478.93	
	$1.49x10^{-4}$	0.027	419.98	3.7053	476.06	
	$7.46x10^{-5}$	0.010	419.98	1.6273	479.93	
	$3.73x10^{-6}$	0.006	419.98	1.0865	473.93	
					Quantum yield	0.01036
AQ2	$5.97x10^{-4}$	0.065	248.00	1.5131	314.07	
	$2.98x10^{-4}$	0.047	248.00	1.4043	314.00	
	$1.49x10^{-4}$	0.036	248.00	1.3285	314.96	
	$7.46x10^{-5}$	0.016	248.00	1.2298	314.00	
	$3.73x10^{-5}$	0.006	248.00	1.1694	314.07	
					Quantum yield	0.00047
AQ3	$5.97x10^{-4}$	0.087	245.99	1.1352	426.06	
	$2.98x10^{-4}$	0.054	245.99	0.8976	426.06	
	$1.49x10^{-4}$	0.049	245.99	0.8799	426.03	
	$7.46x10^{-5}$	0.025	245.99	0.7135	426.96	
	$3.73x10^{-5}$	0.007	245.99	0.6095	426.96	
					Quantum yield	0.00053

Table 4.5, continued

	Concentration (M)	Absorption (a.u.)	λ (nm)	Intensity (a.u.)	Emission Wavelength (nm)	
AQ4	$5.97x10^{-4}$	0.057	239.00	2.7390	354.03	
	$2.98x10^{-4}$	0.048	239.00	2.5620	354.02	
	$1.49x10^{-4}$	0.027	239.00	2.2380	354.06	
	$7.46x10^{-5}$	0.004	239.00	1.8000	354.03	
	$3.73x10^{-5}$	0.000	239.00	1.7537	354.00	
					Quantum yield	0.00140

4.1.2.5 NMR data of anthraquinone AQ1– AQ10

Nordamnacanthal (AQ1). Yellow-orange amorphous; UV (MeOH) λ_{max} (log ε) 213 (3.37), 259 (3.60), 337 (3.15), 387 (3.06), 416 (3.02) nm; ESI-MS *m/z* 267.0 $[M-H]^-$ (calculated for $C_{15}H_8O_5$-H, 267.0). ^{1}H NMR ($CDCl_3$, 600 MHz) δ 14.05 (1H, s, 1-OH), 12.67 (1H, s, 3-OH), 10.50 (1H, s, 2-CHO), 8.32 (1H, dd, *J* = 8 and 1 Hz, H-8), 8.29 (1H, dd, *J* = 8 and 1 Hz, H-5), 7.84 (1H, m, H-7), 7.84 (1H, m, H-6), 7.33 (1H, s, H-4). ^{13}C NMR ($CDCl_3$, 150 MHz) δ 194.3 (C, 2-CHO), 187.1 (C, C-9), 181.7 (C, C-10), 169.5 (C, C-1), 168.4 (C, C-3), 139.5 (C, C-4a), 135.1 (CH, C-7), 135.0 (CH, C-6), 133.6 (C, C-10a), 133.5 (C, C-8a), 128.1 (CH, C-5), 127.3 (CH, C-8), 112.4 (C, C-2), 109.7 (CH, C-4), 109.4 (C, C-9a).

Damnacanthal (AQ2). Yellow amorphous; UV (MeOH) λ_{max} (log ε) 203 (3.22), 248 (3.17), 279 (3.36), 316 (2.87), 379 (2.65) nm; ESI-MS with m/z 281.0 $[M-H]^-$ (calculated for $C_{16}H_{10}O_5$-H, 281.0). ^{1}H NMR ($CDCl_3$, 600 MHz) δ 12.28 (1H, s, 3-OH), 10.47 (1H, s, 2-CHO), 8.30 (1H, dd, *J* = 8 and 1 Hz, H-8), 8.25 (1H, dd, *J* = 8 and 1 Hz, H-5), 7.83 (1H, td, *J* = 8 and 1 Hz, H-7), 7.78 (1H, td, *J* = 8 and 1 Hz, H-6), 7.68 (1H, s, H-4), 4.13 (1H, s, 1-OMe). ^{13}C NMR ($CDCl_3$, 150 MHz) δ 194.3 (C, 2-CHO), 182.3 (C, C-10), 180.5 (C, C-9), 167.0 (C, C-1), 166.9 (C, C-3), 142.0 (C, C-4a), 135.2 (C, C-8a), 135.2 (CH, C-7), 134.0 (CH, C-6), 132.8 (C, C-10a), 127.7 (CH, C-5), 127.4 (CH, C-8), 118.4 (C, C-2), 118.0 (C, C-9a), 113.4 (CH, C-4), 65.0 (C, 1-OMe).

Rubiadin (AQ3). Yellow amorphous; UV (MeOH) λ_{max} (log ε) 204 (3.63), 245 (3.31), 278 (3.42), 412 (2.78) nm; ESI-MS *m/z* 253.0 $[M-H]^-$ (calculated for $C_{15}H_{10}O_4$-H, 253.1). ^{1}H NMR ($CDCl_3$, 600 MHz) δ 13.11 (1H, s, 1-OH), 8.22 (1H, dd, *J* = 8 Hz, H-8), 8.15 (1H, dd, *J* = 5 Hz, H-5), 7.73 (1H, td, *J* = 8 Hz, H-7), 7.69 (1H, td, *J* = 8 Hz, H-6), 7.16 (1H, s, H-4), 2.14 (1H, s, 2-Me). ^{13}C NMR ($CDCl_3$, 150 MHz) δ 186.8 (C, C-9), 183.8 (C, C-10), 163.3 (C, C-1), 162.8 (C, C-3), 134.1 (CH, C-6), 134.5 (CH, C-7), 134.5 (C, C-8a), 133.6 (C, C-10a), 132.1 (C, C-4a), 127.2 (CH, C-5), 127.0 (CH, C-8), 119.2 (C, C-9a), 109.9 (C, C-2), 107.9 (CH, C-4), 8.2 (C, 2-Me).

1-Methoxy-2-methyl-3-hydroxylanthraquinone (AQ4). Yellow amorphous; UV (MeOH) λ_{max} (log ε) 205 (3.97), 239 (3.74), 278 (4.06), 360 (3.11) nm; ESI-MS *m/z* 267.0 $[M-H]^-$ (calculated for $C_{16}H_{12}O_4$-H, 267.1). ^{1}H NMR ($CDCl_3$, 600 MHz) δ 8.21 (1H, dd, *J* = 8 and 1 Hz, H-8), 8.12 (1H, dd, *J* = and 1 Hz, H-5), 7.72 (1H, td, *J* = 8 and 1 Hz, H-7), 7.65 (1H, td, *J* = 8 and 1 Hz, H-6), 7.40 (1H, s, H-4), 3.84 (1H, s, 1-OMe), 2.21 (1H, s, 2-Me). ^{13}C NMR ($CDCl_3$, 150 MHz) δ 184.4 (C, C-10), 181.7 (C, C-9), 162.0 (C, C-3), 161.5 (C, C-1), 135.3 (C, C-8a), 134.6 (CH, C-7), 133.2 (CH, C-6), 132.8 (C, C-10a), 127.7 (C, C-2), 127.4 (CH, C-8), 126.6 (CH, C-5), 118.9 (C, C-9a), 109.7 (CH, C-4), 61.2 (C, 1-OMe), 9.2 (C, 2-Me).

1-Hydroxy-3-methoxyanthraquinone (AQ5). Yellow amorphous; UV (MeOH) λ_{max} (log ε) 203 (3.65), 267 (2.57), 307 (2.05) nm; ESI-MS *m/z* 253.0 $[M-H]^-$ (calculated for $C_{15}H_{10}O_4$-H, 253.1) ^{1}H NMR ($CDCl_3$, 600 MHz) δ 13.33 (1H, s, 1-OH), 8.33 (1H, m, H-5), 8.33 (1H, m, H-8), 7.85 (1H, m, H-6), 7.85 (1H, m, H-7), 7.53 (1H, s, H-4), 6.26 (1H, s, H-2), 3.42 (1H, s, 3-OMe).

1,6-Dihydroxy-2-methylanthraquinone (AQ6). Yellow-orange amorphous. UV (MeOH) λ_{max} (log ε) 201 (3.57), 219 (3.74), 269 (3.79), 411 (3.23) nm; ESI-MS *m/z* 253.0

[M-H]$^-$ (calculated for $C_{15}H_{10}O_4$-H, 253.1). ^{1}H NMR ($CDCl_3$, 600 MHz) δ 13.12 (1H, s, 1-OH), 8.13 (1H, d, J = 8, H-8), 7.63 (1H, d, J = 8, H-4), 7.50 (1H, s, H-5), 7.43 (1H, d, J = 8, H-8), 7.12 (1H, d, J = 8, H-8), 2.30 (1H, s, 2-Me). ^{13}C NMR ($CDCl_3$, 150 MHz) δ 188.3 (C, C-9), 183.5 (C, C-C-10), 163.7 (C, C-6), 160.9 (C, C-1), 136.7 (CH, C-3), 136.1 (C, C-10a), 135.4 (C, C-2), 131.7 (C, C-4a), 130.1 (CH, C-8), 125.8 (C, C-7), 121.7 (CH, C-4), 119.3 (CH, C-9a), 115.4 (C, C-9a), 113.1 (CH, C-5), 16.4 (C, 2-Me).

1,3-Dihydroxy-2-methoxyanthraquinone (AQ7). Yellow amorphous. UV (MeOH) λ_{max} (log ε) 202 (3.55), 247 (3.54), 285 (3.46), 415 (2.92) nm; ESI-MS *m/z* 269.0 [M-H]$^-$ (calculated for $C_{15}H_{10}O_5$-H, 269.0). ^{1}H NMR ($CDCl_3$, 600 MHz) δ 14.81 (1H, s, 1-OH), 12.63 (1H, s, 3-OH), 8.34 (1H, dd, J = 8 and 1 Hz, H-8), 8.28 (1H, dd, J = 8 and 1 Hz, H-5), 7.82 (1H, m, H-6), 7.82 (1H, m, H-7), 7.40 (1H, s, H-4), 4.08 (1H, s, 2-OMe). ^{13}C NMR ($CDCl_3$, 150 MHz) δ 187.8 (C, C-9), 183.0 (C, C-10), 172.1 (C, C-2), 171.2 (C, C-3), 168.5 (C, C-1), 135.0 (CH, C-7), 134.7 (CH, C-6), 133.5 (C, C-8a), 133.5 (C, C-10a), 127.8 (CH, C-5), 127.4 (CH, C-8), 110.0 (C, C-9a), 109.6 (CH, C-4), 106.4 (C, C-4a), 53.4 (C, 2-OMe).

1,5,6-Trihydroxy-2-methylanthraquinone (AQ8). Orange-red amorphous. UV (MeOH) λ_{max} (log ε) 204 (3.61), 230 (3.72), 259 (3.69), 290 (3.39), 447 (3.27) nm; ESI-MS *m/z* 269.0 [M-H]$^-$ (calculated for $C_{15}H_{10}O_5$-H, 269.0). ^{1}H NMR ($CDCl_3$, 600 MHz) δ 7.75 (1H, d, J = 8, H-8), 7.68 (1H, d, J = 8, H-4), 7.45 (1H, d, J = 8, H-3), 7.13 (1H, d, J = 8, H-7), 2.32 (1H, s, 2-Me). ^{13}C NMR ($CDCl_3$, 150 MHz) δ 188.3 (C, C-10), 187.7 (C, C-9), 161.2 (C,C-1), 152.8 (C, C-6), 150.6 (CH, C-5), 136.8 (CH, C-3), 136.1 (C, C-2), 131.4 (C, C-4a), 124.7 (C, C-8a), 121.7 (CH, C-8), 120.6 (CH, C-7), 119.1 (CH, C-4), 116.7 (CH, C-10a), 115.6 (C, C-9a), 16.4 (C, 2-Me).

1-Hydroxy-2-methoxyanthraquinone (AQ9). Yellow amorphous**.** UV (MeOH) λ_{max} (log ε) 202 (3.57), 223 (3.36), 253 (3.54), 327 (2.65), 406 (2.89) nm; ESI-MS *m/z* 253.0 $[M-H]^-$ (calculated for $C_{15}H_{10}O_5$-H, 253.1). ^{1}H NMR ($CDCl_3$, 600 MHz) δ 13.03 (1H, s, 1-OH), 8.32 (1H, m, H-5), 8.32 (1H, m, H-8), 7.86 (1H, m, H-4), 7.82 (1H, m, H-6), 7.82 (1H, m, H-7), 7.79 (1H, d, J = 8, H-3), 4.86 (1H, s, 2-OMe). ^{13}C NMR ($CDCl_3$, 150 MHz) δ 182.0 (C,C-10), 160.0 (C, C-1), 160.0 (C, C-2), 135.0 (CH, C-3), 135.0 (CH, C-8a), 134.5 (CH, C-6), 134.5 (CH, C-7), 133.7 (C, C-4a), 133.7 (C, C-10a), 127.8 (CH, C-8), 127.3 (CH, C-5), 119.8 (CH, C-4), 115.2 (C, C-9a), 61.0 (C, 2-OMe).

1-Methoxy-2-hydroxyanthraquinone (AQ10). Yellow amorphous; UV (MeOH) λ_{max} (log ε) 203 (3.66), 222 (3.60), 249 (3.63), 394 (2.95) nm; ESI-MS *m/z* 253.0 $[M-H]^-$ (calculated for $C_{15}H_{10}O_4$-H, 253.1). ^{1}H NMR ($CDCl_3$, 600 MHz) δ 13.02 (1H, s, 2-OH), 8.27 (1H, m, H-5), 8.27 (1H, m, H-8), 8.14 (1H, d, J = 9, H-4), 7.78 (1H, m, H-6), 7.78 (1H, m, H-7), 7.36 (1H, d, J = 9, H-3), 4.04 (1H, s, 1-OMe). ^{13}C NMR ($CDCl_3$, 150 MHz) δ 181.7 (C, C-10), 155.3 (C, C-2), 146.2 (C, C-1), 134.2 (CH, C-6), 134.2 (CH, C-7), 134.2 (CH, C-8a), 134.2 (C, C-10a), 127.4 (CH, C-4a), 127.4 (C, C-8), 127.1 (CH, C-5), 126.1 (CH, C-4), 126.1 (C, C-9a), 120.6 (CH, C-3), 62.6 (C, 1-OMe).

4.2 Chemical constituents studies of *Boesenbergia stenophylla*

4.2.1 Source and authentication

The roots *Boesenbergia stenophylla* were obtained from Alor Setar, Malaysia on September 2012. The roots were cut into smaller pieces, air-dried, and finally subjected to extraction. A voucher of the specimen is deposited at the Herbarium of Chemistry Department, University of Malaya.

Figure 4.3: The roots of *Boesenbergia stenophylla*

4.2.2 General

The NMR spectra data were obtained from the 600 MHz Bruker AVANCE III with chemical shifts (δ) expressed in ppm and TMS as an internal standard in $CDCl_3$ or CD_3OD. The coupling constants (*J*) are reported in Hz. The ESI-MS data were obtained from the Agilent 6490 Triple Quad (Agilent Technologies, Santa Clara, CA, USA) mass-spectrometer equipped with Agilent 1290 Infinity u-HPLC system. The HRESIMS data were obtained from the Agilent 6530 Q-TOF (Agilent Technologies, Santa Clara, CA, USA) mass-spectrometer equipped with Agilent 1290 Infinity u-HPLC system. The UV measurement was carried out using the Agilent Cary 60 UV Vis spectrophotometer (Agilent Technologies, Santa Clara, CA, USA). The IR measurement was carried out on the Perkin-Elmer RX1 FT-IR (Perkin Elmer, Waltham, MA, USA) spectrophotometer using NaCl cell. The fluorescence measurement was carried out using Horiba Scientific Fluoromax-4 spectrofluorometer (HORIBA Instruments Incorporated, Edison, USA). The FRAP measurement was carried out using the Shimadzu UV-2700 UV-Vis Spectrophotometers (Shimadzu Corporation, Duisburg, Germany).

4.2.3 Plant extraction

2.0 Kg of dry *B. stenophylla* roots were extracted with hexane, chloroform and denatured ethanol consecutively, and each solvent extraction was repeated three times. The extracts were concentrated to dryness under reduced pressure which give 7.55 g of

hexane crude extract, 27.07 g of chloroform crude extract and 35.0 g of ethanol crude extract. The three crude extracts were later subjected to various chromatographic methods for isolation of pure compound.

4.2.4 Chromatographic method

4.2.4.1 Thin layer chromatographic (TLC)

TLC was extensively used for the subsequent isolation of pure compounds. TLCs were performed on pre-coated silica gel plates (Kieselgel 60 F24, Merck, Darmstadt, Germany), and spotted using a fine glass capillary tube, followed by development in a solvent saturated TLC tank with various solvents. The developed TLC plate was then viewed under short wave and long wave UV light, and stained with iodine and anisaldehyde staining reagents.

4.2.4.2 Column chromatography (CC)

CC was carried out using silica gel 60 (0.063-0.200 and 0.040-0.063 mm, Merck, Darmstadt, Germany). The column was packed by preparing silica gel slurry in desired eluting solvent and then settling the gel into the column. The solvent systems used were generally hexane, ethyl acetate, acetone, chloroform and diethyl ether, in different mixing compositions and gradients. TLC was used to aid in monitoring the fractions.

4.2.4.3 Centrifugal thin layer chromatography (CTLC)

CTLC was carried out by using the Kieselgel 60 with gypsum silica gel (Merck, Darmstadt, Germany) prepared on a round glass plate of 24 cm in diameter. The silica gel slurry was prepared by using about 30 g of silica gel dissolved in 90 mL of distilled water (to prepare for 1 cm thickness on the plate). The glass plate was taped on the edge by using cellophane tape before pouring the silica gel slurry evenly on the glass plate. The slurry was air-dried before removing the cellophane tape and the plate was subsequently baked in an oven at 80 °C for 2 hours to remove any water remained. Then, the plate was

allowed to cool at room temperature for 6 hours before scrapping the plate 5 mm from the edge and 30 mm from the centre. Chromatography was carried out by first wetting the spinning plate mounted on the machine with eluting solvent, and then the sample was loaded on the center to form a thin band before eluting with the desired solvent system. TLC was used to aid in monitoring the fractions obtained.

4.2.4.4 Preparative thin layer chromatography (PTLC)

Prep TLC is a useful technique for the purification of the small quantities of sample because it allows rapid separation of a number of components in a reaction mixture. It was carried out using the TLC silica gel 60 F_{254} (Merck, Darmstadt, Germany). The TLC plate were gently marked roughly 1.5 cm from one side of the plate. This is the "origin" line. Using a fine glass capillary tube, a thin line of sample was deposited across the pencil line. After obtained the prep TLC chamber, pour in the eluent, approximately about 150 mL. Then, the plate was placed in and the top sealed with lid. A typical run takes about 1 hour to 2 hours. After that, the plate was removed and visualized under UV. The bands that appear were marked with pencil, cut into pieces by using a scissor and put it in a small bottom flask, then soaked in a mixture of methanol, chloroform, and acetone. The sample then was concentrated to dryness by using the rotary evaporator or speed evaporator. To separate the sample with the silica gel, the sample was soaked with the solvent that the sample can dissolved in (e.g. chloroform and acetone). The supernatant was taken out and concentrated to dryness, and then it was subjected to ^{1}H NMR experiment.

4.2.5 Staining reagents for TLC

4.2.5.1 Iodine staining reagent

A 100 mL wide mouth chamber (with cap) was assembled with a piece of filter paper and a few iodine crystals were added to saturate the chamber with iodine vapor.

TLC plate was then placed in the chamber and incubated for a few minutes to allow reaction between the iodine vapor and the compounds on the TLC plate. When the entire TLC plate turned brownish, the TLC was removed to identify the dark brown spots on the brownish TLC plate. The spots were marked with a pencil. This reagent is normally used to detect unsaturated compounds.

4.2.5.2 Anisaldehyde staining reagent

A 100 mL anisaldehyde staining reagent was prepared by using 1 mL anisaldehyde, 100 mL of denatured ethanol, and 2 mL of 98% sulphuric acid. The staining was carried out by flooding the TLC plate with the stain solution and immediately heated to dry until the TLC plate turned pink or the maximal visualiation of the reacted compounds. The colour changes to violet, blue, red, grey or green according to functional groups namely lichen constituents, phenols, terpenes, sugars and steroids.

4.2.6 Isolation charts

4.2.6.1 Isolation chart of chloroform extract from *Boesenbergia stenophylla*

The chloroform extract obtained from *B. stenophylla* (6.16 g) was subjected to extensive chromatographic separation as summarized in the flow diagram shown in Figure 4.4 to yield one compound.

4.2.6.2 Isolation chart of hexane extract from *Boesenbergia stenophylla*

The hexane extract obtained from *B. stenophylla* (7.56 g) was subjected to extensive chromatographic separation as summarized in the flow diagram shown in Figure 4.5 to yield one compound.

4.2.6.3 Isolation chart of ethanol extract from *Boesenbergia stenophylla*

The ethanol extract obtained from *B. stenophylla* (4.5 g) was subjected to extensive chromatographic separation as summarized in the flow diagram shown in Figure 4.6 to yield two compounds.

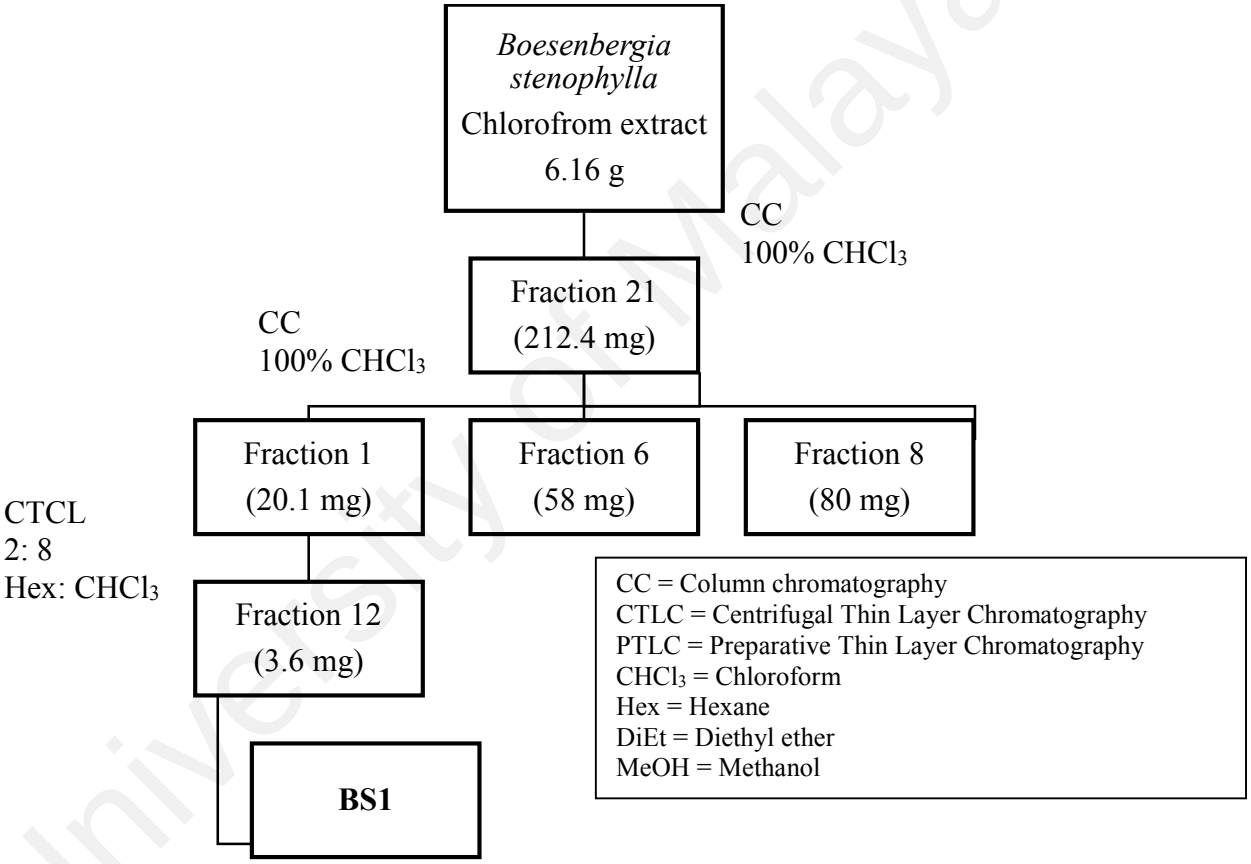

Figure 4.4: Isolation of compounds from the chloroform extract of *Boesenbergia stenophylla*

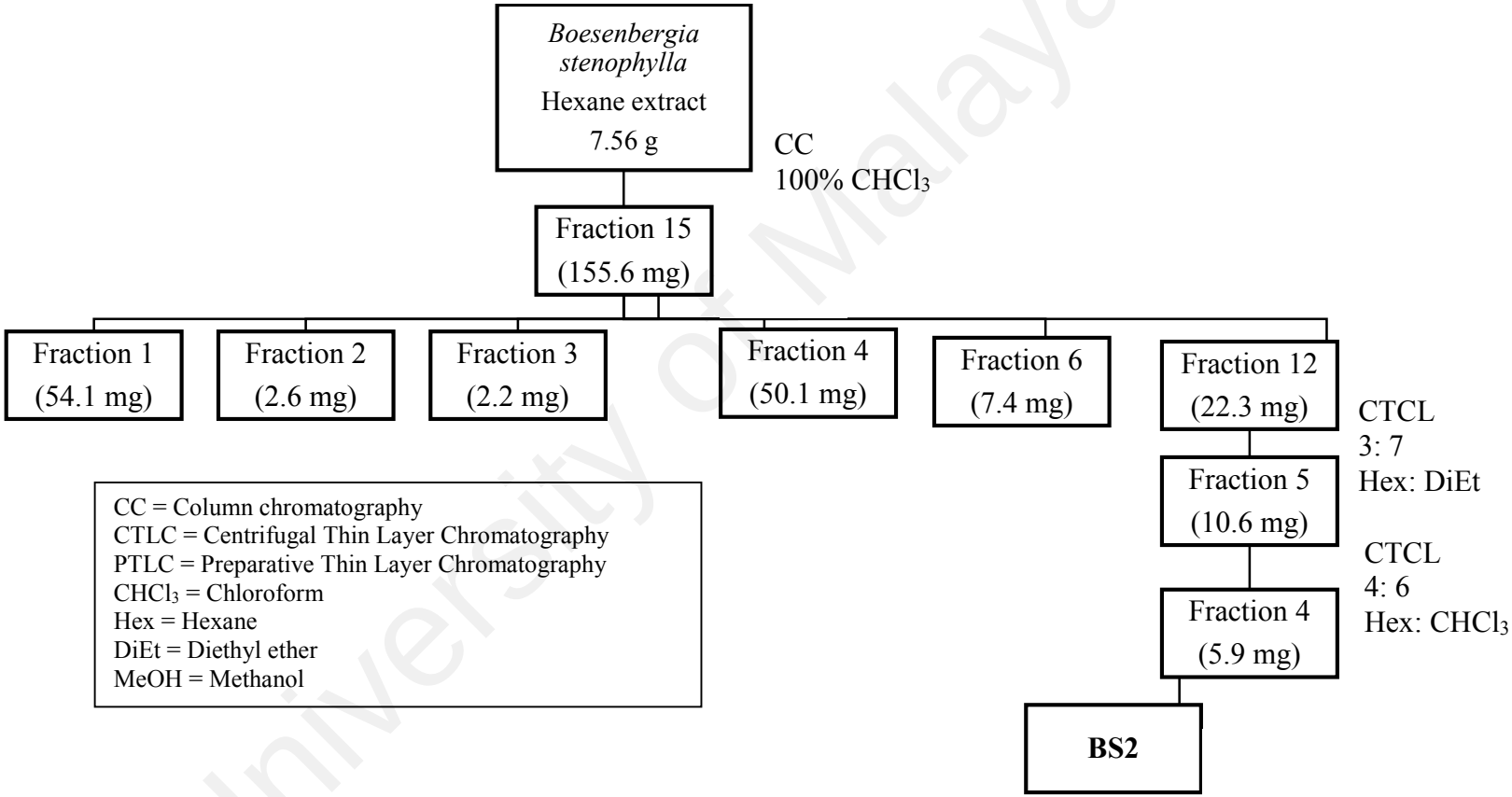

Figure 4.5: Isolation of compounds from the hexane extract of *Boesenbergia stenophylla*

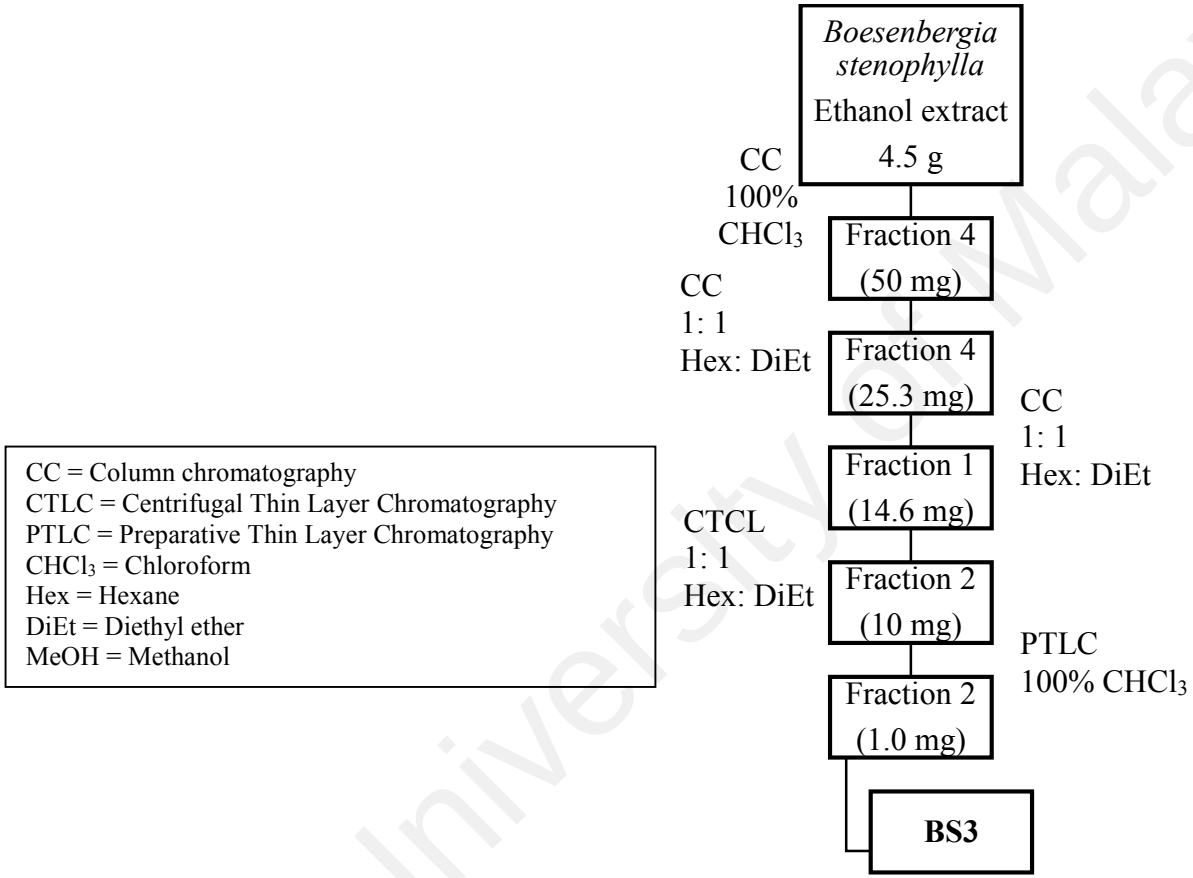

Figure 4.6: Isolation of compounds from the ethanol extract of *Boesenbergia stenophylla* (part 1)

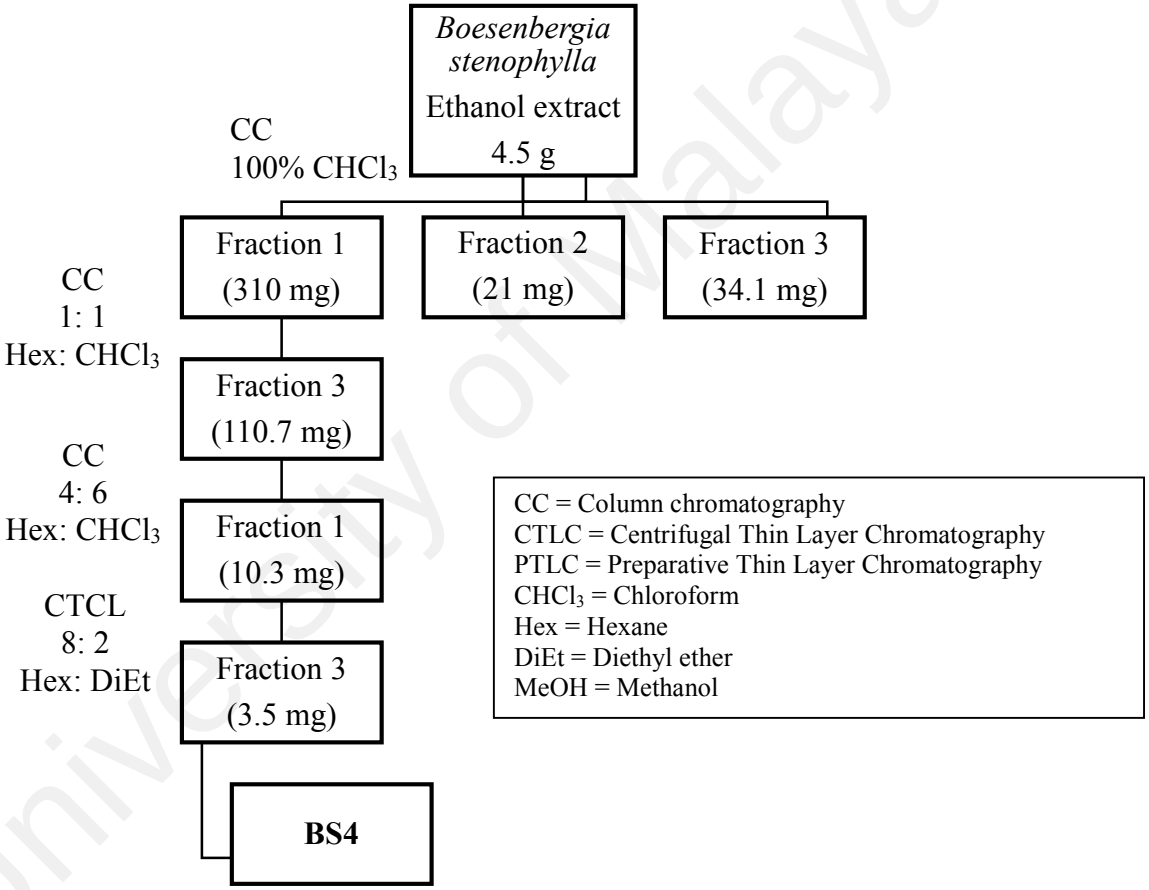

Figure 4.7: Isolation of compounds from the ethanol extract of *Boesenbergia stenophylla* (part 2)

4.2.6.4 Table of R_f Values of extraction of *B. stenophylla*

Table 4.6: The R_f values

Compound ID	100% $CHCl_3$	8:2 = $CHCl_3$:Hex	6:4 = $CHCl_3$:Hex	8:2 = Hex:DiEt
BS1	-	0.12	-	-
BS2	-	-	0.31	-
BS3	0.51	-	-	-
BS4	-	-	-	0.41

4.2.7 Spectroscopic data of compounds isolated from *Boesenbergia stenophylla*

BS1: Light yellow oil; molecular formula $C_{15}H_{14}O_5$; UV (MeOH) λ_{max} (log Ɛ) 203 (3.89), 294 (3.23), 341 (2.92) nm; IR (NaCl) ν_{max} 3227, 2851, 1634, 1644, 1161, 1069 cm^{-1}; HREIMS *m/z* 257.0802 $[M+H-H_2O]^+$ (calculated for $C_{15}H_{14}O_5 + H - H_2O$, 257.0808) and *m/z* 255.0689 $[M-H-H_2O]^-$ (calculated for $C_{15}H_{14}O_5 – H - H_2O$, 255.0663); for ^1H and ^{13}C NMR data, see Table 3.6. HMBC: ^2J C-2 to H-3; C-2' to H'; C-4' to H-3'; C-4' to H-5'; C-6' to H-5'; C-1'' to H-3; ^3J C-1 to H-3'; C-1' to H-3'; C-1' to H-5'; C-3' to H-5'; C-5' to H-3'; C-1'' to H-2; C-1'' to H-3''; C-1'' to H-5''; C-2'' to H-4''; C-3'' to H5''; C-4'' to H-2''; C-4'' to H-6''; C-5'' to H-3''; C-6'' to H-4''.

BS2: Dark brown oil; molecular formula $C_{20}H_{22}O_3$; UV (MeOH) λ_{max} (log Ɛ) 224 (3.76), 282 (3.20), 371 (2.54) nm; IR (NaCl) ν_{max} 3422, 2936, 1656, 1515, 1272, 700 cm^{-1}; HREISM with *m/z* 309.1752 $[M-H]^-$ (calculated for $C_{20}H_{22}O_3$ - H, 309.1728) and *m/z* 293.1808 $[M-OH]^-$ (calculated for $C_{20}H_{22}O_3$ - OH, 293.1779); for ^1H and ^{13}C NMR data, see Table 3.7. HMBC: ^2J C-6 to H-5; C-7 to H-6; C-1' to H-1; C-2' to H-3'; C-1'' to H-7; C-1'' to H-6''; C-4'' to H-3''; C-4'' to H-5''; ^3J C-1 to H-6'; C-3 to H-5; C-4 to H-6; C-6 to H-4; C-7 to H-5; C-1' to H-2; C-1' to H-2'; C-1' to H-3'; C-1' to H-5'; C-2' to H-4'; C-2' to H-6'; C-3' to H-5'; C-5' to H-3'; C-6' to H-2'; C-1'' to H-6; C-5'' to H-3''.

BS3: Light yellow oil; molecular formula $C_{15}H_{10}O_5$; UV (MeOH) λ_{max} (log Ɛ) 213 (3.62), 269 (3.45), 318 (3.12), 367 (3.19) nm; IR (NaCl) ν_{max} 3352, 2929, 2361, 2343, 1599, 772 cm^{-1}; HREIMS *m/z* 269.0481 $[M-H]^-$ (calculated for $C_{15}H_{10}O_5$ - H, 271.0); for ^1H and ^{13}C NMR data, see Table 3.8. HMBC: ^2J C-5 toH-6; C-7 to H-6; C-8a to H-8; C-1' to H-2'; C-1' to H-6'; C-3' to H-2';C-5' to H-6'; C-6' to H-5'; ^3J C-2 to H-2'; C-2 to H-6'; C-4a to H-6; C-4a to H-8; C-6 to H-8; C-1' to H-3'; C-1' to H-5'; C-2' to H-6'; C-4' to H-6'; C-5' to H-3'; C-6' to H-2'.

BS4: Light yellow oil; molecular formula $C_{19}H_{20}O$; UV (MeOH) λ_{max} (log Ɛ) 210 (3.47), 245 (2.90), 280 (2.41) nm; IR (NaCl) ν_{max} 3028, 2955, 1719, 1708, 1458, 1377, 698 cm^{-1}; HREIMS *m/z* 283.1791 $[M+H+H_2O]^+$ (calculated for $C_{19}H_{20}O + H + H_2O$, 283.1698); for ^1H and ^{13}C NMR data, see Table 3.9. HMBC: ^2J C-3 to H-4; C-1' to H-1; C-1'' to H-7; ^3J C-1 to H-2'; C-1 to H-6'; C-2 to H-4; C-3 to H-1; C-3 to H-5; C-4 to H-6; C-6 to H-4; C-1' to H-3'; C-1' to H-5'; C-2' to H-4'; C-2' to H-6'; C-3' to H-5'; C-4' to H-2'; C-4' to H-6'; C-5' to H-3'; C-6' to H-2'; C-1'' to H-6; C-1'' to H-3''; C-1'' to H-5''; C-2'' to H-6''; C-3'' to H-5''; C-4'' to H-2''; C-4'' to H-6''; C-5'' to H-3''; C-6'' to H-2''; C-6'' to H-4''.

4.2.8 Antioxidant assay – Ferric reducing antioxidant power (FRAP) data

Ferric reducing antioxidant power (FRAP) assay FRAP assay was performed according to the methods of Benzie & Strain (1996) with slight modification. The FRAP reagent was prepared fresh by adding 10 mM of 2,4,6-Tris(2-pyridyl)-1,3,5-triazine (TPTZ) (dissolved with 40 mM of HCl), 20 mM of $FeCl_3$ in water and 300 mM of acetate buffer (pH 3.6) in ratio of 1:1:10. 12 µg/mL of samples **BS1** – **BS4** were mixed with 400 µl FRAP reagent and 2% of dimethyl sulfoxide (DMSO) in test tubes. Blank samples were prepared for deionized water extracted samples. Both samples and blank were incubated in water bath for 30 minutes at 37 ^{0}C and the absorbance of the samples was determined against blank at 593 nm. Absorbance at 593 nm was measured by Shimadzu UV-2700 UV-Vis Spectrophotometers (Shimadzu Corporation, Duisburg, Germany). Vitamin C (ascorbic acid), and caffeic acid were used as antioxidant standards and positive controls. Series of stock solution at 2, 4, 8, 12, 16, 20 and 24 µg/mL were prepared (R^2= 0.9984) using aqueous solution of $FeSO_4.7H_2O$ as standard curve (Figure 4.8, Table 4.7). The values obtained were expressed as mmol/g of ferrous equivalent Fe (II) per gram of dried sample (Table 4.8).

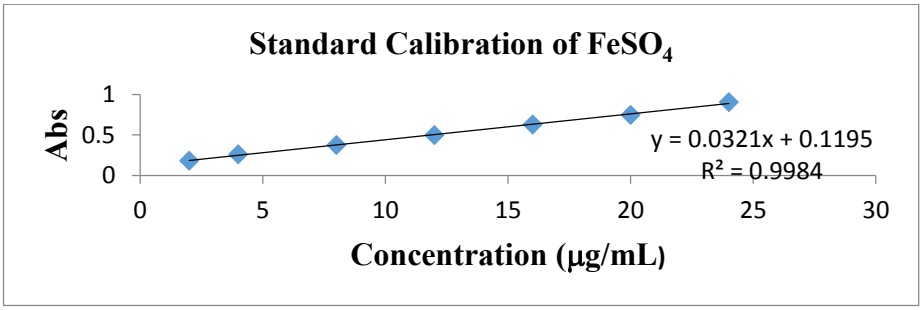

Figure 4.8: $FeSO_4$ standard curve.
Standard equation: y= 0.0321x + 0.1195; R^2 = 0.9984

Table 4.7: $FeSO_4$ data

Concentration (µg/mL)	Absorption
2	0.1793
4	0.2612
8	0.3751
12	0.4975
16	0.6290
20	0.7478
24	0.9038

Table 4.8: Antioxidant capacity value for ascorbic acid, caffeic acid, **BS2** and **BS3**

Sample	**Replicates**	**µg/mL**	**µg/mL**	**mM**	**mmol Fe/g**
Ascorbic acid	12 µg/mL	Y value	X value		
	1	0.5697	14.0249	0.0504	4.20
	2	0.5674	13.9542	0.0502	4.18
	3	0.5891	14.6293	0.0526	4.39
				mean	4.26
				SD	0.11
Caffeic acid	12 µg/mL	Y value	X value		
	1	0.6281	15.8450	0.0570	4.75
	2	0.6282	15.8472	0.0570	4.75
	3	0.6246	15.7350	0.0566	4.72
				mean	4.74
				SD	0.02
BS2	12 µg/mL	Y value	X value		
	1	0.5100	12.1657	0.0438	3.65
	2	0.5151	12.3228	0.0443	3.69
	3	0.5171	12.3849	0.0445	3.71
				mean	3.68
				SD	0.03
BS3	12 µg/mL	Y value	X value		
	1	0.3613	7.5313	0.0271	2.26
	2	0.3626	7.5732	0.0272	2.27
	3	0.3506	7.1986	0.0259	2.16
				mean	2.23
				SD	0.06

SD: Standard Deviation

CHAPTER 5: CONCLUSION

Ten natural anthraquinones have been subjected to photophysical studies and characterized using fluorescence, UV, NMR and MS. This study provides a deep insight on effect of interactions between multiple substitution groups on the photophysical properties of anthraquinones. The results indicate that absorption and emission maxima are deeply affected by presence of electron withdrawing or donating groups, ability to form intramolecular hydrogen bonding, steric configuration, and hyperconjugation effect of the anthraquinone structure.

The second part of the investigation focused on the phytochemical studies of *Boesenbergia stenophylla*. Four compounds were isolated and characterized using various chromatographic methods namely NMR, LCMS, UV and IR. Antioxidant capacity of these compounds have also been evaluated by using the Ferric reducing antioxidant power (FRAP). The phytochemical study of the chloroform extract of *B. stenophylla* yielded a new compound **BS1**. Hexane extract of *B. stenophylla* yielded one new compound **BS2**. While **BS3** and **BS4** was isolated from the ethanol extract of *B. stenophylla*. This is the first report of the occurrence of **BS1** and **BS2** to the best of our knowledge.

All the fourteen compounds from *M. citrifolia* and *B. stenophylla* are summarized in the Table 5.1.

Table 5.1: The compounds isolated from *Morinda citrifolia* and *Boesenbergia stenophylla*

Comp. ID.	Source	Compound structure	Compound name
AQ1	*M. citrifolia*	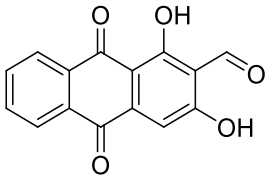	Nordamnacanthal
AQ2		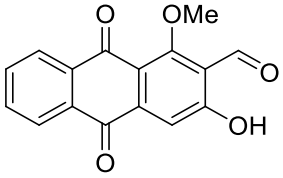	Damnacanthal
AQ3		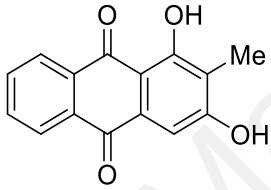	Rubiadin
AQ4		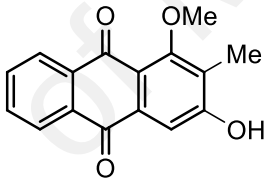	1-Methoxy-2-methyl-3-hydroxyanthraquinone
AQ5		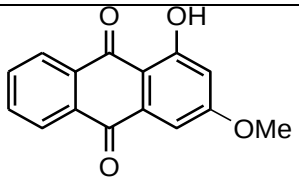	1-Hydroxy-3-methoxyanthraquinone
AQ6		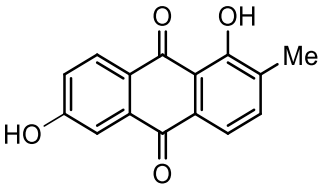	1,6-Dihydroxy-2-methylanthraquinone
AQ7		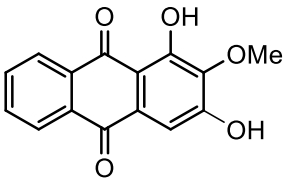	1,3-Dihydroxy-2-methoxyanthraquinone

Table 5.1, continued.

Comp. ID.	Source	Compound structure	Compound name
AQ8		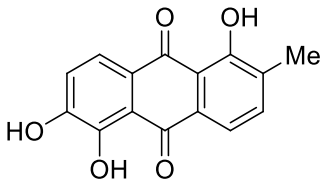	1,5,6-Trihydroxy-2-methylanthraquinone
AQ9		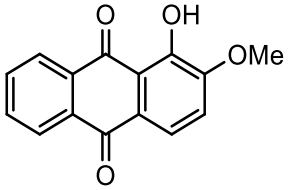	1-Hydroxy-2-methoxyanthraquinone
AQ10		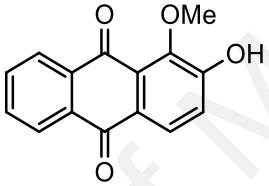	1-Methoxy-2-hydroxyanthraquinone
BS1	*B. stenophylla*	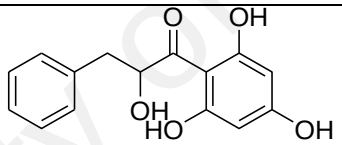	2-hydroxy-3-phenyl-1-(2,4,6-trihydroxy-phenyl)-propan-1-one
BS2		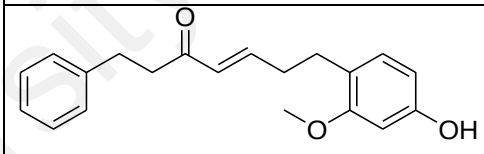	7-(2”-Methoxy-4”-hydroxyphenyl)-1-phenyl-hept-4-en-3-one
BS3		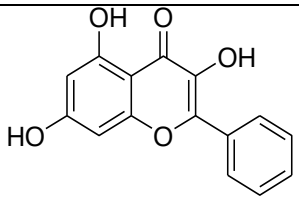	3,5,7-trihydroxy-flavone
BS4		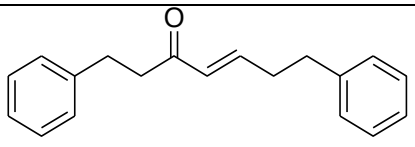	1,7-diphenylhept-4-en-3-one

REFERENCES

Agosta, W. C. (1997). Medicined and Drugs from Plants. *Journal of Chemical Education, 74* (7), 857-860.

Ahmad, F. B., & Jantan, I. B. (2003). The essential oils of *Boesenbergia stenophylla* RM Sm. as natural sources of methyl (E)-cinnamate. *Flavour and Fragrance Journal, 18*(6), 485-486.

Ahn, M. R., Kunimasa, K., Kumazawa, S., Nakayama, T., Kaji, K., Uto, Y., Hori, H., Nagasawa, H., & Ohta, T. (2009). Correlation Between antiangiogenic activity and antioxidant activity of various components from propolis. *Molecular Nutrition & Food Research, 53*, 643 – 651.

Aiyelaagbe, O., & Osamudiamen, P. M. (2009). Phytochemical screening for active compounds in Mangifera indica leaves from Ibadan, Oyo State. *Plant Science and Research, 2*(1), 11-13.

Allen, N. S., Pullen, G., Shah, M., Edge, M., Holdsworth, D., Weddell, I., & Catalina, F. (1995). Photochemistry and photoinitiator properties of 2-substituted anthraquinones 1. Absorption and luminescence characteristics. *Journal of Photochemistry and Photobiology A: Chemistry, 91*, 73-79.

Alothman, M., Bhat, R., & Karim, A. (2009). Antioxidant capacity and phenolic content of selected tropical fruits from Malaysia, extracted with different solvents. *Food Chemistry, 115*(3), 785-788.

An, N., Xu, L. Z., Zou, Z. M., & Yang, S. L. (2006). Diarylheptanoids from Alpinia officinarum. *Journal of Asian Natural Product Research, 8*(7), 637-641.

Anouar, E. L., Osman, C.P., Weber, J. F. F., & Ismail, N.H. (2014). UV/Visible spectra of a series of natural and synthesised anthraquinones: experimental and quantum chemical approaches. *SpringerPlus, 3*, 233.

Antolovich, M., Prenzler, P. D., Patsalides, E., McDonald, S., & Robards, K. (2002). Methods for testing antioxidant activity. *Analyst, 127*(1), 183-198.

Aruna, P., Fred, R., & Eugene, M. (2007). Antioxidant Activity. Retrieved 23rd, February, 2017, from http://www.medallionlabs.com/Downloads/Antiox_acti_

Babu, D., Gurumurthy, P., Borra, S. K., & Cherian, K. M. (2013). Antioxidant and free

radical scavenging activity of triphala determined by using different in vitro models. *Journal of Medicinal Plants Research, 7*(39), 2898-2905.

Bairwa, K., Grover, J., Kania, M., & Jachak, S. M. (2014). Recent developments in chemistry and biology of curcumin analogues. *RSC Advances, 4*(27), 13946-13978.

Bendiner, E. (1989). Alexander Fleming: player with microbes. *Hospital Practice, 24*(2), 283-316.

Benzie, I. F., & Strain, J.J. (1996). The ferric reducing ability of plasma (FRAP) as a measure of "antioxidant power": the FRAP assay. *Analytical Biochemistry, 239*(1), 70-76.

Buchwalow, I. B., and Böcker, W. (2010). *Immunohistochemistry: basics and methods.* Berlin: Springer Verlag.

Butler, M. S. (2004). The role of natural product chemistry in drug discovery. *Journal of Natural Product, 64*(12), 2141-2153.

Caamaño-Tubío, R. I., Pérez, J., Ferreiro, S., and Aldegunde, M. (2007). Peripheral serotonin dynamics in the rainbow trout (*Oncorhynchus mykiss*). *Comparative Biochemistry and Physiology Part C: Toxicology & Pharmacology, 145*(2): 245-255.

Cakir, Y., and Strauch, S. M. (2005). Tricaine (MS-222) is a safe anesthetic compound compared to benzocaine and pentobaritol to induce anesthesia in leopard frogs (*Rana pipiens*). *Pharmacological Reports, 57*: 467-474.

Cameron, A. A., Plenderleith, M. B. and Snow, P. J. (1990). Organization of the spinal cord in four species of elasmobranch fishes: cytoarchitecture and distribution of serotonin and selected neuropeptides. *The Journal of Comparative Neurology, 297*: 201-218.

Chin, Y. W., Balunas, M. J., Chai, H. B., & Kinghorn, A. D. (2006). Drug discovery from natural resources. *AAPS Journal, 8*(2), E239-E253.

Christoph, G. (2012). Basic Principles of Luminescence. Retrieved 17th, March, 2017, from http://www.leica-microsystems.com/science-lab/basic-principles-of-luminescence/

Csepregi, K., Neugart, S., Schreiner, M., & Hideg, É. (2016). Comparative evaluation of total antioxidant capacities of plant polyphenols. *Molecules, 21*(2), 208.

Dahiya, P., Kumbhakar, M., Mukherjee, T., & Pal, H. (2006). Effect of the amino and hydroxy substituents on the photophysical properties of 1, 4-disubstituted-9, 10-anthraquinone dyes. *Journal of Molecular Structure, 798*(1), 40-48.

Dahiya, P., Maity, D., Nayak, S., Mukherjee, T., & Pal, H. (2007). Photophysical properties of 1-N-methylamino-and 1-N, N-dimethylamino-9, 10-anthraquinone dyes: a comparison with 1-amino-9, 10-anthraquinone dye. *Journal of Photochemistry and Photobiology A: Chemistry, 186*(2), 218-228.

Dave, H., & Ledwani, L. (2012). A review on anthraquinones isolated from Cassia species and their applications. *Indian Journal of Natural Product Research, 3*(3), 291-319.

De Silva, S., Watanabe, M., & Snieckus, V. (1979). General route to anthraquinone natural products via directed metalation of N, N-diethylbenzamides. *Journal of Organic Chemistry, 44*(26), 4802-4808.

Deep, M. K., & Siddqui, A.A. (2012). Isolation and Characterization of Some Pharmaceutical Active Flavonoids from Cichorrium Intybus Plant (Kasini). *Ultra Chemistry, 8*(2), 125-134.

Diaz, A. N. (1990). Absorption and emission spectroscopy and photochemistry of 1,10-anthraquinone derivatives: a review. *Journal of Photochemistry and Photobiology A: Chemistry, 53*, 141-167.

Diaz, A. N. (1991). Analytical applications of 1,10-anthraquinones: A review. *Talanta, 38*, 571-588.

Dong, Y., Shi, H., Yanga, H., Peng, Y., Wang M., Li, X. (2012). Antioxidant Phenolic Compounds from the Stems of *Entada phaseoloides*. *Chemistry & Biodiversity, 9*(68-79).

Dudonné, S., Vitrac, X., Coutiere, P., Woillez, M., & Mérillon, J. M. (2009). Comparative study of antioxidant properties and total phenolic content of 30 plant extracts of industrial interest using DPPH, ABTS, FRAP, SOD, and ORAC assays. *Journal of Agricultural and Food Chemistry, 57*(5), 1768-1774.

Eng-Chong, T., Yean-Kee, L., Chin-Fei, C., Choon-Han, H., Sher-Ming, W., Li-Ping, C.T., Gen-Teck, F., Khalid, N., Abd Rahman, N., Karsani, S. A., Othman, S., Othman, R., & Yusof, R. (2012). *Boesenbergia rotunda* : From Ethnomedicine to Drug Discovery. *Evidence- Based Complementary and Alternative Medicine, 2012*, 1-25.

Fabricant, D. S., Farnsworth, N. R. (2001). The value of plants used in traditional medicine for drug discovery. *Environmental Health Perspectives, 109*, 69–75.

Farnsworth, N. R., Akerele, R. O., Bingel, A. S., Soejarto, D. D., Guo, Z. (1985). Guo, Medicinal plants in therapy. *Bulletin World Health Organization, 63*, 965–981.

Flom, S. R., & Barbara, P.F. (1985). Proton transfer and hydrogen bonding in the internal conversion of S1 anthraquinones. *Journal of Physical Chemistry A, 89*, 4489-4494.

Garrido, J., Gaspar, A., Garrido, E. M., Miri, R., Tavakkoli, M., Pourali, S., & Firuzi, O. (2012). Alkyl esters of hydroxycinnamic acids with improved antioxidant activity and lipophilicity protect PC12 cells against oxidative stress. *Biochimie, 94*(4), 961-967.

Gierschner, J., Duroux, J. L., & Trouillas, P. (2012). UV/Visible spectra of natural polyphenols : a time-dependent density functional theory study. *Food Chemistry, 131*(1), 79-89.

Gueritte, F., Fahy, J. (2005). *Anticancer agents from natural products*. Taylor and Francis: Boca Raton, Florida.

Guilbault, G. G. (1990). *Practical Fluorescence*. New York: CRC Press.

Guo, C., Yang, J., Wei, J., Li, Y., Xu, J., & Jiang, Y. (2003). Antioxidant activities of peel, pulp and seed fractions of common fruits as determined by FRAP assay. *Nutrition Research, 23*(12), 1719-1726.

Gurnani, N., Mehta, D., Gupta, M., & Mehta, B.K. (2014). Natural products: Source of potential drugs. *African Journal of Basic & Applied Sciences, 6*(6), 171-186.

Haefner, B. (2003). Druds from the deep: marine natural products as drug candidates. *Drug Discovery Today, 8*(12), 536-544.

Hartwell, J. L. (1982). *Plants used against cancer.* Quarterman: Lawrence, Massachusetts.

Hasnah, M. S., Shajarahtunnur, J., & Neelavany, M. (1995). *Chemical constituents of Boesenbergia species. Chemical prospecting in The Malaysian forest*. Kuching, Malaysia: Pelanduk Publications (M) Sdn. Bhd.

Hassimotto, N. M. A., Genovese, M. I., & Lajolo, F. M. (2005). Antioxidant activity of dietary fruits, vegetables, and commercial frozen fruit pulps. *Journal of Agricultural Food Chemistry, 53*(8), 2928-2935.

He, L., Freeman, H. S., Lu, L., & Zhang, S. (2011). Spectroscopic study of anthraquinone dye/amphiphile systems in binary aqueous/organic solvent mixtures. *Dyes Pigment, 91*(3), 389-395.

Herschel, J. F. W. (1845). Superficial Colour Presented by a Homogeneous Liquid Internally Colourless. *Philosophical Transactions of the Royal Society of London, 135*, 143-145.

Hossain, M. A., Wongsrikaew, N., Yoo, G.W., Han, J., & Shin, C.G. (2012). Cytotoxic effects of polymethoxyflavones isolated from *Kaempferia parviflora*. *Journal of the Korean Society for Applied Biological Chemistry, 55*(4), 471-476.

Huang, D., Ou, B., & Prior, R. L. (2005). The chemistry behind antioxidant capacity assays. *Journal of Agricultural Food Chemistry, 53*(6), 1841-1856.

Huang, G. S., Lopez-Barcons, L., Freeze, B. S., Smith, A. B., Goldberg, G. L., Horwitz, S. B., & McDaid, H. M. (2006). Potentiation of taxol efficacy and by discodermolide in ovarian carcinoma xenograft-bearing mice. *Clinical Cancer Research, 12*, 298-304.

Inoue, H., Hida, M., Nakashima, N., & Yoshihara, K. (1982). Picosecond fluorescence lifetimes of anthraquinone derivatives. Radiationless deactivation via intra-and intermolecular hydrogen bonds. *Journal of Physical Chemistry A, 86*(16), 3184-3188.

Inoue, H., Hoshi, T., Yoshino, J., & Tanizaki, Y. (1972). The polarized absorption spectra of some α-aminoanthraquinones. *Bulletin of Chemical Society of Japan, 45*(4), 1018-1021.

Itokawa, H., Morita, M., & Mihashi, S. (1981). Two new diarylheptanoids from Alpinia officinarum Hance. *Chemical and and Pharmaceutical Bulletin, 29*(8), 2383-2385.

Jantan, I. B., Basni, I., Ahmad, A. S., Ali, M. Azah, N., Ahmad, A. R., & Ibrahim, H. (2001). Constituents of the rhizome oils of *Boesenbergia pandurata* (Roxb.) Schlecht from Malaysia, Indonesia and Thailand. *Flavour and Fragrance Journal, 16*(2), 110-112.

Keirs, R. J., Britt Jr, R. D., & Wentworth, W. E. (1957). Phosphorimetry. *Analytical Chemistry, 29*(2), 202-209.

Khan, M. S., & Khan, Z. H. (2003). Electronic absorption spectra of amino substituted anthraquinones and their interpretation using the ZINDO/S and AM1 methods. *Spectrochimica Acta Molecular and Biomolecular Spectroscopy, 59*(7), 1409-1426.

Kinghorn, A. D. (2001). Pharmacognosy in the 21st century. *Journal of Pharmacy and Pharmacology, 53*, 125-148.

Kirana, C., Jones, G.P., Record, I.R., & McIntosh, G.H. (2007). Anticancer properties of panduratin A isolated from *Boesenbergia pandurata* (Zingiberaceae). *Journal of Natural Medicine, 61*(2), 131-137.

Kong, J. M., Goh, N. K., Chia, L. S., & Chia, T. F. (2003). Recent advances in traditional plant drugs and orchids. *Acta Pharmacologica Sinica, 24*(1), 7-21.

Kozlowski, D., Trouillas, P., Calliste, C., Marsal, P., Lazzaroni, R., & Duroux, J. L. (2007). Density functional theory study of the conformational, electronic, and antioxidant properties of natural chalcones. *The Journal of Physical Chemistry A, 111*(6), 1138–1145.

Kulip, J. (2007). Gingers in Sabah and their traditional uses. *Sepilok Bulletin, 7*, 23-44.

Lahlou, M. (2013). The Success of Natural Products in Drug Discovery. *Pharmacology & Pharmacy, 4*, 17-31.

Lakowicz, J. R. (2006). *Principles of Fluorescence Spectroscopy*. Baltimore, USA: Springer.

Lakowicz, J. R. (2013). *Principles of fluorescence spectroscopy*. New York: Springer Science & Business Media.

Langdon-Jones, E. E., & Pope, S.J.A. (2014). The coordination chemistry of substituted anthraquinones: developments and applications. *Coordination Chemistry Reviews, 269*, 32-53.

Larsen, K. (2010). Further studies in the genus *Boesenbergia* (Zingiberaceae). *Journal of Medicinal Plants Research, 17*(4), 361-366.

Leardkamolkarn, V., Tiamyuyen, S., & Sripanidkulchai, B.O. (2009). Pharmacological Activity of *Kaempferia parviflora* Extract against Human Bile Duct Cancer Cell Lines. *Asian Pacific Journal Cancer Prevention, 10*, 695-698.

Lee, K. H., & Xiao, Z. (2012). *Anticancer agents from natural products.* Taylor and Francis: Boca Raton, Florida.

Li, Y., & Schellhorn, H. E. (2007). New developments and novel therapeutic perspectives for vitamin C. *Journal of Nutrition, 137*(10), 2171-2184.

Lien, E. J., Ren, S., Bui, H. H., & Wang, R. (1998). Quantitative structure-activity relationship analysis of phenolic antioxidants. *Free Radical Biology and Medicine, 26*(3), 285-294.

Lim, Y., Lim, T., & Tee, J. (2007). Antioxidant properties of several tropical fruits: A comparative study. *Food Chemistry, 103*(3), 1003-1008.

Ling, J. J., Maryati Mohamed, D., Rahmat, A., & Bakar, M. F. A. (2010). Phytochemicals, antioxidant properties and anticancer investigations of the different parts of several gingers species (*Boesenbergia rotunda*, *Boesenbergia pulchella* var attenuata and *Boesenbergia armeniaca*). *Journal of Medicinal Plants Research, 4*(1), 27-32.

Lotulung, P. D., Kardono, L. B., & Kawanishi, K. (2008). Antioxidant compounds from rhizomes of *Kaempferia rotunda*. *Pakistan Journal Of Biology and Science, 11*(20), 2447-2450.

Lu, Y., Khoo, T. J., & Wiart, C. (2014). Antioxidant activity determination of Citronellal and crude extracts of Cymbopogon citratus by 3 different methods. *Pharmacology & Pharmacy, 5*(4), 395.

Luximon-Ramma, A., Bahorun, T., Soobrattee, M. A., & Aruoma, O. I. (2002). Antioxidant activities of phenolic, proanthocyanidin, and flavonoid components in extracts of *Cassia fistula*. *Journal of Agricultural and Food Chemistry, 50*(18), 5042-5047.

Madaka, F., Wattanapiromsakul, C., Sudsai, T., & Tewtrakul, S. (2013). Anti-allergic activity of compounds from *Boesenbergia thorelli*. *Songklanakarin Journal of Science and Technology, 35*(2), 197-201.

Mahady, G. (2005). Medicinal plants for the prevention and treatment of bacterial infections. *Current Pharmaceutical Design, 11*(9), 2405-2427.

Marković, Z., Manojlović, N., & Zlatanović, S. (2008). Electronic absorption spectra of substituted anthraquinones and their simulation using ZINDO/S method. *Journal of the Serbian Chemical Society, 2*(2), 73-79.

Moon, J. K., & Shibamoto, T. (2009). Antioxidant assays for plant and food components. *Journal of Agricultural and Food Chemistry, 57*(5), 1655-1666.

Moye, H., & Winefordner, J. (1956). Phosphorescence, Phosphorimetric Study of Some Common Pesticides. *Journal of Agricultural and Food Chemistry, 13*(6), 516-518.

Murakami, A., Kondo, A., Nakamura, Y., Ohigashi, H., & Koshimizu, K. (1993). Possible anti-tumor promoting properties of edible plants from Thailand, and identification of an active constituent, cardamonin, of *Boesenbergia pandurata*. *Bioscience, Biotechnology and Biochemistry, 57*(11), 1971-1973.

Nagia, F., & El-Mohamedy, R. (2007). Dyeing of wool with natural anthraquinone dyes from Fusarium oxysporum. *Dyes Pigment, 75*(3), 550-555.

Nelson, G. M., Ramesh, D., Sunena, C., Robert, K., & Alexander, K. (2016). Marine Invertebrate Metabolites with Anticancer Activities: Solutions to the "Supply Problem". *Marine Drugs, 14*, 98.

Nur Atiqah, M. N. (2016). *Chemical constituents from Marsdenia tinctoria and Morinda citrifolia* (Master dissertation). Retrieved from http://pendeta.um.edu.my

Núñez-Sellés, A. J. (2005). Antioxidant therapy: myth or reality?. *Journal of The Brazilian Chemical Society, 16*(4), 699-710.

O'Donnell, C., & Winefordner, J. (1975). The potential of phosphorescence spectrometry in clinical chemistry—the new generation of instrumentation and methodology. *Clinical Chemistry, 21*(3), 285-299.

Oktay, M., Gulcin, I., & Kufrevioglu, I. O. (2003). Determination of in vitro antioxidant activity of fennel (*Foeniculum vulgare*) seed extracts. *Lebensmittel-Wissenschaft & Technologie, 36*, (263–271).

Omprakash, H. N. (2013). Natural Products from Plant, Microbial, and Marine Species. *International Journal of Science and Technology, 10*(1), 611-646.

Patlak, M. (2004). From Viper's Venom to Drug Design: Treating Hypertension. *FASEB Journal, 18*(3), 421.

Peters, R. H., & Sumner, H.H. (1953). 430. Spectra of anthraquinone derivatives. *Journal of Chemical Society (Resumed)*, 2101-2110.

Philipson, J. D. (2001). Phytochemistry and medicinal plants. *Phytochemistry, 56*(3), 237-243.

Prasad, S., Yadav, V.R., Sundaram, C., Reuter, S., Hema, P.S., Nair, M.S., Chaturvedi, M.M., & Aggarwal, B.B. (2010). Crotepoxide Chemosensitizes Tumor Cells through Inhibition of Expression of Proliferation, Invasion, and Angiogenic Proteins Linked to Proinflammatory Pathway. *Journal of Biology and Chemistry, 285*(35), 26987–26997.

Prior, R. L., Wu, X., & Schaich, K. (2005). Standardized methods for the determination of antioxidant capacity and phenolics in foods and dietary supplements. *Journal of Agricultural Food Chemistry, 53*(10), 4290-4302.

Pulido, R., Bravo, L., & Saura-Calixto, F. (2000). Antioxidant activity of dietary polyphenols as determined by a modified ferric reducing/antioxidant power assay. *Journal of Agricultural and Food Chemistry, 48*(8), 3396-3402.

Ranjitha, S., Aroulmoji, V., Mohr, T., Anbarasan, P., & Rajarajan, G. (2014). Structural and Spectral Properties of 1, 2-dihydroxy-9, 10-anthraquinone Dye Sensitizer for Solar Cell Applications. *Acta Physica Polonica A, 47*(2), 221-227.

Rath, M., Pal, H. & Mukherjee, T. (1996). Pulse-radiolytic one-electron reduction of anthraquinone and chloro-anthraquinones in aqueous-isopropanol-acetone mixed solvent. *Radiation Physics and Chemistry, 47*(2), 221-227.

Sauer, M., Hofkens, J., & Enderlein, J. (2011). *Basic principles of fluorescence spectroscopy. Handbook of Fluorescence Spectroscopy and Imaging: From Single Molecules to Ensembles*. Germany: Wiley-VCH.

Sharma, A., & Schulman, S. G. (2000). *An Introduction to Fluorescence Spectroscopy*. United Kingdom: Perkin Elmer.

Singh, C. B., Chanu, S.B., Bidyababy, T., Devi, W.R., Singh, S.B., Nongalleima, K., Lokendrajit, N., Swapana, N., & Singh, L.W. (2013). Biological and Chemical properties of *Kaempferia galanga* L. Zingiberaceae plant. *NeBio, 4*(4), 35-41.

Somparn, P., Phisalaphong, C., Nakornchai, S., Unchern, S., & Morales, N. P. (2007). Comparative antioxidant activities of curcumin and its demethoxy and hydrogenated derivatives. *Biological and Pharmaceutical Bulletin, 30*(1), 74-78.

Sons, J. H. (1987). *Notes from the Royal Botanic Garden, Edinburgh*. Edinburgh: Oliver & Boyd, Edinburgh.

Sri, A. (2014). *Phytochemical of Kaempferia Plant & Bioprospecting for Cancer Treatment.* Paper presented at the In Proceeding of International Conference On Research, Implementation And Education Of Mathematics And Sciences 2014, Yogyakarta State University, Yogyakarta, Indonesia.

Stevenson, P. C., Veitch, N. C., & Simmonds, M. S. (2007). Polyoxygenated cyclohexane derivatives and other constituents from *Kaempferia rotunda* L. *Phytochemistry, 68*(11), 1579-1586.

Stokes, G. G. (1852). XXX. On the change of refrangibility of light. *Philosophical Transactions of the Royal Society of London*, *142*, 463-562.

Sudsai, T., Wattanapiromsakul, C., Nakpheng, T., & Tewtrakul, S. (2013). Evaluation of the wound healing property of *Boesenbergia longiflora* rhizomes. *Journal of Ethnopharmacology, 150*(1), 223-231.

Sun, Y., Matsubara, H., Kitanaka, S., & Yasukawa, K. (2008). Diarylheptanoids from the rhizomes of Alpinia officinarum. *Helvetica Chimica Acta, 91*(1), 118-123.

Tao, M., Zhou, X., Jing, M., Liu, D., & Xing, J. (2007). Fluorescence and electrochemical properties of naphthylporphyrins and porphyrin–anthraquinone dyads. *Dyes Pigment, 75*(2), 408-412.

Tewtrakul, S., Subhadhirasakul, S., Karalai, C., Ponglimanont, C., & Cheenpracha, S. (2009). Antiinflammatory effects of compounds from *Kaempferia parviflora* and *Boesenbergia pandurata*. *Food Chemistry, 115*(2), 534-538.

Tewtrakul, S., Subhadhirasakul, S., Puripattanavong, J., & Panphadung, T. (2003). HIV-1 protease inhibitory substances from the rhizomes of *Boesenbergia pandurata* Holtt. *Songklanakarin Journal of Science and Technology, 25*(6), 503-508.

Thaipong, K., Boonprakob, U., Crosby, K., Cisneros-Zevallos, L., & Byrne, D. H. (2006). Comparison of ABTS, DPPH, FRAP, and ORAC assays for estimating antioxidant activity from guava fruit extracts. *Journal of Food Composition and Analysis, 19*(6), 669-675.

Thomson, R. (2012). *Naturally occurring quinones*. New York: Academic Press Inc.

Thongnest, S., Mahidol, C., Sutthivaiyakit, S., & Ruchirawat, S. (2005). Oxygenated pimarane diterpenes from *Kaempferia marginata*. *Journal of Natural Product, 68*(11), 1632-1636.

Trakoontivakorn, G., Nakahara, K., Shinmoto, H., Takenaka, M., Onishi-Kameyama, M., Ono, H., Yoshida, M., Nagata, T., & Tsushida, T. (2001). Structural Analysis of a Novel Antimutagenic Compound, 4-Hydroxypanduratin A, and the Antimutagenic Activity of Flavonoids in a Thai Spice, Fingerroot (*Boesenbergia pandurata* Schult.) against Mutagenic Heterocyclic Amines. *Journal of Agricultural and Food Chemistry, 49*(6), 3046-3050.

Uzum, A., Toprak, O., Gumustas, M. K., Ciftci, S., & Sen, S. (2006). Effect of vitamin E therapy on oxidative stress and erythrocyte osmotic fragility in patients on peritoneal dialysis and hemodialysis. *Journal of Nephrology, 19*(6), 739.

Valeur, B., & Berberan-Santos, M. N. (2012). *Molecular fluorescence: principles and applications*. Germany: John Wiley & Sons.

Wcisło, P., Niedziałkowski, P., Wnuk, E., Zarzeczan´ska, D., & Ossowski, T. (2013). Influence of different amino substituents in position 1 and 4 on spectroscopic and acid base properties of 9, 10-anthraquinone moiety. *Spectrochimica Acta Molecular Biomolecular Spectroscopy, 108*, 82-88.

Weisstuch, J., & Testa, A.C. (1970). Fluorescence study of 2-(N,N-Dimethylamino)pyridine and related molecules. *Journal of Physical Chemistry, 74*, 2299-2302.

Williams, A. R. (1981). *An Introduction to Phosphorescence Spectroscopy*. United Kingdom: Perkin-Elmer.

Win, N. N., Awale, S., Esumi, H., Tezuka, Y., & Kadota, S. (2008). Panduratins DI, Novel Secondary Metabolites from Rhizomes of *Boesenbergia pandurata*. *Chemical and Pharmaceutical Bulletin, 56*(4), 491- 496.

Woerdenbag, H. J., Windono, T., Bos, R., Riswan, S., & Quax, W. J. (2004). Composition of the essential oils of *Kaempferia rotunda* L. and *Kaempferia angustifolta* Roscoe rhizomes from Indonesia. *Flavour and Fragrance Journal, 19*(2), 145-148.

Wohlmuth, H. (2008). Phytochemistry and pharmacology of plants from the ginger family, Zingiberaceae. Retrieved 20th, January, 2015, from http://epubs.scu.edu.au/cgi/viewcontent.cgi?article=1298&context=theses

Wollenweber, E., Stevens, J.F., Dörr, M., & Rozefelds, A.C. (2003). Taxonomic significance of flavonoid variation in temperate species of Nothofagus. *Phytochemistry, 62*(7), 1125-1131.

Wu, X., Chao, Z., Wang, C., & Yu, L. (2015). Separation of chemical constituents from three plant medicines by counter-current chromatography using a three-phase solvent system at a novel ratio. *Journal of Chromatography A, 1384*, 107-114.

Yasukawa, K., Sun, Y., Kitanaka, S., Tomizawa, N., Miura, M., & Motohashi, S. (2008). Inhibitory effect of the rhizomes of Alpinia officinarum on TPA-induced inflammation and tumor promotion in two-stage carcinogenesis in mouse skin. *Journal of Natural Medicine, 62*(3), 374.

Yoshida, Z., & Takabayashi, F. (1968). Electronic spectra of mono-substituted anthraquinones and solvent effects. *Tetrahedron Letters, 24*, 933.

Zhang, D., Chen, W., Chen, W., Song, X., Han, C., Wang, Y., & Chen, G. (2013). Three new ursane-type triterpenoids from the stems of *Saprosma merrillii*. *Molecules, 18*(12), 14496-14504.

LIST OF PUBLICATIONS AND PAPERS PRESENTED

Nabila, E. A., Nur Atiqah, M. N., Zanariah, A., Choo, Y. M., Hairul, A. T. (2018). Isolation and Photophysical Properties of Di- and Tri-substituted Natural Anthraquinones from Malaysian *Morinda citrifolia*. *Sains Malaysiana, 47* (5), 901-906. *http://dx.doi.org/10.17576/jsm-2018-4705-05.*